2-24-2021

Characterization, Immobilization, and Polymer Related Applications of Watermelon Seed Powder, a Practical Source of Urease Enzyme

Anthony Quan Quoc Mai
Louisiana State University and Agricultural and Mechanical College

CHARACTERIZATION, IMMOBILIZATION, AND POLYMER RELATED APPLICATIONS OF WATERMELON SEED POWDER, A PRACTICAL SOURCE OF UREASE ENZYME

A Dissertation

Submitted to the Graduate Faculty of the
Louisiana State University and
Agricultural and Mechanical College
in partial fulfillment of the
requirements for the degree of
Doctor of Philosophy

in

The Department of Chemistry

by
Anthony Quan Quoc Mai
B.S., University of Louisiana at Lafayette, 2007
B.S., University of Louisiana at Lafayette, 2007
May 2021

To my loving husband and my encouraging family

My family has always pushed me to better myself, knowing my capabilities sometimes better than I do myself. I would not be in STEM if it not for my mom and dad's reinforcement of the sciences and mathematics. Of course, my brothers and I tinkered away at our house, much to the chagrin of my mom, doing every science competition possible. And last but surely not least, to Tyler, my better half of 10 years. I wouldn't be who I am today without you. Thank you for supporting me through it all, even when times got rough, or I procrastinate ad absurdum. I love you with all my heart--Lienny, Bobi, Nam, Bi, and Tyler.

ACKNOWLEDGEMENTS

I wish to thank and acknowledge *Meus Magister*, Dr. John Anthony Pojman. Your guidance and approach to all things made my journey at LSU most memorable. I never understood why people at my past profession said, “enjoy your grad years,” but I truly do now. I don’t think I could have been more compatible with any other mentor, scientifically and of course in demeanor. We’ve had similar upbringings and shared similar interests which made this experience only more gratifying.

Next I’d like to give my profound gratitude to my committee members, Dr. David Spivak and Dr. Donghui Zhang. In the class and in conversation, I have learned a tremendous amount of polymer chemistry from both of y’all and appreciate every interaction we’ve had. To my collaborators and other mentors, Dr. Ted Gauthier, Dr. Don Labonte, Dr. Jeff Beasley, Dr. Annette Taylor, Dr. Guido Panzarasa, Dr. Michael Vincent, Dr. Rafael Cueto, and Dr. Doug Gilman, I am grateful to have met, interacted, and worked with each of you.

Lastly to my fellow graduate students and undergrads, thank you for the support you all bring, it surely would have been boring without y’all. To Anowar, Daniel, Fahima, Brecklyn, Sam, Kylee, Dennel, Baylen, and Michael, I’ll always cherish all our memories together. To Douglas, Ethan, Tu, Amber, Terry, Clay, Jackie, Colton, Noah, and Dan, I couldn’t have done it without all your help.

Thanks to everyone for the wonderful journey together, onward to the next.

TABLE OF CONTENTS

LIST OF TABLES

LIST OF FIGURES

LIST OF ABBREVIATIONS

AA	Aconitic acid
BET	Brunauer, Emmet, and Teller
BJH	Barrett, Joyner, and Halenda
BuOH	Butanol
CLO	Campylobacter-like organism test
DI	Deionized
EDDT	2,2′-(Ethylenedioxy)diethanethiol
EGDMA	Ethylene glycol dimethacrylate
ELO	Epoxidized linseed oil
ETTMP	Ethoxylated trimethylolpropane tri(3-mercaptopropionate)
FTIR	Fourier-transform infrared
ATR	Attenuated total reflectance
GWMS	Ground watermelon seed
MW	Molecular weight
MWMS	Milled watermelon seeds
PE	Phenoxyethanol
PEDGE	Poly(ethylene glycol) diglycidyl ether
PEGDA	Poly(ethylene glycol) diacrylate
pHi	Initial pH
PSD	Particle size distribution
PV	Pore volume
PVOH	Polyvinyl alcohol

QS	Quorum sensing
RT	Room temperature
RUT	Rapid urease test
SA	Surface area
SEM	Scanning electron microscopy
SLS	Sodium lauryl sulfate
TMPTA	Trimethylolpropane triacrylate
TMPTGE	Trimethylolpropane triglycidyl ether
TMPTMP	Trimethylolpropane tris(3-mercaptopropionate)
TPO	Diphenyl(2,4,6-trimethylbenzoyl)phosphine oxide
UV	Ultraviolet
WMS	Watermelon seed
WMSP	Watermelon seed powder

ABSTRACT

Urease enzyme was crystallized almost a century ago, and to this day its intrinsic stability is not ideal for everyday applications. This work introduces a new process by which a naturally encapsulated material, watermelon seed powder (WMSP), is characterized for its stability and activity. WMSP enzymatic activity has been measured for over a year at various storage conditions—exposed to ambient atmosphere for a year, WMSP retained above 90% activity. In aqueous conditions, the enzyme maintained above 60% activity after two months; with the addition of a preservative that number stays at about 90%. There is a pH shift of the maximum activity at 8.1 pH in addition to a broadening of the activity curve allowing for a wider range of reactions.

In Chapter 3, immobilization techniques were employed on these powders, enhancing their usability and in turn presented some interesting dynamics. One of the techniques physically encapsulated the WMSP inside a porous resin, essentially creating a urea-ammonia exchange resin. These particles were subject to 10 cycles of urea hydrolysis, without any change in the urea-urease clock reaction. The agar immobilized WMSPs exhibited a behavior called quorum sensing. That is a biological communication process by which bacteria express certain genes when a “quorum” or sufficient number are in proximity of each other. With certain parameters, the particles will not clock individually, but when in a cluster of particles, the autocatalysis occurs. This property was then coupled with a hydrogel polymerization that gels in basic conditions. The WMSP particles in principle are biofilm generating analogues. Lastly, Chapter 4 presents an application of WMSP as a base generator for several adhesive formulations and outlines some potential future uses of WMSP.

CHAPTER 1. INTRODUCTION: UREASE ENZYME DISCOVERY AND APPLICATIONS

1.1. The 1946 Nobel Prize for the Crystallization of Urease

In 1926 James B. Sumner phoned his wife and said, “I have crystallized the first enzyme[1].” Like many scientists, he was eager to share a breakthrough or discovery he made in the laboratory. There, J. B. Sumner crystallized urease from jack bean seeds. He began studying urease from jack beans over a decade earlier. By using the jack bean[2] in a crushed meal-form he was testing the urea content in various bodily fluids and tissues.[1, 3] Using this crude product from a coffee grinder, he was able to catalyze the decomposition of urea into ammonia to be analyzed.

Professor Sumner, while working on the jack bean meal, noticed that there were variabilities in the activity of this plant-derived material. He had some batches of seeds which were rich in enzyme, and others when received showed much lower amounts. Lack of reproducibility and huge sample variability are typical problems encountered when working with natural materials. To circumvent this, he had a plant physiologist grow jack beans from a batch of seeds he knew had high activity. The corresponding seeds then in turn exhibited high enzyme amounts. This is one of the challenges when working with natural materials.

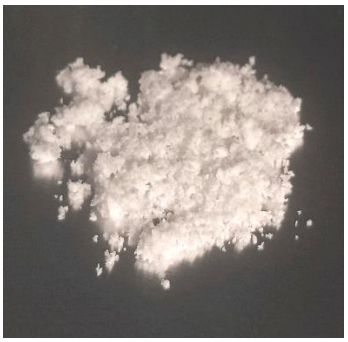

Figure 1.1. Lyophilized urease enzyme from jack bean seeds.

To standardize and overcome these variabilities, Sumner would have to determine if it were possible to extract or purify the enzyme. Using various combination of solvents from alcohol to acetone he was able to determine that using water and acetone in a certain ratio, a purified substance was precipitated.

The crystalline material had a very regular morphology to it. These particulates then of course had high purity, with recrystallization increasing the purity.[1] This laid the foundation for which Professor Sumner would go on to win the Nobel in 1946—the discovery that enzymes are in fact proteins. The urease enzyme has been further shown to be nickel-centered, with jack bean urease specifically having two nickel centers per active site.[4]

1.2. Urease in Plants

$$H_2NCONH_2 + H_2O \xrightarrow{\text{Urease}} 2NH_3 + CO_2$$

Figure 1.2. Hydrolysis of urea catalyzed by urease.

Urease plays an important role in a plant's metabolic cycle. Urease catalytically converts urea into ammonia and carbon dioxide, Fig. 1.2. This means that the plant can use urea internally or externally from uptake of urea, as urea is a common source of

nitrogen in fertilizer. Internally, urease is proposed to work in conjunction with the ornithine cycle and glutamine synthase to produce glutamine.[5-8]

Germination of many seedlings is highly impacted by imbibition of water. When plants were treated with urease inhibitors, germination was stunted for 36 hours and completely with aged seeds.[9]

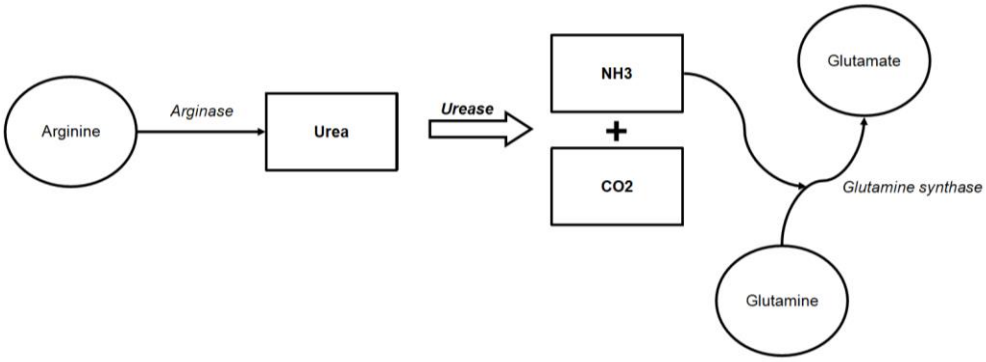

Figure 1.3. Proposed plant metabolism of urea.

Other legumes are also rich sources of urease enzyme. By following a similar process to the extraction of urease from jack beans, studies on garden pea (*Pisum sativum*)[10], pigeon pea (*Cajanus cajan*)[11], and even soybeans (*Glycine max*)[12] have been done. By using an aqueous mixture of acetone the investigators then characterize and can further purify the resulting enzyme.

1.3. Urease in Helicobacter pylori

Another notable source of urease is the bacteria *H. pylori* commonly found in the mucosal lining of the stomach. To survive the low pH environment, *Helicobacter pylori* not only is chemotactic in that it seeks areas of more favorable pH but it also secretes urease enzyme to increase its surrounding pH.[13, 14]

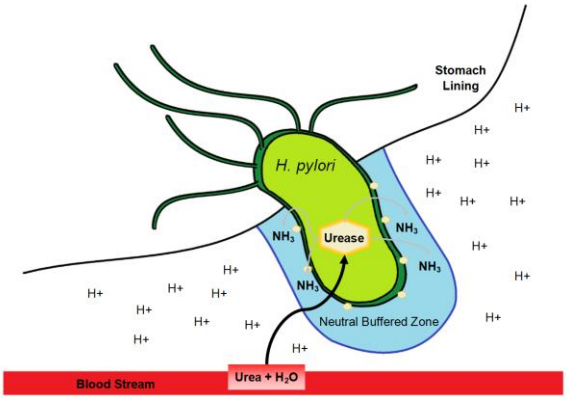

Figure 1.4. Helicobacter pylori diagram of urease stabilizing the surrounding pH in the stomach lining.

In the steps leading to gastritis and peptic ulcers, the bacteria must burrow into the lining of the stomach. To establish a colony and grow, the bacteria produce urease enzyme. Researchers at Boston University, Harvard Medical School, and MIT discovered that not only does the urease enzyme allow for colonization but it also increase the motility of the bacteria.[15] By measuring the viscoelasticity of the mucin at high and low pH and observing the bacteria in mucin within those conditions, they saw at 4 pH the flagella move but no movement of the head, whereas at 6 pH the mucin was much thinner allowing for the bacteria to freely traverse its surroundings.

Using this behavior that *H. pylori* secretes urease enzyme into the surrounding mucosa, there are several diagnostic tests to detect the enzyme, which in turn indicates infection with *H. pylori.*[16] Two notable tests that use the hydrolysis of urea are the rapid urease test, known as the Campylobacter-like organism test (CLO), and the urea breath test. In the rapid urease test, a biopsy of the stomach mucosa is taken to be analyzed. The tissue sample is then placed on a testing kit that contains urea and a pH indicator, i.e., phenol red, that changes color with the production of base. This qualitative test works due the secreted enzyme in the mucosa hydrolyzing the urea in the test. One

potential issue is that if the sample were slightly basic, then the test would show a false positive for infection. To mitigate this, samples can be acidified prior to analysis.[17]

Figure 1.5. CLO test and Hp fast test, both with pH indicators that detect an increase in pH from the hydrolysis of urea with a tissue sample containing urease enzyme.[18]

The other common diagnostic test is the breath test in which a sample of ^{13}C or ^{14}C marked urea is orally given to the patient. Prior to ingesting the urea, the patient blows into a sample bag as a breath control to be analyzed. With the marked urea in your system and if *H. pylori* were present and had secreted urease, the hydrolysis would occur producing ammonia and carbon dioxide. This carbon dioxide is now either $^{13}CO_2$ or $^{14}CO_2$, and then is captured in the next breath sample. Both bags of the patient's breaths would then be analyzed on a mass spectrometer—first the control breath sample would be a baseline and then the post-urea-ingestion breath would show the isotopic carbon dioxide presence. This is a non-invasive and relatively fast method to diagnose infection with *H. pylori*. [17, 18]

CHAPTER 2. WATERMELON SEEDS AND UREASE ENZYME

2.1. Introduction

The specific origin of the watermelon is up for debate[19-21], but it is generally accepted that the fruit originated in Africa and was then spread through the Mediterranean and surrounding areas. From the ancient Egyptians, the fruit has been found in old burial tombs as old as 4,000 years ago including King Tut's tomb.[21] It is theorized that the Egyptians used the fruit as a source of water, as the watermelon back then was not the sweet fruit we know today.

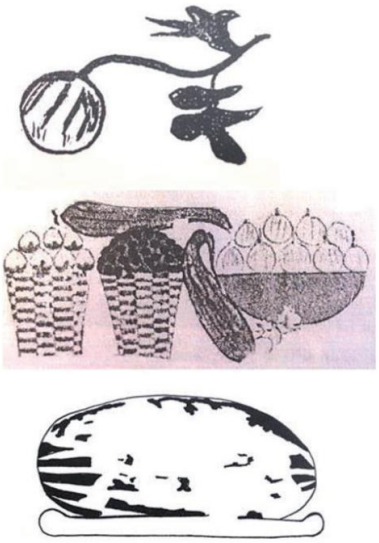

Figure 2.1. Images of watermelons seen in Egyptian tombs, with the first two images detailing the wild spherical type. The elongated kind in the third image most likely is a cultivated version.[20]

In ancient Greece, Hippocrates in 400 BCE wrote in *Regimen* of the *pepon*, a sun-ripened fruit. Dioscorides in 70 CE wrote about the *pepon* having a rind that can be placed on a child's head to cool the child down. This practice is done even to today for amusement purposes. Galen wrote in *On the Properties of Foods* about the *pepon* being cold and wet. During the Roman Empire, Pliny the Elder wrote about the *pepo* as

a “refrigerant mixime” in book 20 of his *Historia Naturalis*. The Roman Emperor Diocletian even mentions the *pepones* in his edict on maximum prices, *De Pretiis Rerum Venalium.*[20]

As people throughout the region began the breed these plants, it was desired to cultivate a sweeter plant. The change from white fleshed to yellow then to our familiar red is attributed to selective breeding for the sweet variants. In the 14th century, an illuminated manuscript, *Tacuinum Sanitatis*, first depicts the red watermelon we know today[22], Figure 2.2.

Figure 2.2. Watermelons drawn in an illuminated manuscript with the familiar red flesh, A) Vienna 2644 folio 21r, B) Paris 9333 folio 18r.[22]

With the fruit being made sweeter with each iteration, particular attention and care must have been shown to the seeds. Different cultures today eat the seeds, similar to roasted pumpkin seeds, which may be more familiar.

In these seeds are the biological blueprint for the plant that has spanned over 5,000 years of our world's history. Many nutrients, DNA, proteins, and enzymes are contained in each seed. One enzyme that is of particular interest is urease. Besides the previously mentioned legumes, watermelon seeds are a source of an abundance of urease. With this in mind, much research has been done on the extraction[23-27] and utilization[28-31] of this enzyme.[32-35]

2.2. Watermelon Seed Powder (WMSP)

The urease enzyme in watermelon seeds (WMS) can be utilized in many different applications that require a change in pH, specifically basic conditions as ammonia is produced (see Figure 1.2). These examples will be presented subsequently. In order to utilize the urease enzyme in watermelon seeds, an extraction or exposure of the enzyme must be done. Initial use of the WMS was through hand-grinding by mortar and pestle. Though this worked to expose the enzyme to aqueous urea, the variation and effort required to produce ground watermelon seed (GWMS) was intensive. To facilitate reproducibility of samples, a coffee grinder was used to grind batches of seeds. The resulting GWMS was more easily produced; however, homogeneity was still an issue.

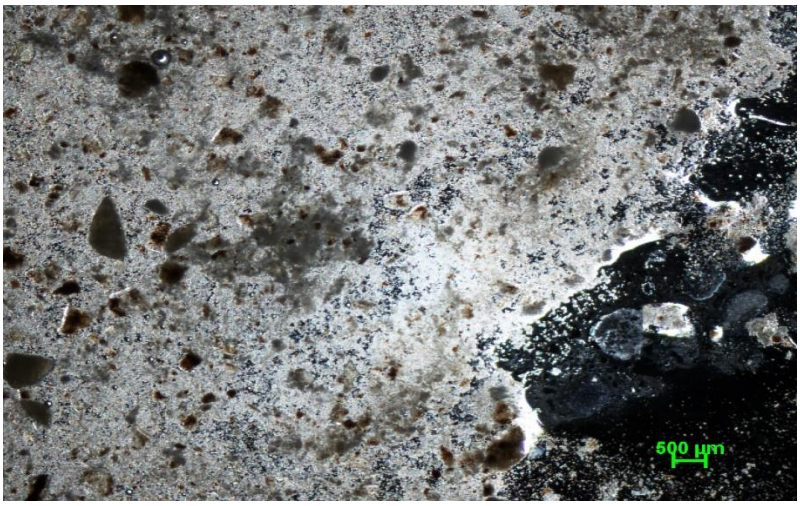

Figure 2.3. Ground watermelon seeds from coffee grinder, with heterogeneous husks seen in image produced from light microscopy 5X.

The GWMS from the coffee grinder seen in Figure 2.3 showed large pieces of the seed husk still present in the mixture. This becomes problematic when trying to disperse the GWMS in a media or solution. Buoyancy of the heterogeneous components are all different, thus some pieces float, some sink, and some remain buoyant.

To further increase the homogeneity of the sample, a flour mill that grinds at 25,000 rpm was purchased to mill the WMS into a fine powder, husks included. Since the milling was quite vigorous, the shear friction from the process generated heat. This then limited the milling process to 1-2 minutes of milling as to not overheat and preserve the enzyme's integrity. Freezing the seeds or subjecting them to liquid nitrogen does allow for 1-2 more minutes of milling as the temperature starts off lower, but this was shown to not be necessary. The milled watermelon seeds (MWMS), were much more homogenous and smaller in particle size, as expected.

Figure 2.4. MWMS (left), watermelon seeds milled with flour mill at 25k rpm and WMSP (right), watermelon seed powder extracted from MWMS with acetone sedimentation and filtration.

From this step, it was noticed that the milled seeds are quite clumpy, almost like a wet-cake material. Since Sumner managed to crystallize urease enzyme from acetone, this then indicates that the enzyme is insoluble or slightly soluble in acetone. This also means that it is possible to use acetone as a drying agent for the MWMS without unwanted extraction of the urease enzyme from the seeds. Using a minimum ratio of 2 to 1 by volume acetone to ground watermelon seeds, the mixture was left stirring overnight to fully extract the water. Upon observation of the acetone seed mixture the following day, a suspended layer was seen above the seed husks, which easily settle when agitation is stopped.

The acetone seed mixture was then passed through a 120-mesh screen (aperture 125 microns) to remove the husks. The resulting turbid solution then was then filtered through a Büchner funnel with a Whatman® #1 filter with an aperture size of 11 microns. Initially when building the wet-cake on the Büchner funnel, some material will be loss due to the particle size being smaller than the filter paper's pore size. This filtrate was then re-filtered through the cake-layered filter paper to recover all solids. The

acetone that passed through is yellow in color most likely due to other extractives, such as lipids. This acetone step in an actual enzyme extraction is called a de-fattening step.

The acetone attained after filtration was high in seed oil and was a transparent yellow in color. By evaporating the acetone in successive steps, it was possible to concentrate the oil to be analyzed. This seed oil was then tested on a Bruker Tensor 27 FTIR spectrometer equipped with an ATR MIRacle™ diamond attachment. 32 scans were performed from 4000 to 650 cm^{-1} with a resolution of 4 cm^{-1}. Using the peaks attained from the scans, comparing to an FTIR database showed a high match for castor oil[27, 36], see Figure 2.5. Castor oil is primarily comprised of a triglyceride of ricinoleic acid[37] and some oleic and linoleic acid components. It is also pressed from castor beans. Though the peaks are not a perfect match, they share many of the strong bands indicating that the WMS oil is most likely a mixture of triglycerides of fatty acids as well.

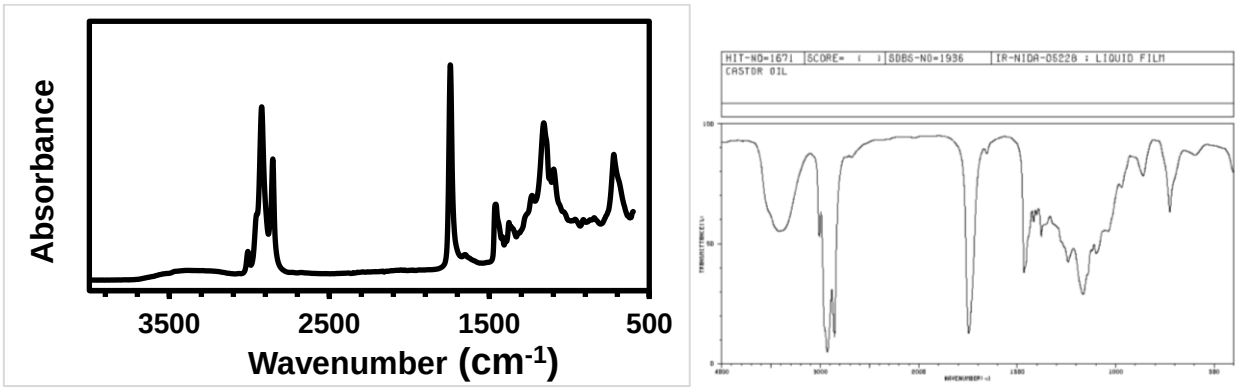

Figure 2.5. FTIR ATR scan (left) of oil from acetone de-fattening of watermelon seeds, (right) FTIR scan of liquid film of castor oil standard copied from AIST.[36]

Once the acetone passed through and the wet-cake was drying out, a secondary wash of clean acetone is recommended to wash any remaining oils left in the sample. If the

filter paper wet-cake is too thick, acetone may not easily pass through and a second filter paper filtration may be required for any remaining acetone and seed solution.

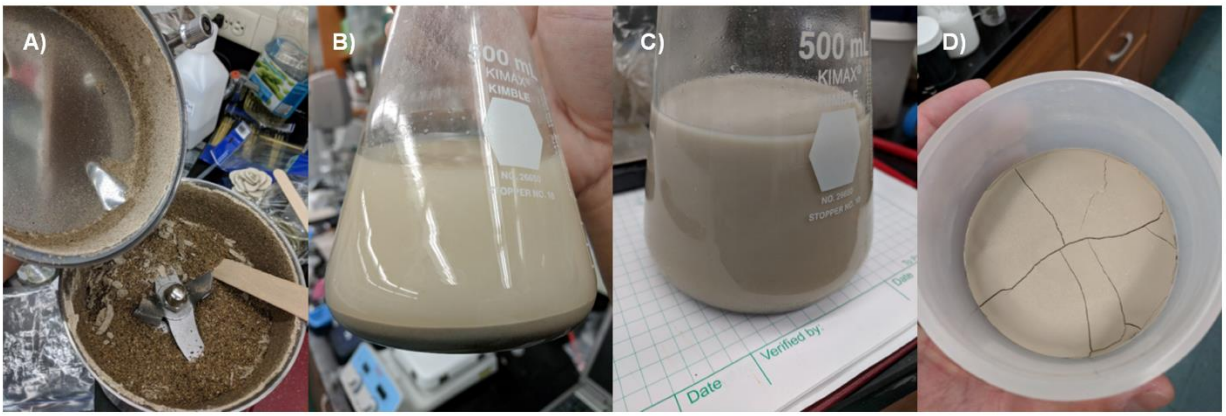

Figure 2.6. Milling, extraction, and filtration steps for producing WMSP: A) milling of WMS with flour mill, B) acetone addition to milled WMS, C) 120 mesh filtrate after overnight stirring of MWMS in acetone, D) wet-cake from Buchner funnel filtration

After the clean acetone wash was done, the tan-colored wet-cake material can be vacuum oven dried for expedience or allowed to dry overnight in the hood. The material will become lighter in color as it dries from a dark brown to a light tan powder. This powder is watermelon seed powder (WMSP) and will be shown to have high amounts of protein content, namely urease enzyme.

2.3. Characterization of the Watermelon Seed Powder

2.3.1. Morphology and Physical Properties

The fluffy tan powder has a bulk density of 0.21 g/cc measured by a 10 mL graduated cylinder with funnel. With every batch made the yield hovered around 25% ± 2% by weight of seeds used. Under light microscopy using a Nikon Eclipse 50i microscope with a Nikon DS-Fi1 camera attachment, this powder has a regular shape that can be dispersed in aqueous or organic systems with little aggregation. Initially it was hypothesized that the particles were formed from the milling process; however,

observation of the highly regular particles leaves doubt to the 25,000 rpm milling's efficiency to make such particles in such a short time of 1-2 minutes.

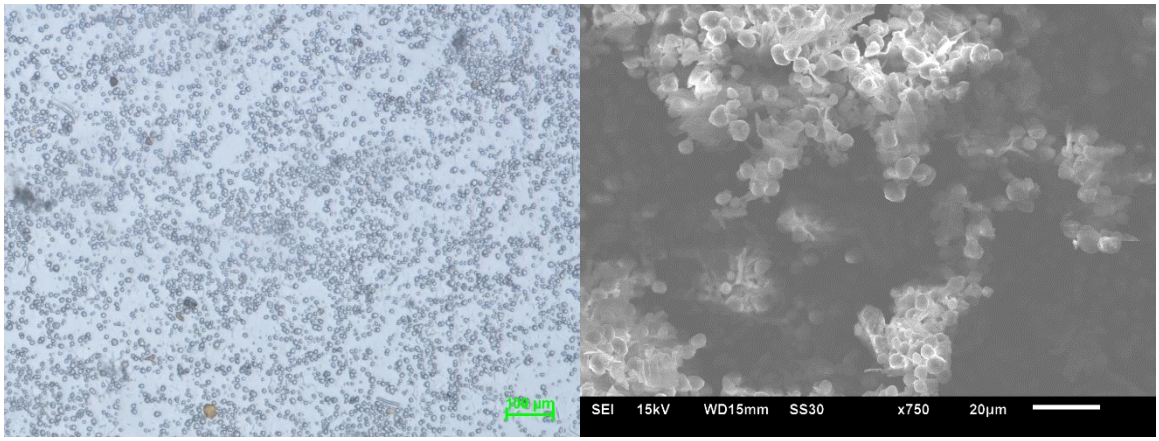

Figure 2.7. Light microscopy 20X (left) and secondary SEM 750X images of the watermelon seed particles, WMSP

To substantiate the claim of these particles being inherent to watermelon seeds, it would have to be seen in the seeds prior to any processing. Using SEM one can see morphological surface textures that could indicate the presence of these particles. The Shared Instrument Facility, SIF, at LSU has a JEOL JSM-6610LV that can view up to 75,000X to easily see the seeds and their structures. Sample preparation for the seeds included submersion in liquid nitrogen to freeze them. This allowed for a clean cross section both laterally along the seed and across the seed's midsection. The sectioned seeds were then placed on SEM aluminum stubs and platinum coated for two coating reps of 4 minutes for a nominal coating of 5 nm each.

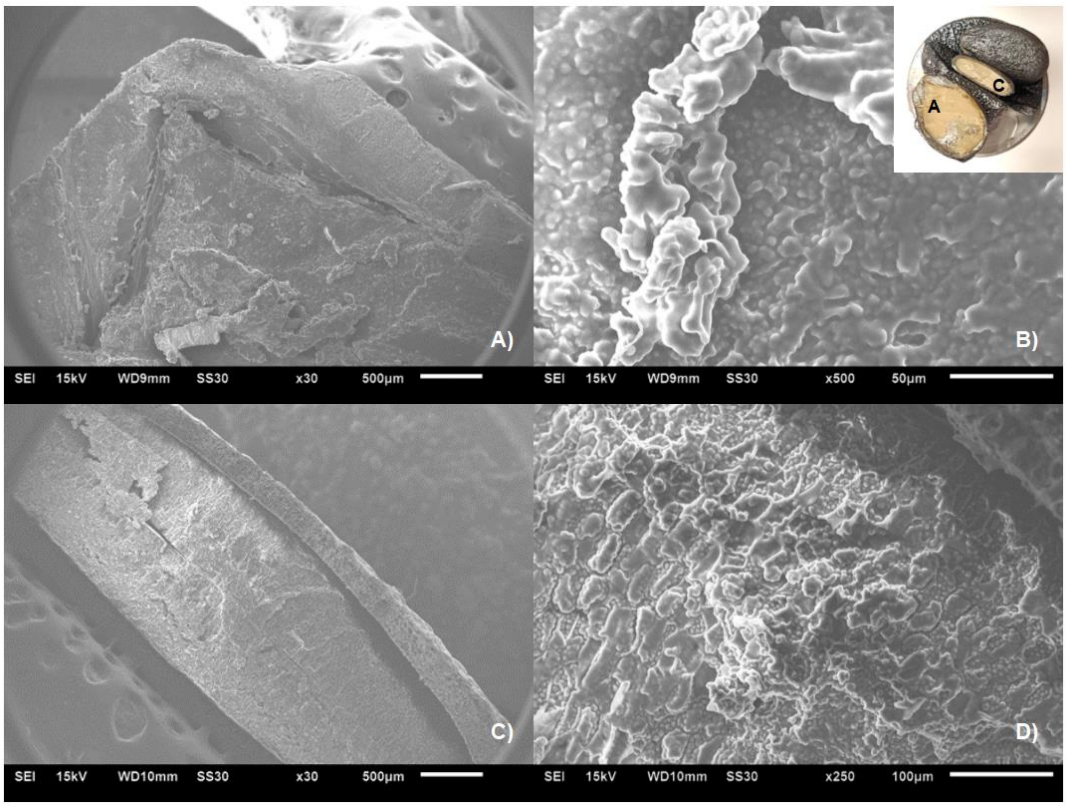

Figure 2.8. Secondary SEM imaging of cross sections of WMS: A & B) lateral cross section of WMS and zoomed-in image showing small structures, C & D) mid-cross section of the WMS also showing small structures, inset shows the seeds prior to platinum coating

Through secondary electron imaging, both cross sections revealed microstructures in the seed cotyledon part of the WMS. This then confirms that the WMSPs were present in the watermelon seeds prior to any processing. Using Sudan red, an indicator that dyes lipids and proteins, the WMSPs were able to be stained red meaning some lipid content is present still in the powder. They were not able to be stained with an iodine solution, 5% iodine in 10% potassium iodide aqueous solution, meaning no starch content.

One possible conjecture is that these particles are some organelle or plant cellular structure. Previous histological work on seeds[30, 38-41] mention “protein body” or “protein globules.” These structures are high in protein content, and this further points to the

location of high urease enzyme. Wang et al. show an image detailing protein bodies in watermelon seeds, Figure 2.8. They are both abundant and in the size range of the watermelon seed powder.

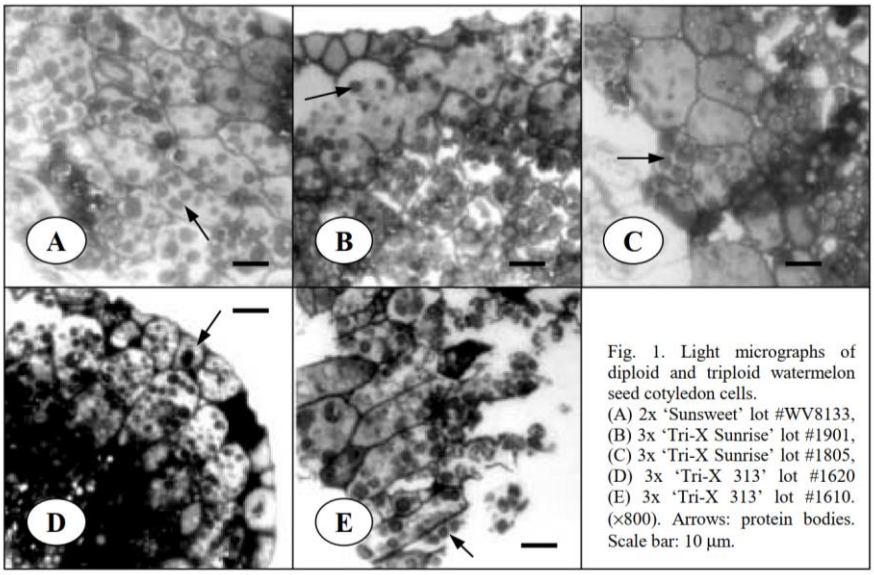

Figure 2.9. Watermelon seed cotyledon cells showing protein bodies as dark spheres.[39]

To determine the size distribution of WMSPs, the powder was measured on a Coulter LS200 laser diffraction particle size analyzer. The sample was first dispersed in deionized water, and then sonicated for 15 minutes to de-aggregate any clumps. The mean particle diameter was 4.8 microns, with a mode particle of 5.4 microns. The standard deviation was 3.6 microns due to the large distribution from some aggregates and fines (Figure 2.9). Scans were measured for 60 seconds with an obscuration of the laser at 15%. The obscuration is a measure of sample loading into the cell.

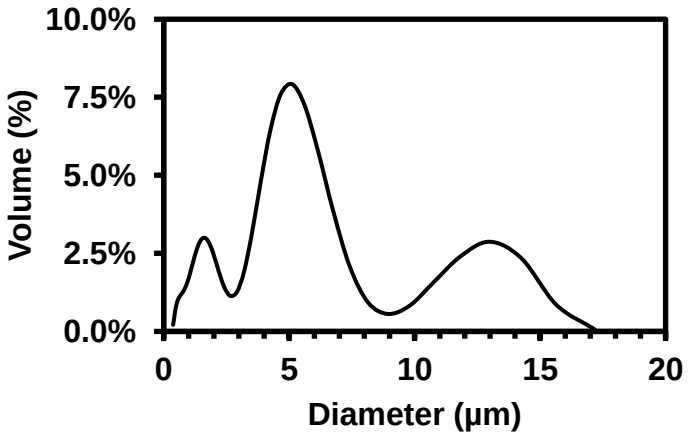

Figure 2.10. Particle size distribution via laser diffraction of watermelon seed powder dispersed in deionized water.

2.3.2. Varieties of Watermelons

The entirety of this study was performed on the crimson sweet variety watermelon seed purchased from Eden Brothers® Vista Horticultural Group. However, to expand the assertion that these watermelon seed powder particles are indeed protein bodies, they should be omnipresent in watermelons regardless of variety. Also, from a materials standpoint, it is beneficial to have multiple sources of a raw material. Three additional varieties of watermelon seeds were purchased—jubilee improved, tendersweet orange, and black diamond yellow belly. The WMSP percentage weight extraction for the crimson sweet variety was around 25% the weight of seeds. The corresponding weight percentage yields for the other varieties are as follows: jubilee improved 30.2%, tendersweet orange 22.8%, and black diamond yellow belly 23.3%. Examining the cross sections of these seeds showed similar results to the crimson sweet variety—that the WMSPs are ubiquitous through the cotyledons of the seeds.

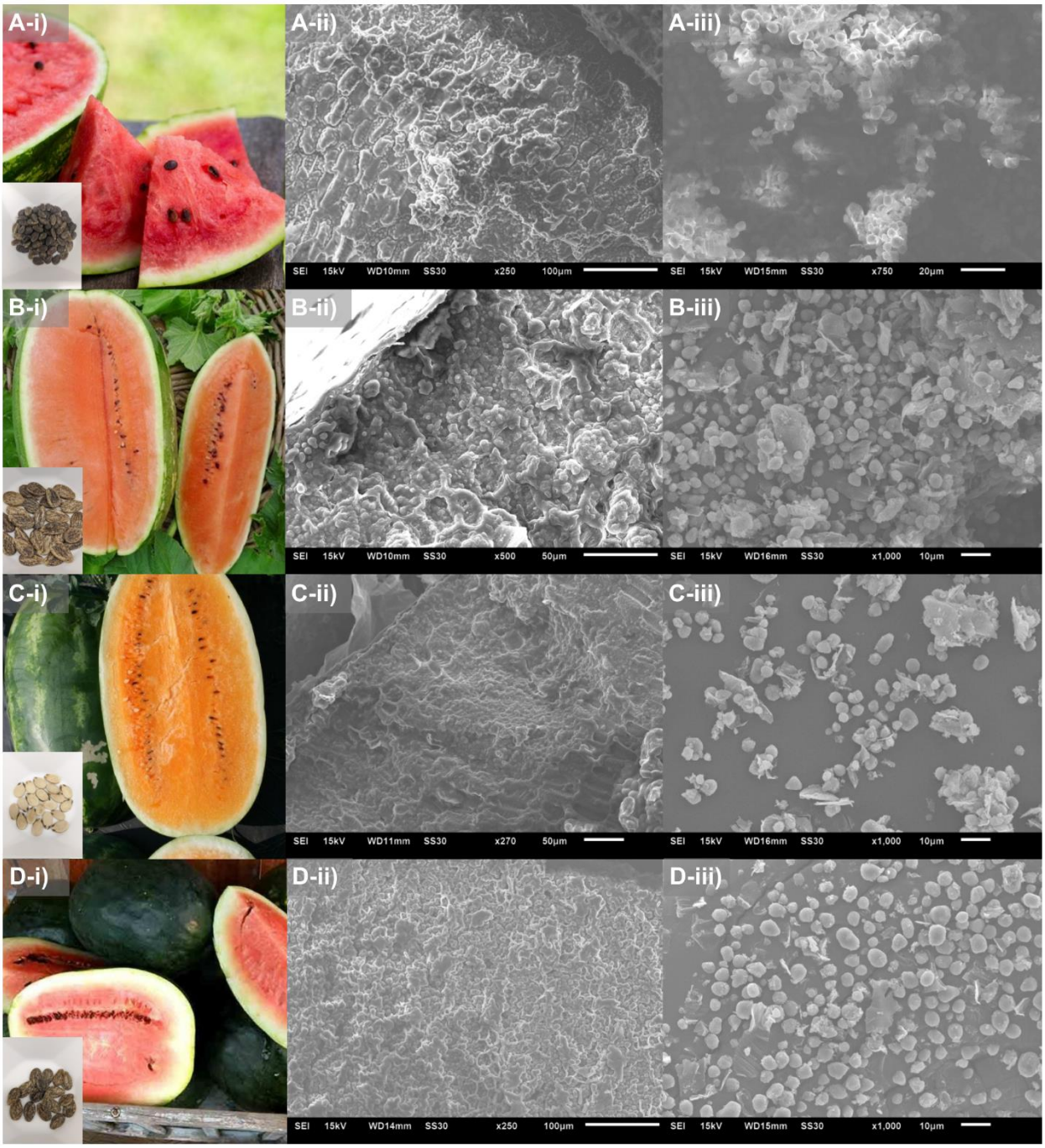

Figure 2.11. Watermelons[42], their seeds, and SEM images of the cross sectioned cotyledons: A i-iii) crimson sweet, B i-iii) jubilee improved, C i-iii) tendersweet orange, and D i-iii) black diamond yellow belly.

2.3.3. Nessler's Reagent Assay

The urease enzyme in watermelon seeds activity is usually measured in units per gram of solid powder. This unit is defined as the amount of enzyme able to liberate 1 µmole of NH_3 from urea per minute at pH 7.0 at 25 °C. To determine this metric, an accurate measure of ammonia production per given time is to be done. One analytical method is a colorimetric assay using Nessler's reagent. Nessler's reagent is a solution comprising of an alkaline solution of potassium tetraiodiomercurate(II), $K_2[HgI_4]$. The reagent was made by adding 10 g of potassium iodide in water and adding a solution of saturated (60 g/L) mercury(II) chloride slowly. When a precipitate is formed, 80 mL of 9M potassium hydroxide was added, then diluted to 200 mL. Using sodium hydroxide is also possible by first creating a 100 mL solution of 23 g of mercury(II) iodide and 16 g of potassium iodide in water, and to that, add 100 mL of 6M sodium hydroxide. Both reagents should be allowed to combine overnight in the dark.[43] The detection of ammonia is around 0.3 µg NH3 in 2 µL of solution forming a yellow to brown precipitate.[44]

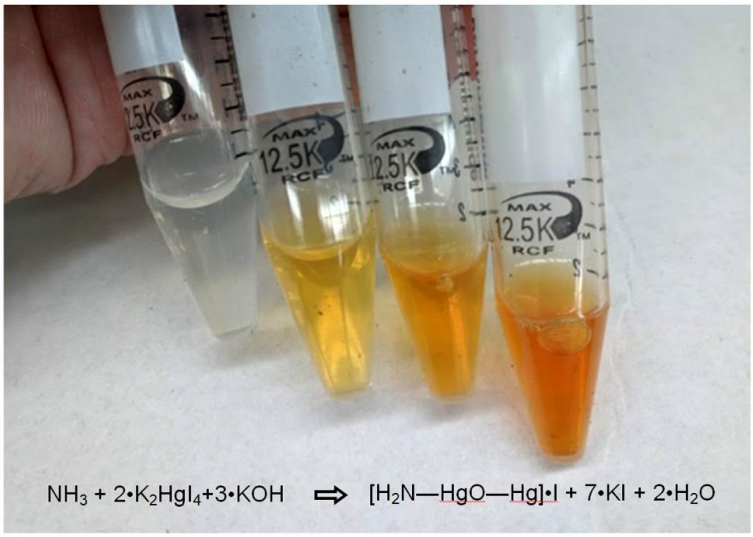

Figure 2.12. Solutions of Nessler's reagent and vials of increase ammonia content from left to right.

The precipitate that forms, an iodide form of Millon's base, was yellow to brown in color depending on the concentration of ammonia in solution. Using this color gradient, it is possible to make a calibration curve of varying ammonia amounts. The use of ammonium sulfate is preferable to weigh out accurate amounts; prior to use, the ammonium sulfate was dried in the vacuum oven at 30 °C in 30 inHg. A stock solution of 1.322 g of ammonium sulfate was dissolved in 100 mL of ammonia free water. This gave an ammonia concentration of 3.41 mg/mL.

The Nessler's assay procedure starts with 2 mL of aqueous solution to be analyzed. (If using dry powder, combine with 2 mL of ammonia free water.) A standard 0.2 M solution of phosphate buffer at 7.0 pH is made from the combination of phosphate monobasic and dibasic salts. 7.744 g of phosphate dibasic heptahydrate is combined with 2.914 g of phosphate monobasic hydrate then filled to 250 mL with deionized water.[45] This buffer solution should be sonicated or stirred until complete dissolution

occurs. Utilizing this buffer solution, a fresh daily solution of 3% by weight of urea is made to be used in the assay.

Prior to spiking the sample to be analyzed with the urea in buffer solution, a 2.0 M solution of sulfuric acid is to be prepared. The concentrated sulfuric acid used had a purity of 96.3% with a density of 1.83 g/mL. Using these specifications, 20.4 g concentrated sulfuric was added to 88.9 g of deionized water (2.0 M). The use of acid in the assay is to crash the pH of the solution low enough to halt the enzyme from hydrolyzing urea. With the creation of these solutions, each 2 mL sample is then spiked with 200 µL of 3% urea in 2 M phosphate buffer. The sample is then left to produce ammonia for 5 minutes with intermittent vortex mixing. After the 5-minute interval is up, 200 µL of 2 M sulfuric acid is added to the reacted vial. Now the sample is ready to be combined with the Nessler's reagent to be analyzed on the spectrophotometer. To a larger vial with 4.3 mL of water, 500 µL of Nessler's reagent is added. 200 µL of the urea-urease-sulfuric acid reacted sample is added to this larger vial. Upon combining the solutions, the characteristic yellow-brown precipitate should be observed. If it is not, then the assay was a false negative or there was no ammonia produced. Samples are to be tested within the same day, with vortex mixing prior to analysis on the spectrometer to redisperse the precipitate. Absorbance at 420 nm is then recorded for each assay.

For the calibration curve, a set of dilutions of the stock ammonium sulfate solution that was made previously will be used for each point. Each vial must contain only 2 mL of solution to be analyzed, e.g., that means if a spike of the stock solution is 200 µL then 1.8 mL of deionized water is to be added. Refer to Figure A.1 for the

calibration curve obtained from the Nessler's reagent assay. Even though the ammonia was already present in the system, addition of the 200 µL 3% urea in buffer solution and 200 µL of 2 M sulfuric should still be done to maintain the proper concentrations. These can be done without the needed 5-minute timing since no reaction is taking place. In the same regard, the samples then are added to the larger vials with deionized water and Nessler's reagent. The absorbance at 420 nm is recorded for each calibration point. Using Beer's law, a linear regression relating absorbance to the concentration or in this case ammonia produced is plotted. This calibration curve will then be used to analyze absorbances of unknown analytes to determine their ammonia production and in turn the enzyme activity of the unknown.

2.3.4. WMSP Urease Activity Assay

Through various trial and error tests with the watermelon seed powder, since the activity was unknown, it was determined that a sample size of 5 – 10 mg of WMSP was more than sufficient to fall within the calibration curve using the method detailed above. Once the amount of ammonia produced is known, a normalization by the sample weight is used to yield an activity with the units of mg NH_3 / g WMSP / 5 minutes reaction time. This can in turn be converted to the conventional unit / g or µmole NH3 / g WMSP / minute. For ease of comparison, the mg NH_3 / g WMSP unit will be used to show activity.

The specific location of the urease enzyme is hypothesized to be in the protein bodies, that is, the watermelon seed powder. Three samples were assayed to determine the location of the enzyme and to see if the addition of an aqueous washing of the WMSPs would result in loss of activity. The husks versus WMSP samples when

assayed showed a significant difference in activity, which is expected. WMSPs had 60X more activity than the little to no activity of the husks.

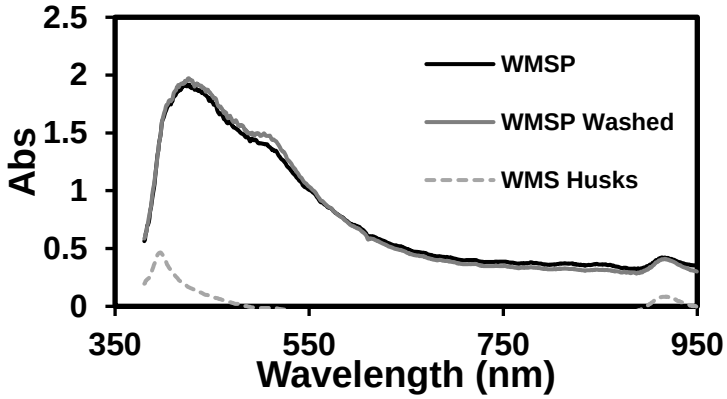

Figure 2.13. Plot given from Vernier Spectrometer of watermelon seed powder, its washed counterpart, and the husks after screening.

The washed seeds were prepared with two 200 mL aqueous washes done when the WMSPs were being filtered on the Büchner funnel.

To further study this behavior of potential free enzyme, several leeching studies were carried out on two older batches of seeds and several new batches with filtration through a syringe filter. 0.5 g WMSP was added to 30 g of deionized water and stirred overnight. The solution was filtered through 0.45 µm PTFE syringe filters, and a 200 µL spike of this filtrate was assayed. Three different watermelon seed powder batches (091518, 020619, and 052119) had less than 0.33% activity versus their corresponding WMSP. One subsequent WMSP batch that was sent to a colleague in Switzerland did show activity in the filtrate. 0.5 g of WMSP was added to 15 g of deionized water, one assay was performed on the filtrate after 1 hour of magnetic bar stirring and one assay was performed on the filtrate after 1 week of intermittent stirring with storage in 5 °C

conditions. The aqueous filtrates of these samples were prepared with first syringe filtration through a 0.45 µm PTFE filter then a 0.2 µm PTFE filter.

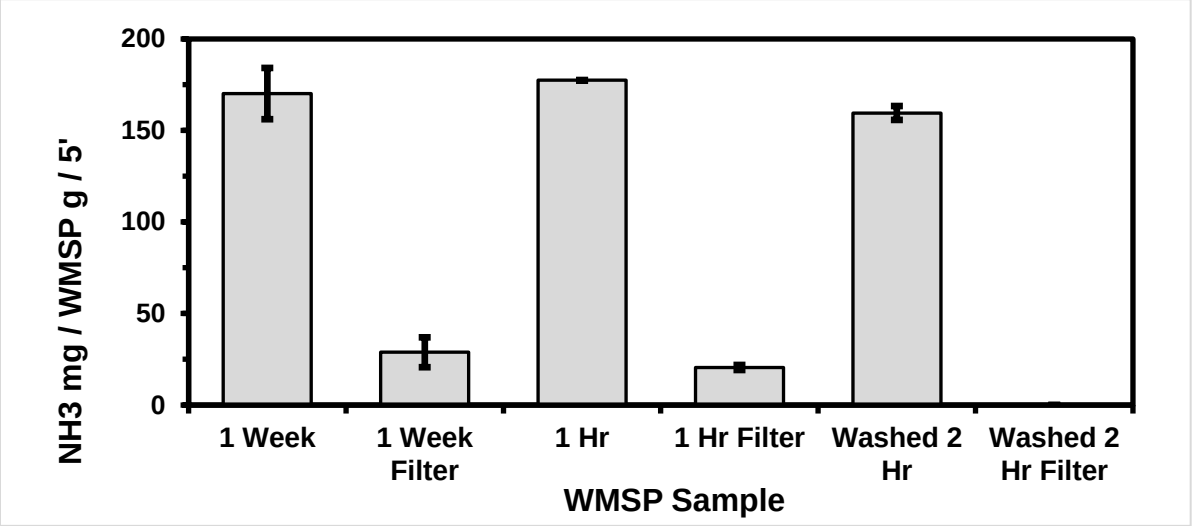

Figure 2.14. Leeching study performed on WMSP showing activities of an aqueous dispersion of powder and its corresponding aqueous filtrate.

This batch was the largest batch of extracted WMSPs made so far at ~400 g of watermelon seeds. There was extended acetone mixing time as well as longer milling time required to attain the desired MWMS size. This most likely contributed to some damaged particles or the WMSPs having more free enzyme on the powder surface than previous batches. Between the filtrate of the 1-hour extraction and the 1 week extraction, if there were leeching involved there should be a wider margin of as the enzyme concentration in the aqueous phase should have increased. To confirm this, 10 g of the same batch of WMSP was soaked in 100 mL of deionized water for 1 day then Büchner funnel filtered followed with 2 subsequent washes of 200 mL of acetone to facilitate even drying. The same process was repeated with 1 g of this washed powder being added to 15 g deionized water and stirred for 2 hours then syringe filtered following the same regimen.

The last two bars in Figure 2.14 detail the assay attained from this wash testing. Since removal of potentially free or surface-bound enzyme, the assay in turn was a little bit lower by about 10%. This, though, is additive with the removal of the 11% free enzyme measured in the previous two samples. In addition, the washed sample was also soaked in deionized water, the filtrate then showed no activity as no leeching had occurred. Additionally, samples of watermelon seed were frozen in a -15 °C freezer and some with liquid nitrogen. These samples were then subjected to the same protocol to extract WMSP, and the assays for these samples showed no difference between those sample which were milled at ambient temperature.

2.3.5. Assay on Varieties of Watermelon Seed Powder

From the WMSP extraction performed on the three additional varieties of watermelons, the same assay using Nessler's reagent can be performed. Since morphologically they do not significantly differ, it was to be seen if each of the powder's urease enzyme content was also similar. Each variety was run in triplicate with 5 – 10 mg of WMSP in each sample tested.

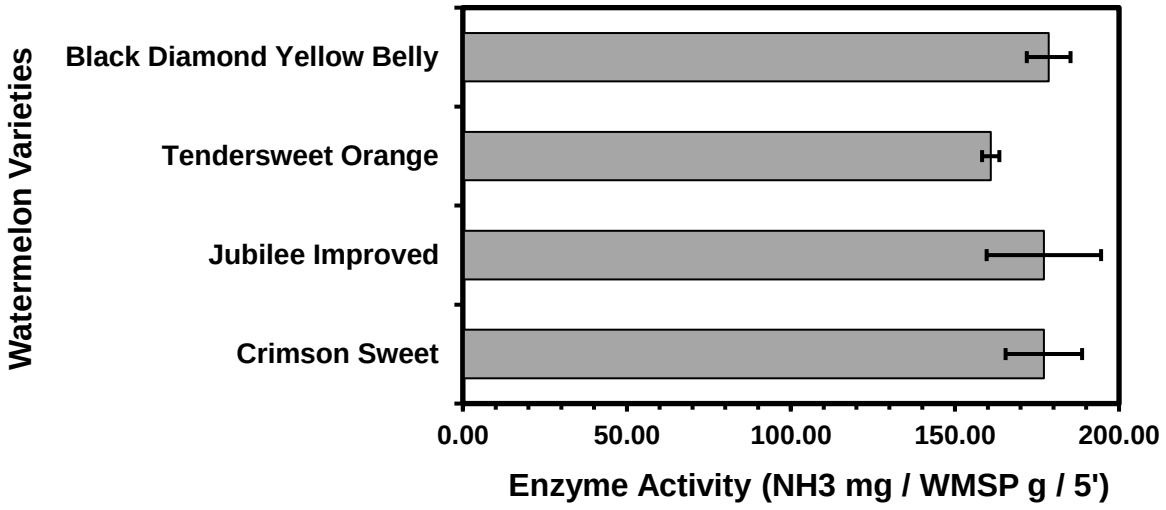

Figure 2.15. Urease activity of different varieties of watermelons.

The tendersweet orange's assay was slightly lower than the rest, and it can be noted that its seed coloration was starkly contrasting being completely off white, where three other varieties were dark brown. Nevertheless, the assays in turn resulted in activities for each of the watermelon seed varieties ranging in close values of 2 – 8% of each other, tendersweet included. With the WMSP yields between varieties being similar and the urease activity also being comparable, crimson sweet seeds may be substituted with any of the three other kinds.

2.3.6. pH and Temperature Dependence of Urease in WMSP

Works focusing on extracted urease enzyme[23, 24, 46-49] often quantify the pH dependence of the enzyme activity. This gives an activity curve of the enzyme and its dependence on pH. Pure urease enzyme generally has a maximum activity at around 7 – 7.5 pH.

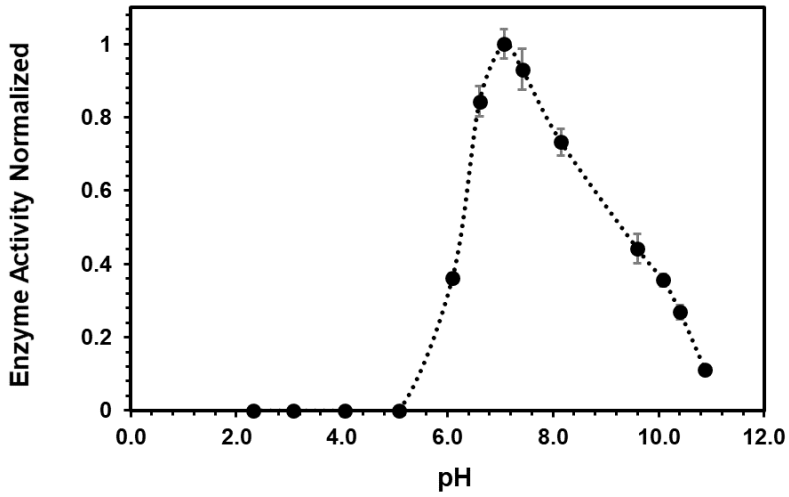

Figure 2.16. pH dependence of urease from jack beans.

The reason for the autocatalytic property of the urea-urease reaction is due to this characteristic bell-shaped activity curve—starting at low pH, the hydrolysis of urea produces ammonia that raises the pH, which in turn increases the activity of the enzyme. This curve also means that the enzyme is self-regulating, in that the activity reaches a maximum activity then begins to slow down as the surrounding pH is getting more basic.

The enzyme's activity is also temperature dependent. Though the standard urease unit is measured at 25 °C, this is not necessarily its maximum activity.

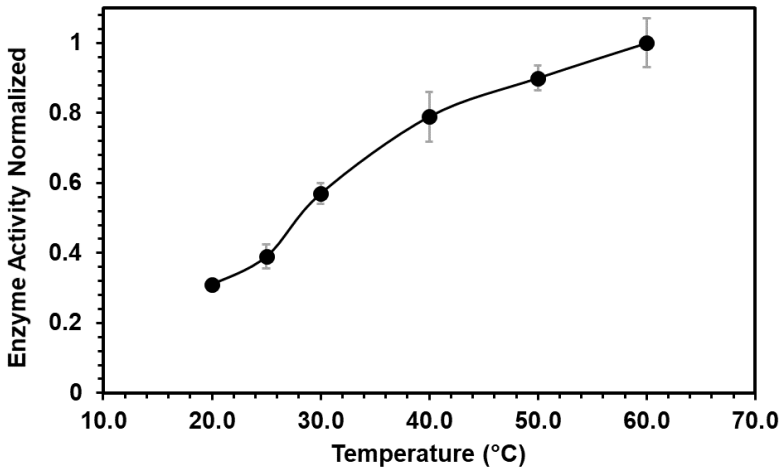

Figure 2.17. Enzyme activity temperature dependence profile of urease enzyme from jack beans.

Since the urease enzyme in watermelon seed powder is naturally encapsulated, it expected to see different pH and temperature dependence profiles. First, several buffer solutions of different pH must be created. For the range of 2 – 8 pH units, the McIlvaine (or citrate-phosphate) buffer was chosen. This requires different volumes of a standard dibasic phosphate solution and citric acid solution. To a 100 mL volumetric flask, 5.368 g of dibasic phosphate heptahydrate was added then filled to volume with deionized water (0.2 M). For the citric acid solution, 1.922 g of anhydrous citric acid was added to a 100 mL volumetric flask and filled to volume with deionized water (0.1 M). For the buffer range of 9 – 11 pH, a mixture of sodium bicarbonate and sodium hydroxide solutions were made. 0.424 g of sodium bicarbonate was added to a 100 mL volumetric flask and filled to volume with deionized water (0.05 M). Likewise, 0.397 g of sodium hydroxide was added to a 100 mL volumetric flask then filled to volume (0.1 M). Each buffer mixture was then tested on a VWR-sympHony™ pH meter with 4.0, 7.0, and 10.0 pH calibrations performed the day of testing.

Table 1. Buffers for pH dependence activity curve, ranges 2-8 pH were made with phosphate and citric acid buffers, 9-11 pH buffers were made with bicarbonate and sodium hydroxide solutions.

Buffer Name	**0.2 M Phosphate (g)**	**0.1 M Citric (g)**	**pH**
b1	0.41	19.61	2.320
b2	4.12	15.91	3.083
b3	7.74	12.32	4.062
b4	10.30	9.73	5.077
b5	12.64	7.38	6.096
b5.5	14.56	5.98	6.610
b6	16.48	3.58	7.071
b6.5	17.97	2.08	7.418
b7	19.47	0.57	8.150
Buffer Name	**0.05 M Bicarbonate (g)**	**0.1 M Hydroxide (g)**	**pH**
b8	18.18	1.85	9.599
b8.5	16.80	3.25	10.088
b9	15.38	4.64	10.403
b9.5	14.54	5.45	10.882
b10	13.75	6.29	11.126

With the creation of these buffers, assays of watermelon seed powder and standard jack bean urease were carried out in these solutions instead of the 2 mL solution of deionized water.

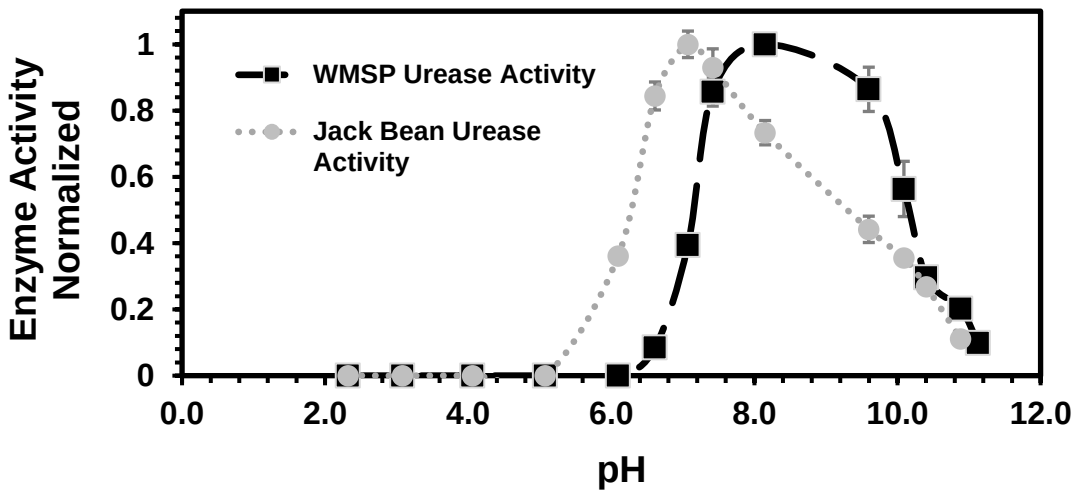

Figure 2.18. WMSP and jack bean pure urease activity curve.

The standard jack bean urease assays show corresponding values to that of the commercial activity curve. The activity curve for the WMSP shows a 1 pH unit shift to a maximum activity at around pH 8. The whole bell-shaped curve is slightly broader as well, possibly due to the diffusion of urea and ammonia across the natural WMSP plant material.

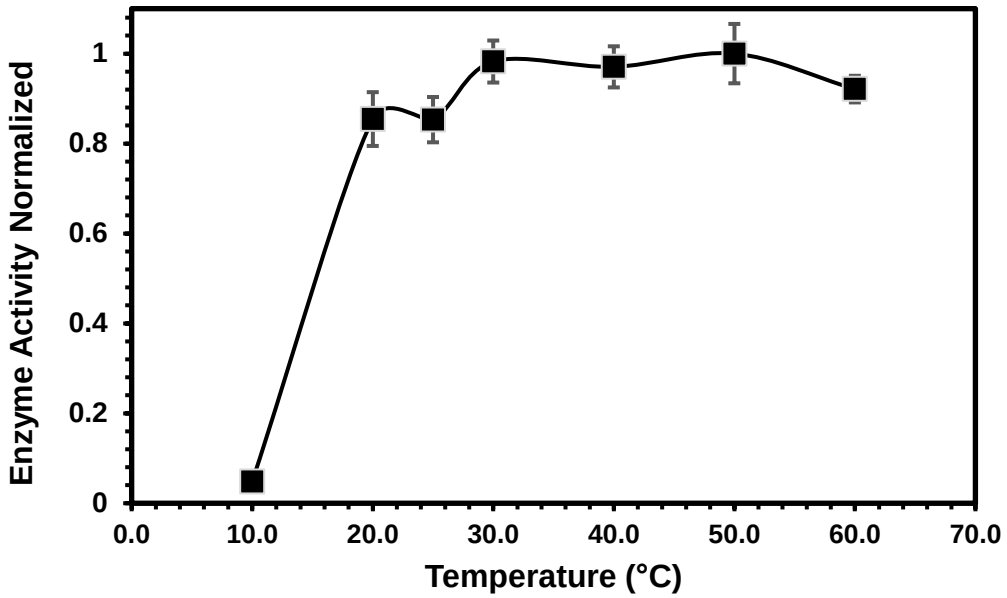

Figure 2.19. Temperature dependence curve of WMSP urease activity.

To measure the temperature dependence of WMSP, the assay was carried out in a water immersion bath at various temperatures. The analyte vials containing the weighed out WMSP and 2 mL of deionized water were equilibrated in the bath at the desired temperature for 5 minutes prior to spiking with the urea solution. After spiking the vials with the urea solution, the vials were returned to the bath for the 5-minute reaction time. When the 5 minutes had elapsed, the vials were taken out of the bath and spiked with the 0.2 M sulfuric and was left to be analyzed with the Nessler's reagent on the spectrometer. When the sulfuric was added, the reaction is complete so the bath can then be incrementally increased in temperature for the next sample to be acclimated and tested. The temperature dependence curve shows the activity is of WMSP is relatively high over a broad range of temperatures. Compared to the commercial jack bean urease 40% activity at 25 °C, the WMSP showed above 80% activity at 20 °C.

2.3.7. Dry Stability of WMSP

Enzymes with high stability are desirable, as experiments may be conducted over several days. [46, 50-52]. If the enzyme's activity fluctuates in the experimental window, it becomes necessary to repeatedly assay the enzyme, especially if the stability is poor. Several strategies are employed to increase the stability an enzyme: addition of buffers, chelating agents[50], and preservatives, or enzyme immobilization.[46, 51-65]

Since the watermelon seed powder is already a natural type of immobilization, studies on its stability both as a dry powder and in an aqueous dispersion can be performed. Additionally, since it has been shown to not leech overtime in an aqueous environment, the enzyme's activity should be maintained in that aqueous dispersion. Since the powder is extracted via large quantities of acetone, residual moisture is dependent on its storage conditions. To three 20 mL scintillation vials, about 15 mL of WMSP was added to the vials. Storage conditions were as follows: 1) capped vial left in ambient, 2) uncapped vial left in ambient, and 3) capped vial in 5-10 °C refrigerator. Conditions 3 and 2 are the most different and should be an ideal storage versus worst case scenario, respectively. Prior to sampling of each vial, the dry WMSP was be vortex mixed to ensure a representative sample was taken.

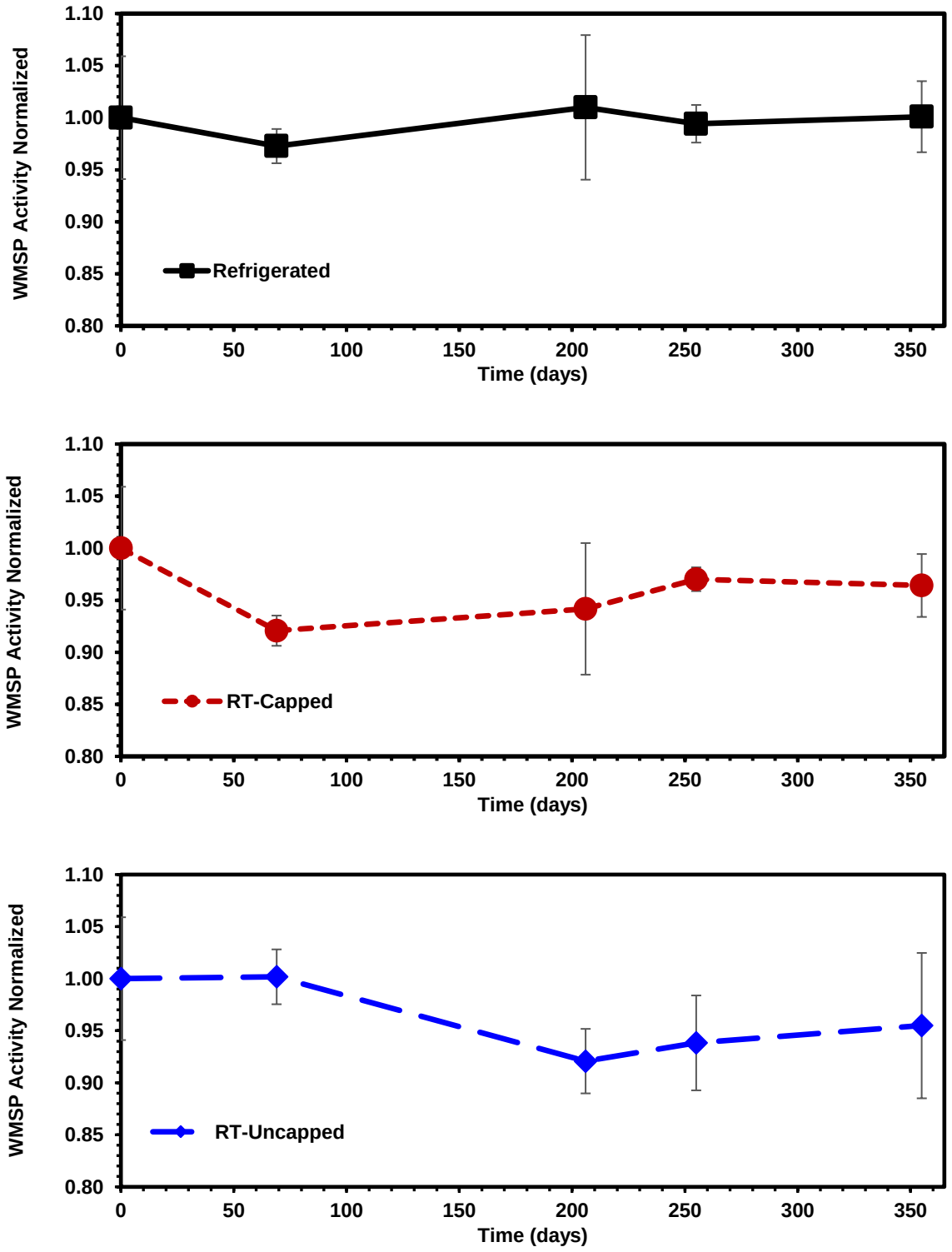

Figure 2.20. Urease activity stability plots of dry WMSP in three conditions: Refrigerated (5-10 °C) capped vial, ambient capped vial, and ambient uncapped vial.

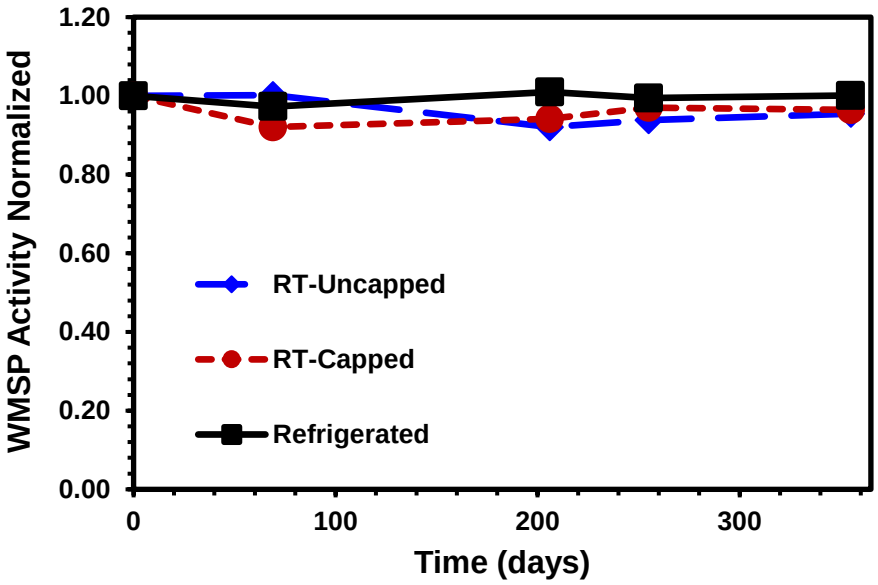

Figure 2.21. Combined plot of dry stability WMSP samples

The dry stability assays show little to no degradation or change in activity of the WMSP. Even the sample left in ambient laboratory conditions in the southern humid Louisiana climate had no noticeable decrease in activity. The opened vial was exposed to the atmosphere and humidity; visually it had darkened slightly with perhaps more clumps. A gravimetric analysis on the three samples showed moisture contents all within 1% of each other; this may be due to each sample being opened at least 5 times for assay. The gravimetric analysis was done by placing a weighed sample with the dish's tare weight into a vacuum oven at 35 °C and pulling above 30 inHg of vacuum. The samples were let dry for 1 hour then weighed. The refrigerated capped sample had 5.8% moisture, the ambient capped had 6.1% moisture, and surprisingly though visually possibly different the ambient exposed sample had 5.3% moisture. These values were then be used to correct for the assay variations.

2.3.8. Aqueous Stability of WMSP

It was advantageous to know that the various storage conditions of the watermelon seed powder had no real impact on its stability. As the WMSPs are generally never utilized in dry conditions, a realistic stability metric to determine would be its urease activity over time in solution. To study this, samples of WMSP were placed in deionized water, specifically Nanopure™ to ensure that no residual metal ions could potentially inhibit the enzyme and stored under different conditions–refrigerated at 5-10 °C and ambient room temperature. Initially two amounts of WMSP in water were studied to observe if there were a difference in the powder concentration stability. In one scintillation vial, 0.5 g of WMSP was added to 15 g of deionized water, and in another vial, 0.3 g of WMSP was added to 15 g deionized water. To each vial, 270 mg of fumed silica was added to keep the seeds in suspension during sampling. After the addition of fumed silica, the vials were homogenized on a VWR25D rotor-stator homogenizer at 10 krpm for 10 seconds. One set of high and low WMSP concentration was placed in refrigeration (B3 and B4) and the other left in ambient (B1 and B2). To assay each vial, it is critical to use an amount of solution that would fit within the calibration curve of the Nessler's assay. Determining the WMSP concentration and then back calculating how much to spike yields 280 µL of the 3 g WMSP vials and 435 µL of the 5 g WMSP vials.

Prior to taking a sample, every vial was sonicated for 5 minutes then vortexed for 10 seconds. Even though the spikes were performed with functioning micropipettes, an accurate weight was measured to compensate for density differences due to trapped air bubbles. The volume was assumed to be correct for the micropipettes, and then total volume was made up to the assay's 2 mL.

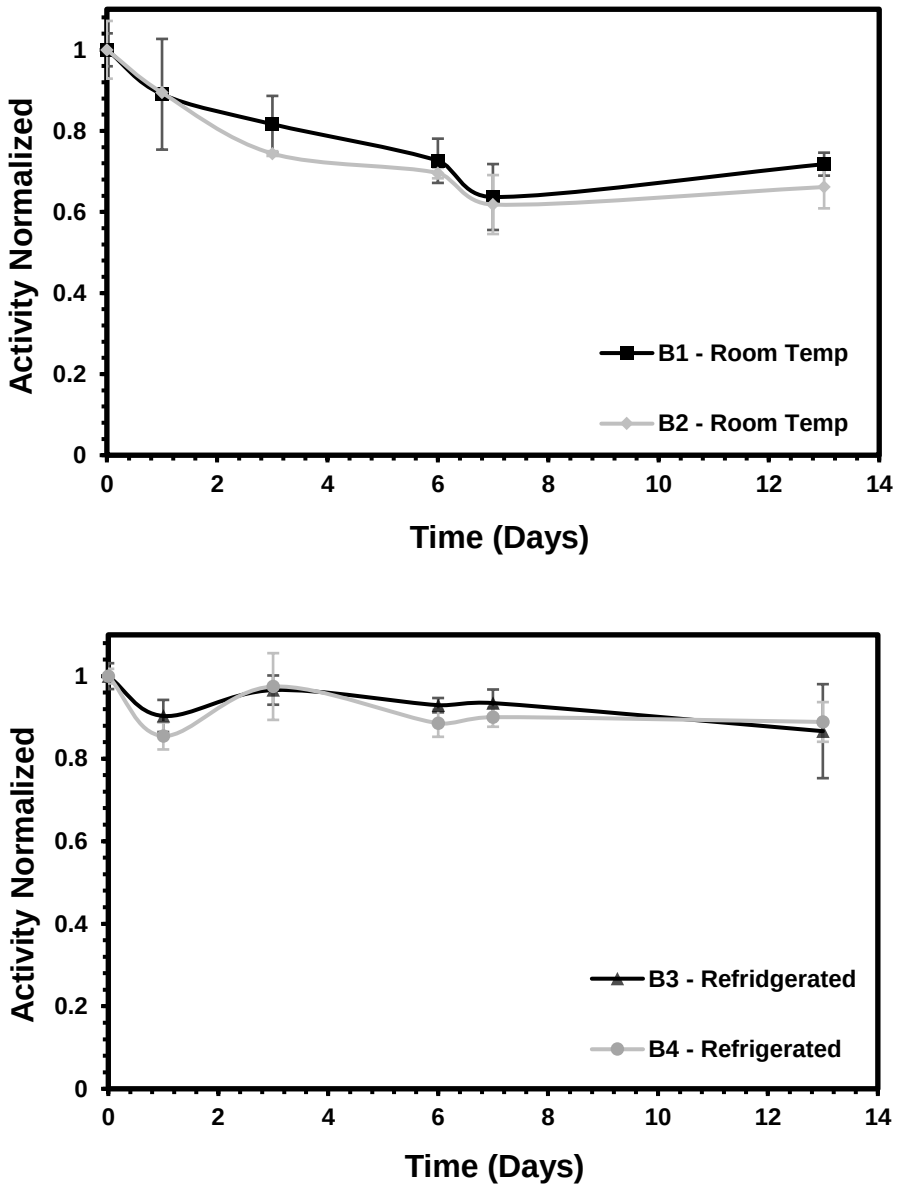

Figure 2.22. Stability plots of the activity of WMSP in 0.02 M 7.0 pH phosphate buffer with fumed silica. B1 and B3 were the lower concentrated WMSP, with B2 and B4 were the higher concentrate WMSP vials.

The assays were taken over a span of 12 days, and it was noticed on day 4 that a strong odor emanated from the ambient samples. This putrid smell became more intense as time passed. It is thought that since the WMSP was a natural material, bacterial or mold may be growing especially enhanced in the samples left at room

temperature. The refrigerated samples were found to have a faint smell after 10 days, which affirms that the lower temperature is simply preserving the sample integrity.

In any case, the urease enzyme is still present at above 60% activity after 12 days in ambient conditions even with the rancidity. The refrigerated samples also maintained above 80% activity after 12 days. Previous research in immobilization and preservation showed fast degradation or complete denaturing of the enzyme within 1-3 days/[46, 51, 52]

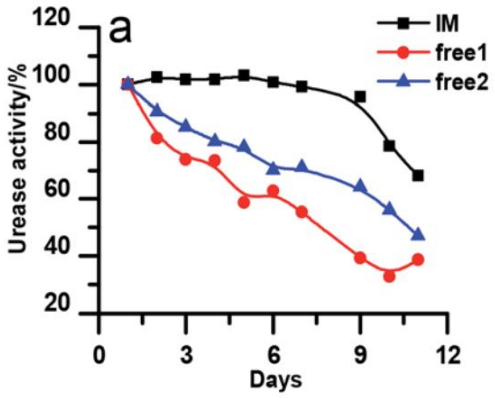

Figure 2.23. Yang et al. measured stability of immobilized urease and free urease enzyme stored 25C (free1) and 4C (free2).[52]

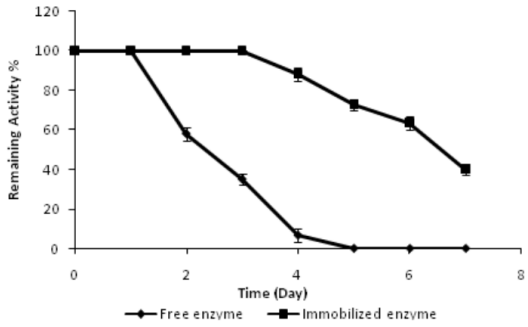

Figure 2.24. Tetiker et al. measured stability of immobilized urease and free enzyme, storage conditions are 4 °C.[51]

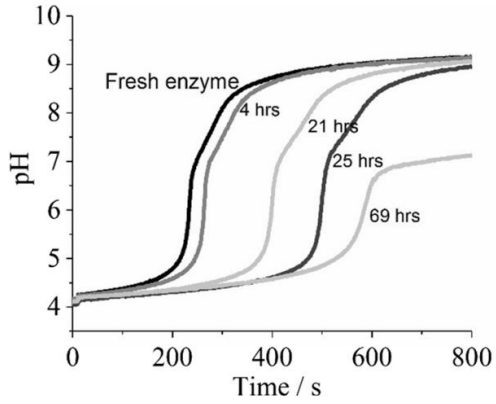

Figure 2.25. Bubanja et al. studied the clock reactions for enzyme in un-buffered aqueous solutions over time.[46]

The sharp decrease and high variation of the enzyme activity of the WMSP is most likely due to microbial action since the refrigerated sample retained more activity and the sharp drop in the ambient samples occurred after noticing the odor. To address this issue, a germicidal could potentially stabilize the aqueous WMSP dispersions. Phenoxyethanol is a germicidal glycol ether[37] that works against gram-negative and gram-positive bacteria and *Candida albicans*. It is an FDA approved preservative, which is also used in vaccines, personal care applications, and in antiseptics.[66] Besides conforming to regulatory commissions, it is relatively inexpensive and is slightly soluble (2.6%) in aqueous and soluble in organic environments.

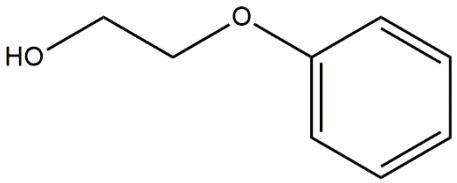

Figure 2.26. Phenoxyethanol is a germicide that is effective in aqueous and organic environments.

In cosmetic applications, the phenoxyethanol is added at maximum of 1.0%. It was decided to add this preservative at 0.5% by weight in the aqueous phase. The stability study was continued for the non-preserved samples with the addition of two more

samples with 0.5% phenoxyethanol—one placed in refrigeration 5 °C and one in ambient room temperature.

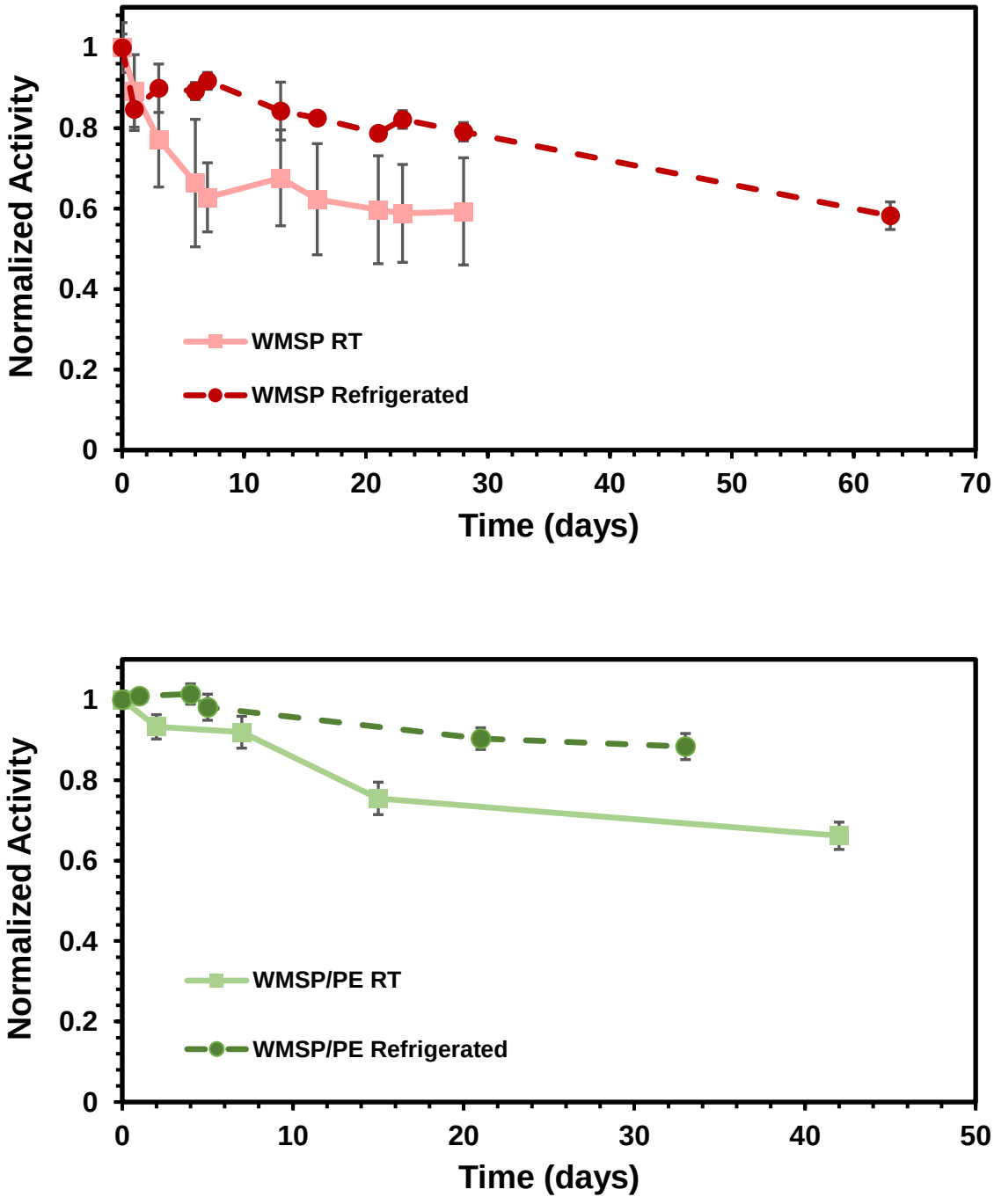

Figure 2.27. Aqueous stability WMSP urease activity testing, top plot has no preservative and bottom plot has 0.5% phenoxyethanol added.

The longevity of activity of WMSP in an aqueous dispersion was greatly enhanced by the addition of phenoxyethanol. Since it is primarily a germicidal, the degradation of the enzymatic activity seen from the non-preserved samples most likely were attributed to microbial action. Even without the preservative, however putrid the samples may smell, the room temperature dispersion of WMSP retained at least 50% activity after about a month. With refrigeration, the WMSP dispersion in turn had around 60% activity in 2 month's passing. The phenoxyethanol did stave off the putrefaction, and notably both preserved samples showed 90% activity after 1 week, with the sample kept in refrigeration showing 88% activity after 1 month. By utilizing WMSPs, urease activity can be maintained at the desired U/mL concentration for much longer intervals than pure enzyme.

2.4. Clock Reaction Kinetics of the Urea-Urease Reaction Using WMSP

The clock behavior in the urea-urease reaction is well documented.[46, 48, 52, 67-69] This occurs due the enzyme's activity exhibiting maximum activity as a function of pH. This is seen from the bell-shape curve of Figure 2.16 and 2.18 of WMSP. By hydrolyzing urea, ammonia is produced, which increases the pH. With this increase in pH, urease's activity is increased producing more ammonia. The system then self regulates, as the enzyme's activity decreases past its maximal activity. The induction period, i.e. time prior to acceleration, the clock's shape, and final pH can be tuned with three variables: initial pH, urease amount, and urea concentration.

To study these three parameters, one of them will be in variation where the other two will be kept constant. To compare the behaviors with WMSP, a standard jack bean type IX urease with assay value of 76440 units / g solid was utilized. The WMSP batch

used has an assay value of 2124 units / g powder. All reactions were performed starting at 4 pH, chosen specifically to be a comparison point between WMSP and free enzyme. Large volumes of 4 pH solution were made with taking 2 L of deionized water and titrated with dilute solutions of aqueous hydrochloric acid. This was done by magnetic stirring the solution with a VWR sympHony™ pH probe immersed, and the meter was correspondingly set to continuous read. To easily use the jack bean urease, since its activity is so high, a stock solution was made with the acidified water: 33.6 mg urease enzyme was added to 5.1644 g H_2O (4 pH HCl). This results in an enzyme concentration of 497 units/mL. Furthermore, a stock solution of 10% (wt/wt) urea in 4 pH water was created to spike in each trial. This solution's density was measured at 1.029 mg/µL. Finally, the total volume for every analysis was 60 mL taking into account each spike of stock solutions. Each trial was well stirred with a magnetic stirrer set at 300 rpm.

2.4.1. Variation of Urease Concentration

Since enzyme concentration was being studied, the amount of urea was fixed at a 200 µL spike. This results in a urea concentration of 5.7 mM in each trial. In the WMSP experiments, the weights used were 10 mg, 20 mg, 30 mg, 50 mg, 100 mg, and 150 mg. This corresponds to WMSP enzyme concentrations of 0.35 U/mL, 0.71 U/mL, 1.06 U/mL, 1.77 U/mL, 3.54 U/mL, and 5.31 U/mL, respectively. Likewise, in the free enzyme experiments a spike of 42 µL, 128 µL, and 427 µL of the jack bean enzyme stock was used. This in turn gives free enzyme concentrations of 0.35 U/mL, 1.06 U/mL, and 3.54 U/mL, respectively.

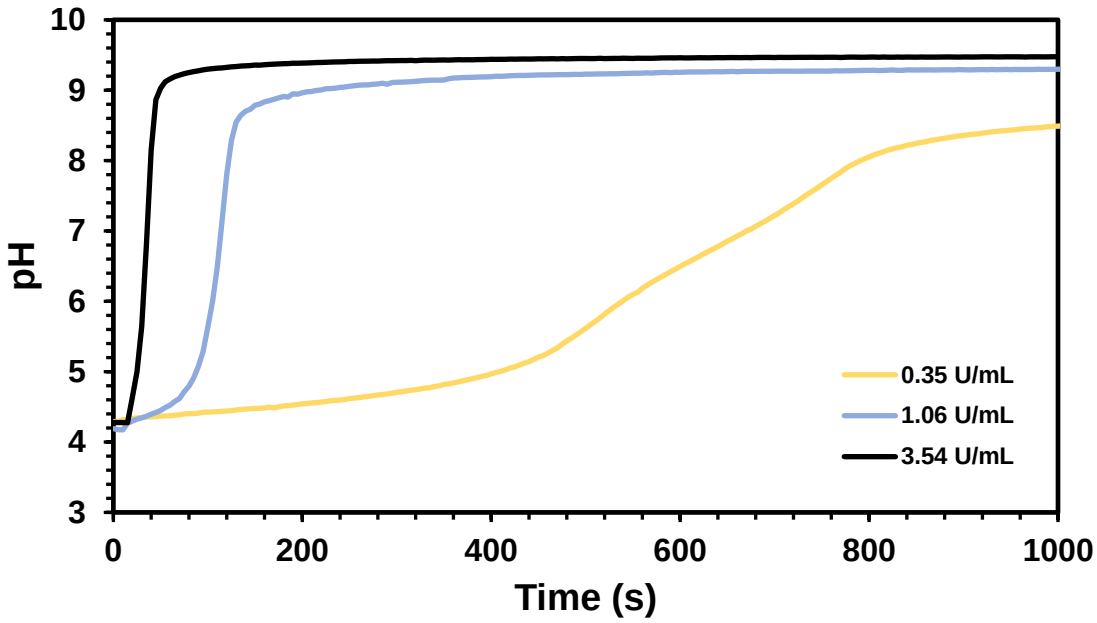

Figure 2.28. Variation of free enzyme concentration pH profile, [Urea] = 5.7 mM.

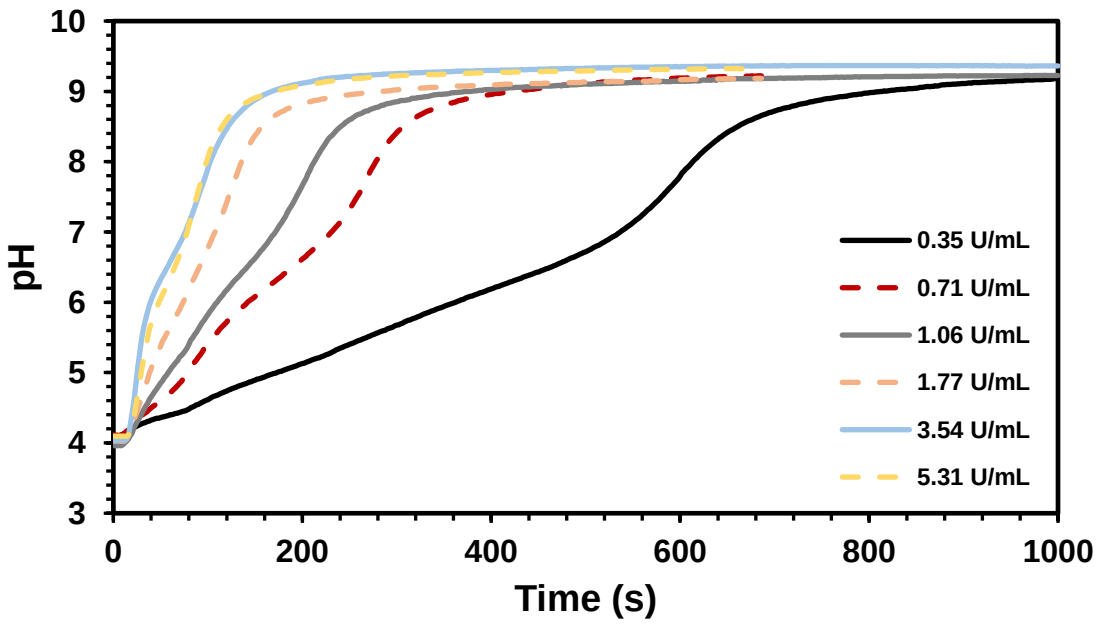

Figure 2.29. Variation of WMSP enzyme concentration pH profile, [Urea] = 5.7 mM.

The pH profiles of both free enzyme and WMSP exhibited the clock behavior of the rapid pH increase, and since the urea concentration was fixed the final pH were similar between enzyme sources. Though the ramp in WMSP seems to exhibit an inflection point around 6.8 pH. One potential explanation is the initial ramp to around 6.8 pH is diffusion limited since the WMSP is a carrier. After 6.5 pH the clock happens, as the bell-shaped activity curve from Figure 2.18 starts around 6 pH with a maximum activity at 8.1 pH. This maximum corresponds to the steep-most point along the curve for all trials. Accordingly, the free enzyme clocks faster since there is no diffusion component, yet at the low enzyme concentration (0.35 U/mL), both plots are similar in behavior.

2.4.2. Variation of Initial pH

The next parameter to study was initial pH. This in turn means that the concentration of urea was fixed at 5.7 mM, a 200 µL spike of the 10% urea solution, and the amount of free enzyme, 427 µL spike of stock, and WMSP, 100 mg, was fixed (3.54 U/mL). Solutions of deionized water of various pH were to be made. Following a similar protocol to create the 4 pH stock: a pH probe was immersed and set to continuous read in 2L of deionized water. Dilute $HCl_{(aq)}$ was then added slowly to titrate the water to each desired stopping point. When the desired pH value was reached, the solution was allowed to equilibrate for 1 minute and then about 150 mL of the solution was decanted for use. The pH levels to study the clock reaction are 4.2 pH, 3.9 pH, 3.7 pH, 3.5 pH, 3.2 pH, and 3.0 pH.

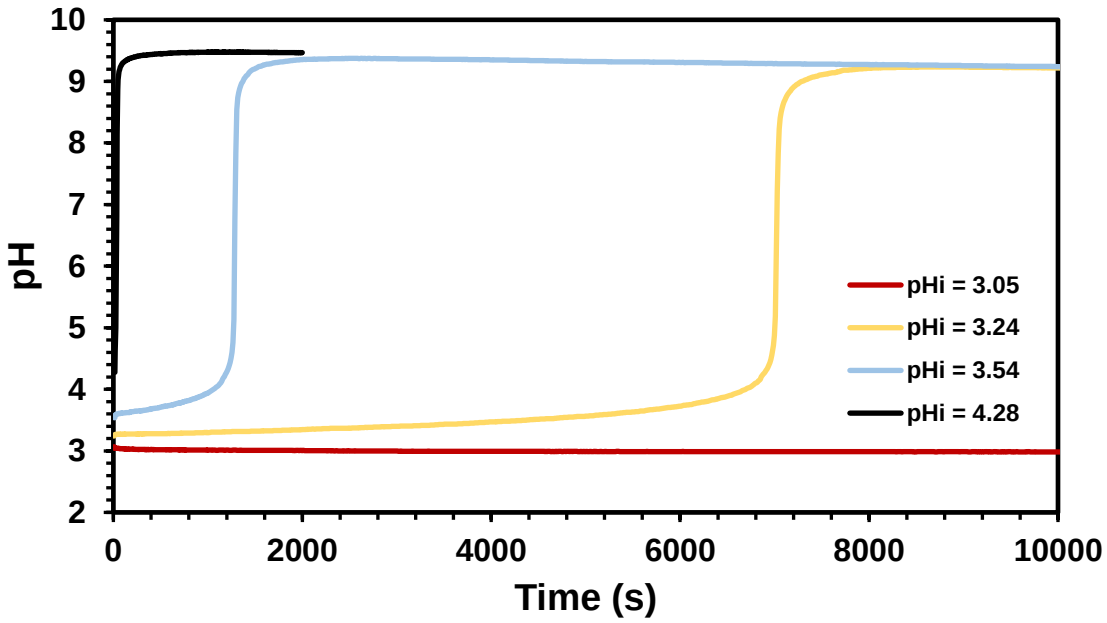

Figure 2.30. Variation of initial pH profile for free enzyme, [Urea] = 5.7 mM and [Urease] = 3.54 U/mL.

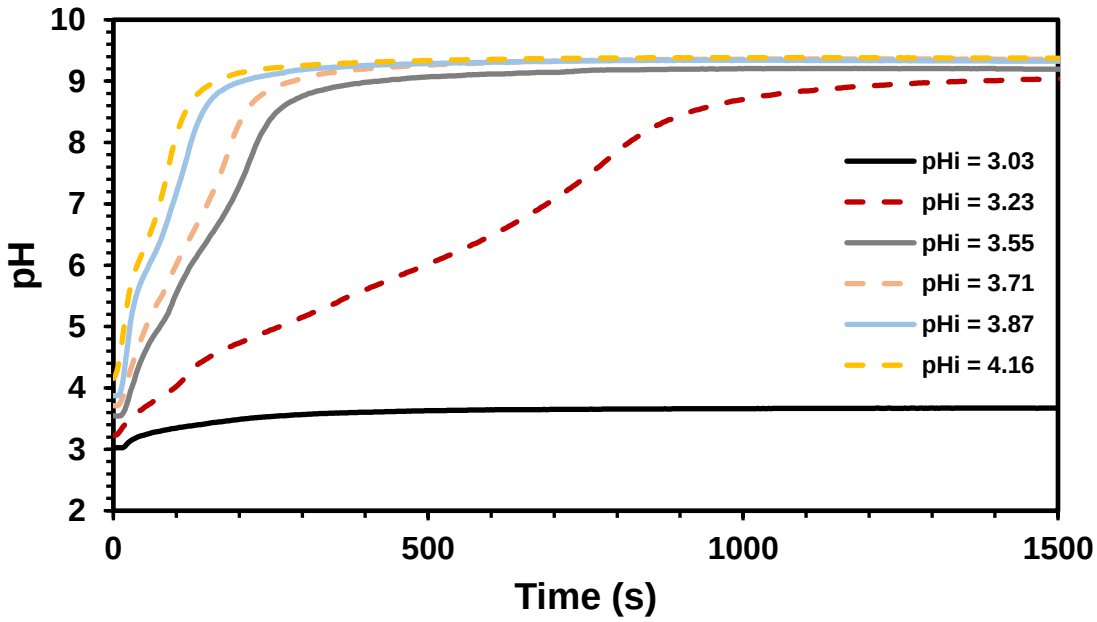

Figure 2.31. Variation of initial pH profile for WMSP enzyme, [Urea] = 5.7 mM and [Urease] = 3.54 U/mL.

The free enzyme pH profiles show the characteristic clock behavior also with increasing induction times for lower the initial pH. The WMSP profiles look completely different,

though somewhat similar to the WMSP variation curves of Figure 2.29. Since the WMSP has a diffusion component, even though it is well stirred, and the particles are small, perhaps the ammonia produced by enzyme in the WMSP raises the pH of the immediate surroundings of the urease, contributing to higher activity. Another conjecture on diffusion would be that the acid component is not diffusing fast enough to neutralize the ammonia produced around the enzyme. With both these factors, the WMSP was able to react at 3.2 pH an order of magnitude faster than the free enzyme.

2.4.3. Variation of Urea Concentration

The amount of urea in solution was the last parameter to investigate. Similar to the previous study, free enzyme and WMSP was fixed at 3.54 U/mL. The amount of 10% urea to be varied was as follows: 10 µL, 20 µL, 25 µL, 50 µL, 75 µL, 100 µL, 150 µL, and 200 µL. This corresponded to concentrations of 0.3 mM, 0.5 mM, 0.7 mM, 1.4 mM, 2.1 mM, 2.9 mM, 4.3 mM, and 5.7 mM, respectively.

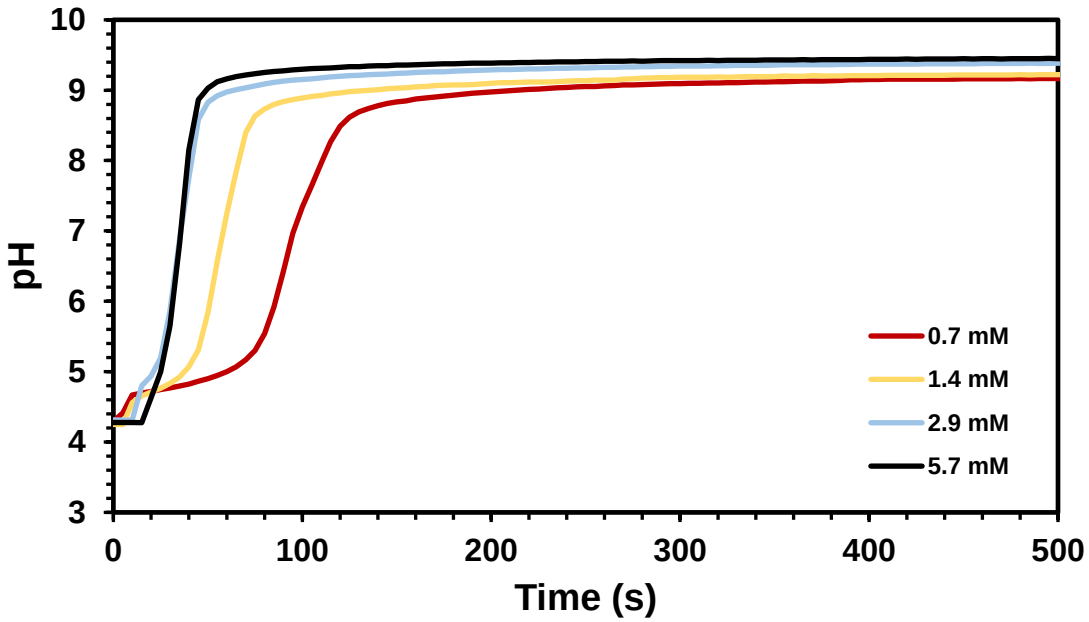

Figure 2.32. Variation of urea concentration pH profile for free enzyme, [Urease] = 3.54 U/mL.

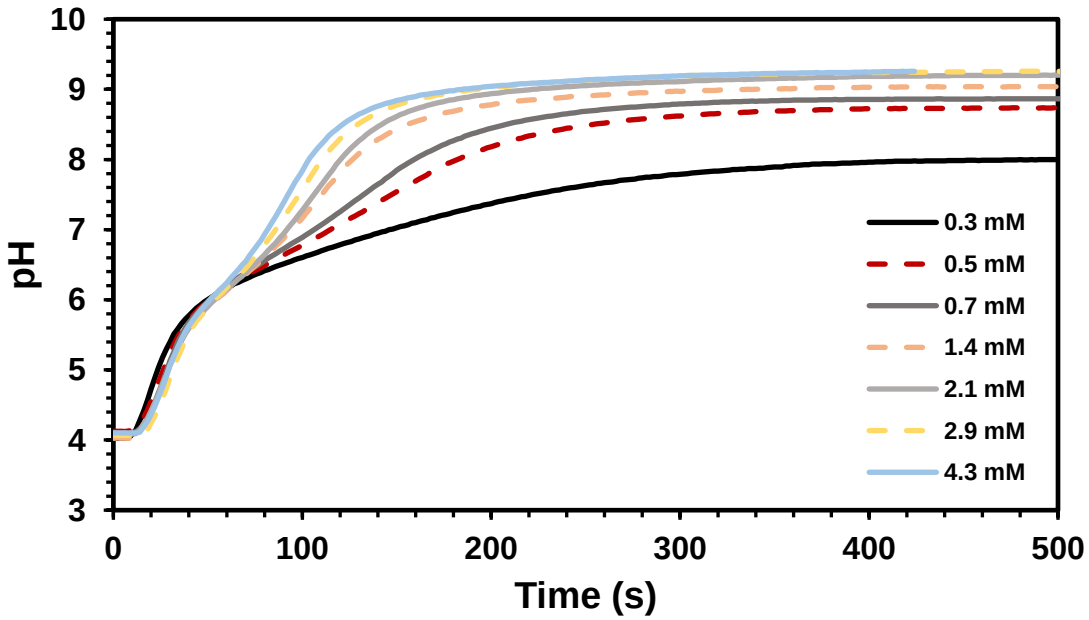

Figure 2.33. Variation of urea concentration pH profile for WMSP enzyme, [Urease] = 3.54 U/mL.

Comparatively, the clock reaction for the free enzyme was faster than WMSP. Only at the low 0.7 mM were there some similarities in timing. It is interesting to note that the curves in the WMSP plot seem to collapse from 4 – 6 pH. This means that the activity in

this region is independent of the urea concentration. As mentioned previously, the inflection at 6 pH and clock reactions thereafter are due to the WMSP's bell-shaped activity dependence on pH.

2.5. WMSP Components: Post-Reaction with Urea and Presence of Catalase

When performing the assay on the WMSP, it was noted that there is a change in the macroscopic properties of the dispersion. Even if the particles were sonicated and left to fully de-aggregate, certain conditions cause a lightening of the solution or even flocculation to occur. Understandably this material is not synthetic, and its make up is wholly up to nature. That being said, most likely it is a protein body which contains urease enzyme and potentially other enzymes as well.

2.5.1. Observations of WMSP Post-Reaction with Urea

The WMSP sample in the Nessler's assay starts in 7 pH due to the phosphate buffer, reacts with urea, and then was subjected to 2 M sulfuric acid. Prior to the acidification the sample is slightly yellow, and after the acid was added, the sample is white. If the vial was left undisturbed for 30 seconds, the solids portion begins to flocculate and may float. Since these physical phenomena occur macroscopically, a view of the individual WMSP reacting with urea may give some explanation as to what is happening.

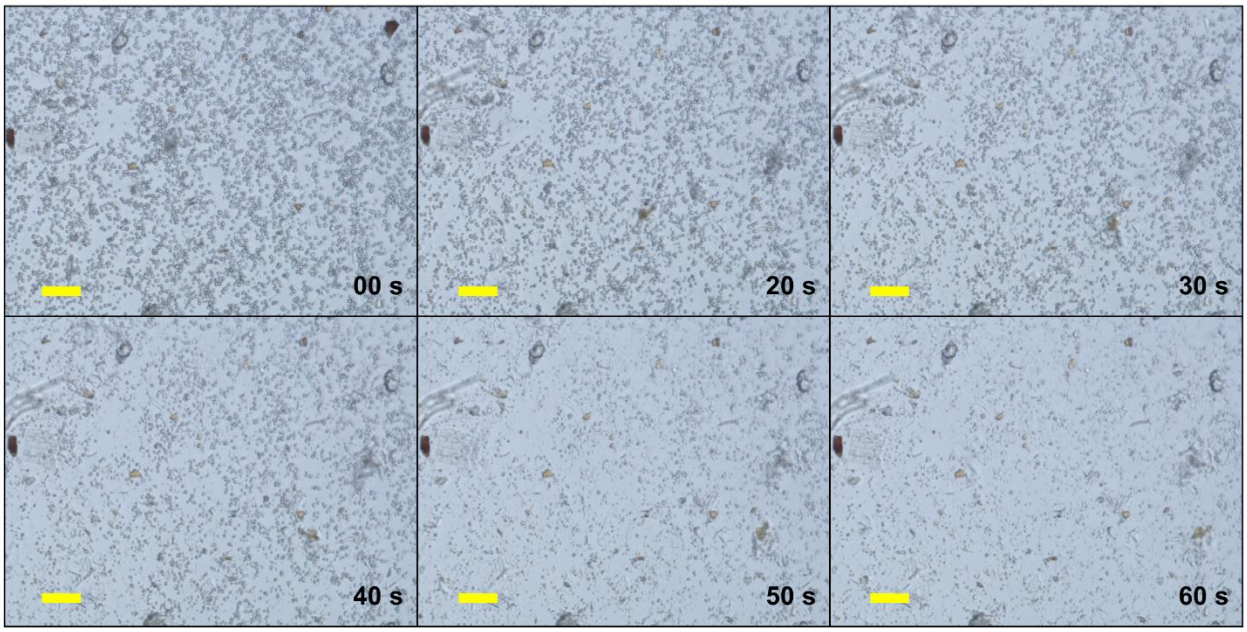

Figure 2.34. Light microscopy image time lapse of WMSP in deionized water at 7 pH. Time 00 s is immediately after addition of 3% urea in 7 pH buffer. Scale bar is 50 µm.

By viewing the reaction of urea with WMSP, the particles seemed like they were dissolving after the reaction, or that there was a refractive index change of the particle occurring. Running the same reaction with un-buffered 10% urea, it was thought that the reaction should be even faster. It ended up taking a longer time to dissolve but it nevertheless did; this ruled out that the buffer was the culprit of the “dissolution.” Viewing the WMSP during the reaction-dissolution and then adding acid also showed no reformation of the particle or reverse of the probable refractive index change.

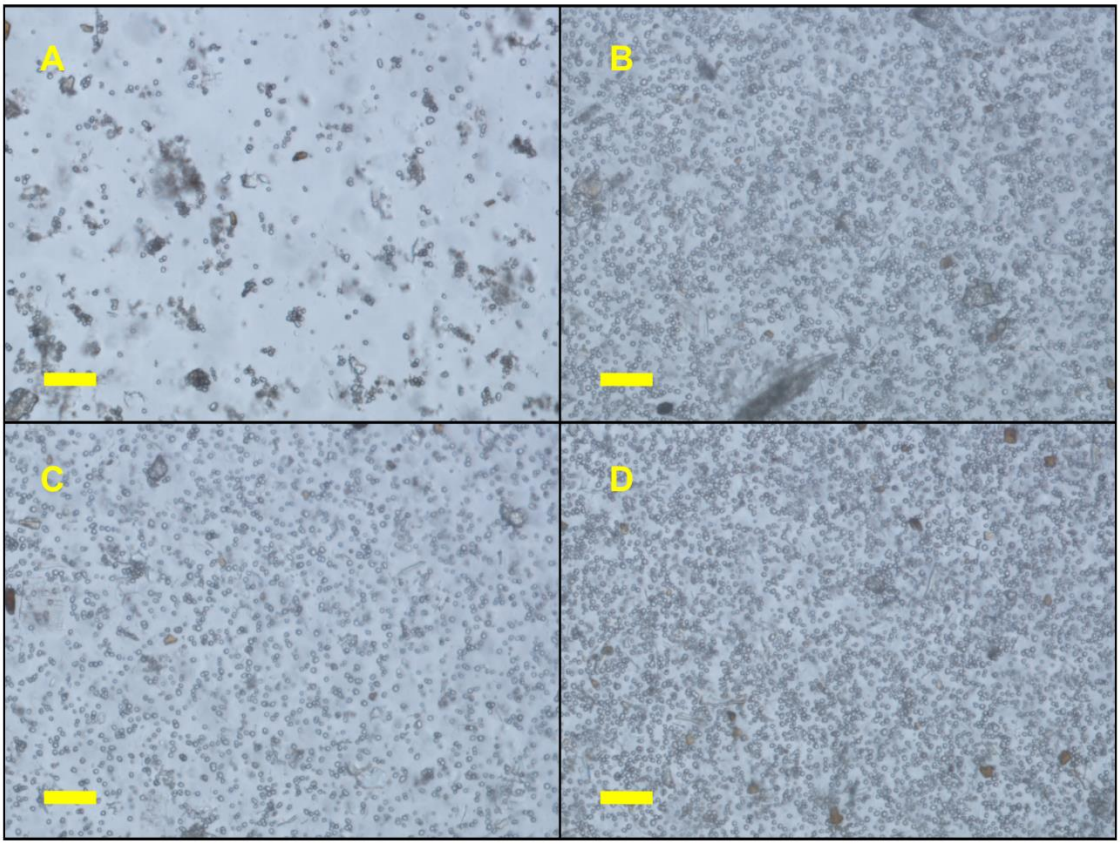

Figure 2.35. WMSP in different pH solutions: a) 2 pH, b) 4 pH, c) 8 pH, d) 10 pH.

Putting the WMSP in various pH solutions (acidic conditions from HCl_{aq} and basic conditions from $NaOH_{aq}$) became more confounding, as the WMSP at 10 pH showed no change, no dissolution. From the multiple pH profiles ran on the urea-urease reaction, 10 pH was an unobtainable upper limit, yet the particles still remain. One observation was at the 2 pH, Figure 2.35 (a), there were some aggregation seen from the well distributed mixture.

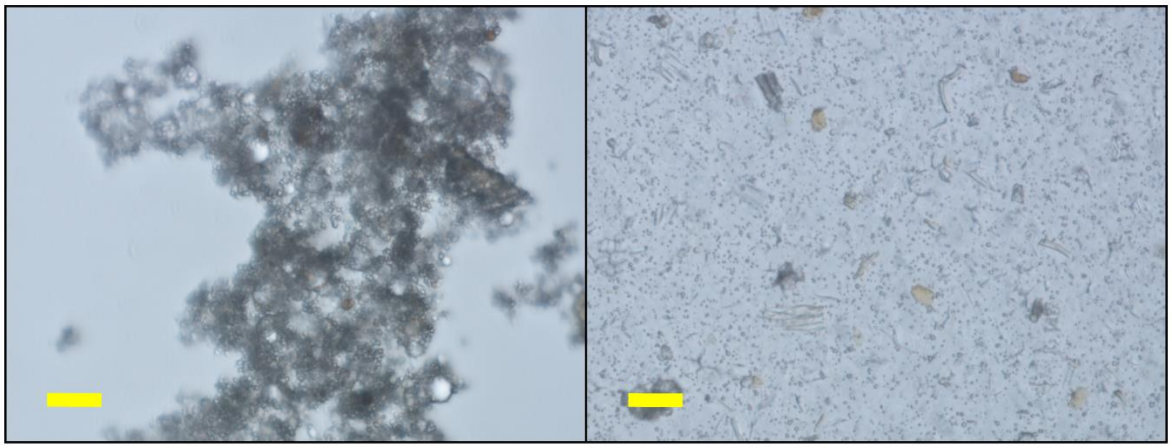

Figure 2.36. WMSP in 0.2 M sulfuric acid (left) and WMSP in 10% ammonium hydroxide (right).

Only by going to extremes were the macroscopic behaviors really observed. Putting WMSP in 0.2 M sulfuric quickly aggregated the well sonicated dispersion. Furthermore, the WMSP in high basic conditions finally showed the dissolving behavior seen before. Making different aqueous sodium hydroxide solutions from 10 – 13 pH, it was then possible to determine at what specific pH would dissolve the WMSP.

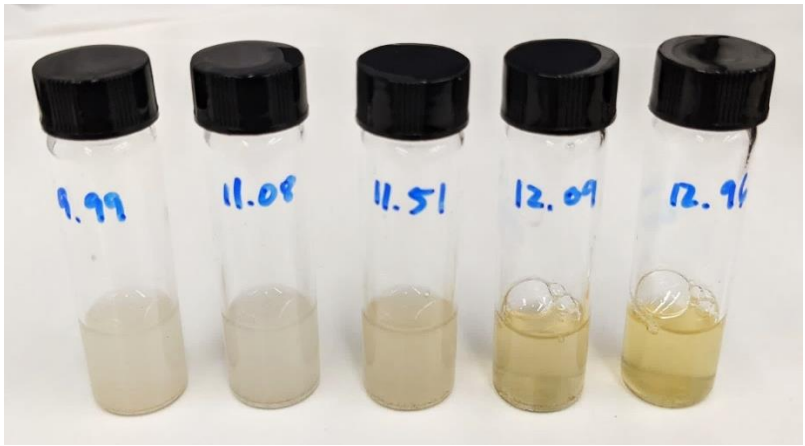

Figure 2.37. WMSP in aqueous solutions of NaOH with different pH, from left to right: 9.99 pH, 11.08 pH, 11.51 pH, 12.09 pH, and 12.96 pH.

Adding WMSP to 10% urea or 3% urea in buffer does not always exhibit the dissolving behavior. Viewing the well reacted solutions, still showed presence of WMSP. Only by

being on the microscope slide for some time did they dissolve. From Figure 2.37, a minimum of 11.5 pH was required to start any dissolution, and at 12 pH the solution is clear and/or the particles had dissolved. The dissolving phenomenon is most likely a localized problem combined with diffusion effects again—since the microscope slide is a thin layer the ammonia produced cannot easily be dispersed. This means that the dissolving particles observed probably had produced enough ammonia to at least 11.5 pH in their immediate surroundings. In most urea-urease systems, the amount of total solution with stirring rate will prevent any spikes in local pH to cause for WMSP dissolution.

2.5.2. Presence of Catalase Enzyme

Since the WMSP are conjectured to be protein bodies, it would follow that there are other enzymes in the particles.[34, 38, 70, 71] One enzyme that is common in seeds, and could be easily tested for, is catalase. Catalase rapidly decomposes hydrogen peroxide to water and oxygen. A qualitative test was first done with 0.1 g WMSP being added to 30 mL of deionized water, then 1 mL of 30% hydrogen peroxide was added to the vial.

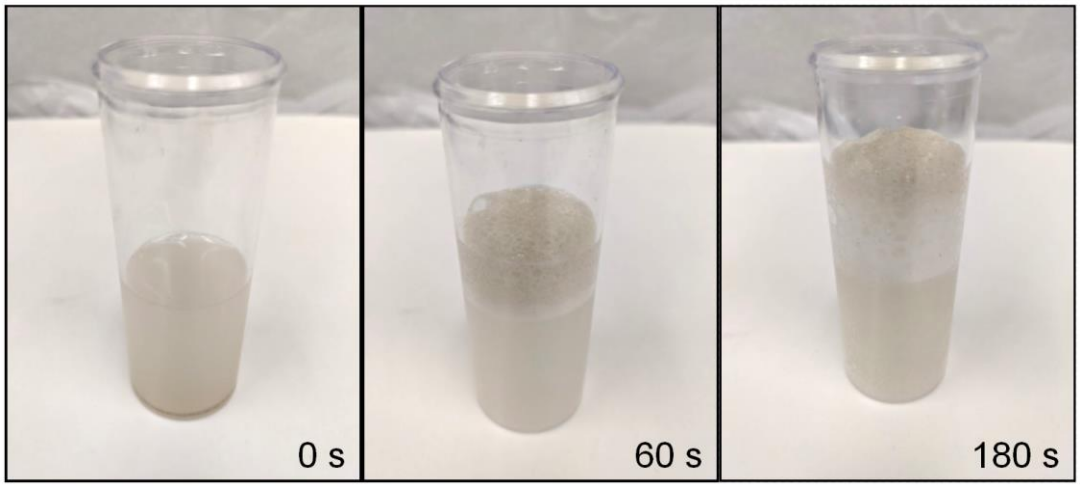

Figure 2.38. Qualitative test of WMSP for decomposition of hydrogen peroxide, from left to right, t = 0 s prior to hydrogen peroxide spike, t = 60 s after spike, t = 180 s after hydrogen peroxide spike.

As seen from Figure 2.38, the evolution of bubbles was quite fast and vigorous. To confirm that hydrogen peroxide was being decomposed, a titration of potassium permanganate and hydrogen peroxide was performed. A 1:3 wt/wt solution of water to sulfuric acid and a 0.1 M $KMnO_4$ solution were made for the analysis. Testing of the 30% hydrogen peroxide reagent was done as a method verification and to determine the starting H_2O_2 concentration. 0.5 g H_2O_2 was added to 100 g DI H_2O with 19.7 g of the sulfuric solution. This mixture was titrated with the permanganate, until a persistent pink was achieved for over 1 minute. The 30% H_2O_2 was assayed to be 31.8% purity. 0.5 g H_2O_2 was added to 75 g DI H_2O and 0.5 g WMSP was added; the mixture was stirred for 10 minutes. The solution was then filtered through a #1 filter and assayed accordingly. All that remained in solution was 1.3% H_2O_2 from the original 31.8% H_2O_2. Thusly, it is confirmed that catalase is present from the decomposition of hydrogen peroxide.

2.6. Conclusions

Watermelon seed powder is a stable and inexpensive source of urease enzyme. One motivation for using WMSPs is that the unit/g cost versus pure enzyme is an order of magnitude less expensive. Not only is it economical for commercial or trial applications, but also the stability of the powder is exceptional. When kept dry, the powder had retained its activity for almost a year no matter the storage conditions. When dispersed in solution with phenoxyethanol, experiments can be run for a month with 90% activity retention if they are stored at 5 °C. Though there are some differences to the pure enzyme, like the shift in pH activity or diffusion characteristics of the clock reaction, these can be accounted for to utilize this stable material.

CHAPTER 3. IMMOBILIZATION OF WMSPS

3.1. Introduction

Enzyme immobilization is a well-established strategy of prolonging stability, enhancing activity in certain conditions, or provide a more accessible matrix.[46, 51-58, 62, 63, 65] There are several ways that immobilization can be achieved—physical encapsulation[46, 52, 56, 58, 60], covalent bonding[52, 57, 60], non-covalent bonding.[57, 65] Additionally, by grafting the usually solution soluble enzyme to a substrate, the potential for recyclability is also apparent. This is definitely a cost savings especially on the commercial scale. Physical encapsulation can be performed on porous matrices or hydrogel-type formulations. Covalent and non-covalent bondings uses surface manipulation schemes to affix the enzyme to a carrier.

Polymeric and porous media are generally the main substrates used in enzyme immobilization and encapsulation. One method of making polymer fibers is

electrospinning, which combines extrusion of a fiber either in melt or solvent to produce micro or nano-sized fibers or mats to be used.[72, 73] The same strategies that go into immobilization on particles or membranes can then be employed on the fibers. From Figure 3.1 A and B, an enzyme can be adsorbed to the surface or core either possibly from ionic interactions or hydrogen bonding. It can be covalently linked via crosslinking agents in Figure 3.1 D, or be spun directly in the polymer fiber matrix as in Figure 3.1 C. Wang et al. immobilized lipase onto polysulfone fibers.[74] Their immobilization increased the stability and temperature behavior of the enzyme.

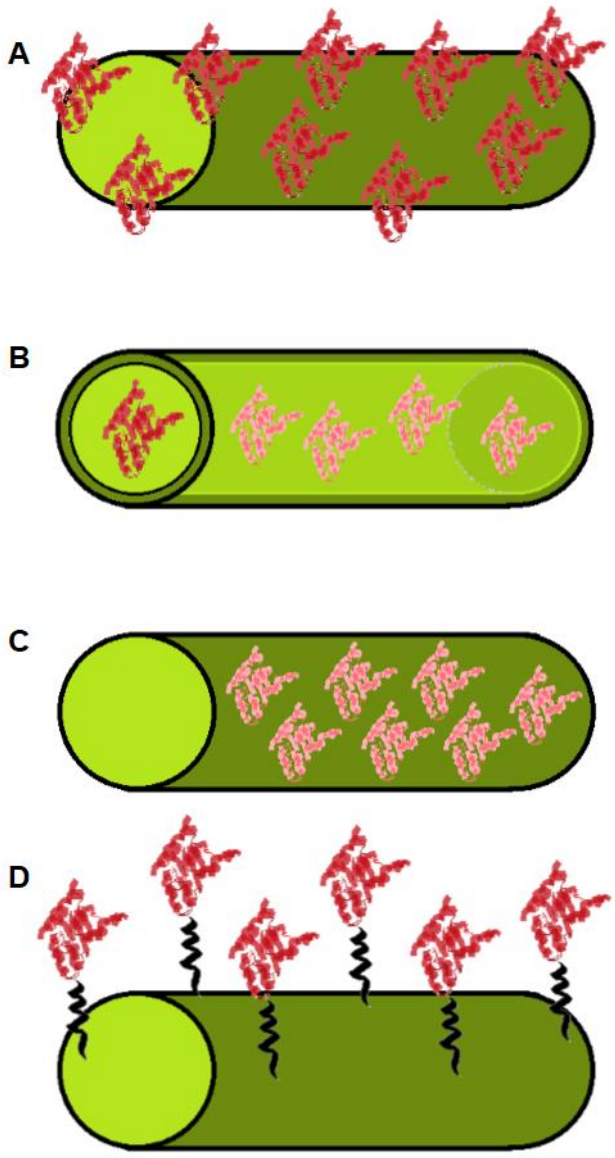

Figure 3.1. Polymeric fiber with different enzyme immobilizations: A) adsorption to the surface, B) adsorption in the core, C) encapsulated in the matrix, D) covalently linked.

Yujin et al. also immobilized lipase on a membrane reactor by first filtration onto the membrane combined with glutaraldehyde crosslinking.[75] By grafting the enzyme to the reactor, flow studies were done by testing the activity of the enzyme's hydrolysis of olive oil and monitoring the fatty acid content in the aqueous phase. Again, activity was enhanced with better stability resulting from the immobilization.

3.2. Immobilization of WMSP in Agar

3.2.1. Hydrogels and Urease

Since urease is highly soluble in water, hydrogels are an inexpensive, fast, and generally biocompatible material to immobilize the enzyme. Synthetic approaches include polymerization of hydrophilic monomers in aqueous environments with the enzyme loaded inside the gel.[46, 56, 60] One type of biocompatible hydrogel are those based on the thiol-acrylate system[76, 77], in which base addition triggers a Michael addition type polymerization. Bubanja et al.[46] coupled this with the clock of the urea-urease reaction, using the urease, which is to be immobilized, in the aqueous phase to polymerize the hydrogel. The aqueous phase, which contains the monomers, urea, urease, and stabilizer is first injected into hexane and then stirred to attain particles. Then after the induction period, urea is hydrolyzed producing ammonia which deprotonates the thiol triggering polymerization resulting in the formation of hydrogel particles.

Biopolymers that form hydrogels are of particular interest in that they are commercially available with inherent compatibility; these can include alginates, agar-agaroses, or gelatins. In another urease hydrogel embodiment[51], alginate is combined with a urease extract from chickpeas and dropwise added to a solution of calcium chloride. The alginate then immediately crosslinks with the calcium producing beads of the size of the droplet. The hydrogel beads are then tested with commercial animal feed for the urea content.

3.2.2. WMSP Encapsulated in Agar

Since the urease in WMSPs are technically immobilized in a natural plant particle but the powder is still micron-sized, physical encapsulation is ideal for handling and usage purposes. In a similar fashion to the hydrogels mentioned previously, agar can be a gelling agent used to entrap material. Agar powder is a biological product of algae that is comprised primarily of a biopolymer, agarose, and other sugars.[78, 79] Using this material is ideal since it is relatively inexpensive and easy to process since the solidification occurs above room temperature (30-40 °C), in comparison to gelatin which requires refrigeration.

Since the hydration and dissolution of agar requires high heat in water (> 90 °C), the addition of the WMSP containing urease has to be done at a lower temperature. The batch size for the WMSP-agar particles can vary based on need, but 100 g is a standard size used. The process consisted of an aqueous phase of the agar-WMSP solution suspended in an oil phase of vegetable oil then cooled. The composition of the particles by weight was 5% WMSP, 4% iron oxide (magnetic powder), and 2% agar. To 65 g of deionized water, 2 g of agar powder was added and brought to a minimum of 92 °C. Since the addition of WMSP should be done at a maximum of 60 °C, addition of ambient WMSP could potentially gel the agar solution at contact of the colder powder. To mitigate this, a separate amount of deionized water was heated to 55 °C to add to the WMSP and iron oxide to incorporate warmed material. Since the batch had an 11% solids content, 89% should be water or in this current formulation 89 g, 65 g of which are already being used for heating the agar. The remaining 24 g of water was used from the heated 55 °C water.

In addition to having a warmed WMSP and iron oxide to prevent agar solidification, this pre-mixing step allows for the powders to be easily dispersed, as the 2% agar solution is much more viscous than the pre-mixing step's warmed water. Once the agar solution had hit the minimum 90 °C temperature, it was held for 30 minutes or until the solution clarified. After this step, the aqueous agar mixture was taken off heating and let cool to 60 °C. Nearing that temperature, the WMSP and iron oxide powders were dispersed in 24 g of deionized water at 55 °C—this can be performed with simple vortex mixing or using a dispersion blade. Next, this pre-dispersion was then added to the agar mixture and homogenized at 5000 rpm for at least 10 seconds. To make the particles, the now agar-WMSP-iron oxide aqueous mixture was dispersed into the oil phase and sheared with a paddle blade. If smaller sized particles were required, a dispersion blade may be used here instead.

Once the desired particle size distribution was achieved, the oil is cooled down by an ice bath to fully solidify the agar. The particles were then screened from the oil and washed with successive amounts of hexane to remove any residual oil from the particles. This step was then improved by using an oil phase comprised of hexane and dichloromethane (DCM) in a 2.1:1 (wt/wt) ratio. This yielded a hydrophobic solution that has a density measured around 0.99 g/mL. This density can then be tuned higher by addition of DCM or lower with hexane. This is important due to the variability of the agar-WMSP-iron oxide mixture density due to air incorporation. A sample of this mixture can be quickly dropped in the hexane:DCM phase prior to full addition to see the buoyancy, then the solvents can be added to tune the density. This allows for proper particle sizing from agitation, due to the agar mixture not completely sinking to the

bottom or floating. In addition, from the stability trials of WMSP in water, phenoxyethanol was added in the aqueous phase at 0.5% by weight to stabilize the particles from microbial growth. After screening the particles from the solvent, they were simply air dried since both hexane and DCM solvents are highly volatile. Another embodiment would be the addition of a surfactant to the oil phase, if fine particles are desired. This could be sorbitan monolaurate or sorbitan monooleate with HLBs[80] at 8.6 and 4.3, respectively.

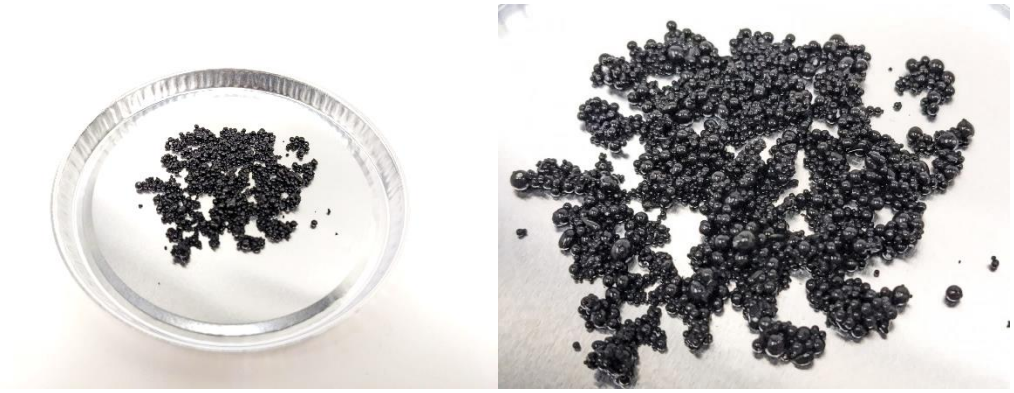

Figure 3.2. Suspension separation prepared 2% Agar particles with 5% WMSP and 4% iron oxide.

The storage of these particles is either in an air-tight container or covered with hexane and placed in 5 °C refrigeration. They can then be used with the appropriate WMSP stability constraints mentioned previously.

Another form of the agar encapsulation came about from an idea of quasi two dimensional urea-urease systems. To study this, the batch formulation is simply 3% agar, 5% WMSP, in deionized water with 0.5% phenoxyethanol. The same measures of the pre-dispersion step were done for the WMSP with the same addition regimen at < 60 °C. The preservative and water solution can be made beforehand and can withstand the agar heating step. Once the pre-dispersed WMSP was added to the agar mixture,

this solution was much more viscous the making the particles due to the increase agar amount. Homogenization was then increased to at least 12000 rpm. Preparation of the casting surface required coating two sheets of glass with a silicone mold release spray. The glass sheets were separated by two 1/8 inch thick glass pieces of appropriate size (1 cm x 10 cm). Once the sheets were sprayed with the release agent, the warm agar-WMSP mixture was poured on one ambient sheet between the separator pieces. The top sheet was then sandwiched on top pressing down to touch the separators, ensuring the now sandwiched agar mixture to be the appropriate size. A weight was placed on top, and the setup was let come to ambient temperatures to solidify the agar. After a few minutes the gel should be hardened, and the sample was placed in refrigeration (5 °C) overnight to fully cool.

Figure 3.3. Sheet casted and proportionately cut 3% agar pieces with 5% WMSP and deionized water with 0.5% phenoxyethanol.

After refrigeration, the agar sheet now was fully hardened and can be manipulated to any shape preferred. One example is Figure 3.3 in which these uniform 1/4 inch squares were cut by a metal grid. The uniformity is crucial when doing certain studies, in which the particles could technically be screened for the same size but with much more

effort required. These squares were refrigerated and covered to maintain the water content in the agar gel.

3.3. Immobilization of WMSP in Polymer Particles

3.3.1. Urease on Solid Substrates

Either through covalent linkages or ionic interactions, urease enzymes can also be immobilized on solid materials, usually with high surface area or porosity. Mesoporous silica can be used as a substrate by which enzymes may be immobilized. The synthesis of the silicas can tune the porosity and surface physical characteristics through the aging conditions[64]. Silica gel is also another support that was used to immobilize urease. By using a diazo coupling agent Mondal et al. linked urease to a nitro-aryl modified surface of a 184 m^2/g silica[62]. Another approach is to use ionic interactions using a urease solution at 6.8 pH (slight negative charge) with a positively charged imidazole functionalized styrene-divinylbenzene aggregates[65].

3.3.2. Synthesis of Porous Polymers

The polymerization of porous polymer systems is a field of polymer chemistry well studied. From adsorbents of all kinds to drug carriers, the porosity of the monoliths or particles are tuned for the application.[81-89] Specifically, particles are of particular interest in packing columns or as resins used in exchange or separation reactions.[86, 90-95] One method to make porous polymer particles is through suspension polymerization combined with a pore forming agent or porogen.[86, 89, 92, 93] These agents can be solvents, solids (e.g. salts), or even supercritical gasses. They are generally solubilized or dispersed with the monomer phase prior to polymerization. When the particles are polymerized, the porogens are removed and the resulting particles have pores defined by the interaction with the monomer and polymer phases.

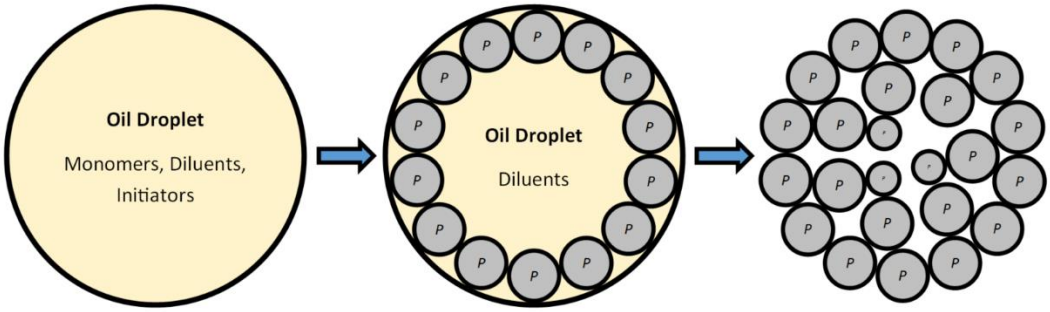

Figure 3.4. Scheme of oil phase droplet with porogen: Polymer is beginning to be formed in the second droplet, with the final droplet an example of porous particle from removal of the porogen.

With this in mind, incorporation of WMSP into the droplets would be a viable carrier with tunable properties. First a screening of various porogens, monomers, and initiators were carried out to determine which system would be ideal to study in the encapsulation. With so many variables, it was deemed necessary to fix some parameters to study. Since the end goal was to entrap WMSP in the matrix, thermal initiators were not studied. By using photo-initiators the porogen choice can be more diverse, due to non-existent solubility issues with the porogen solvent and the continuous aqueous phase that could have arisen from thermal polymerization. One system used in past experiments was a simple combination of a difunctional monomer, ethylene glycol dimethacrylate (EGDMA) polymerized with a photo-initiator, diphenyl(2,4,6-trimethylbenzoyl)phosphine oxide (TPO). Using 365 nm fluorescent lamps or LEDs, the polymerization can take less than a minute to cure.

The aqueous phase was made of 0.5% polyvinyl alcohol of 120,000 MW with an average hydrolyzed content of 88%. This can be premade in large volumes for later use, as the set ratio between the organic to aqueous phase was 1 to 4 by weight, though if polymer yields were a concern that ratio can be increased. Three solvents to

be studied were toluene, n-heptane, and n-butanol, all of which are hydrophobic with different properties of polarity. The organic phase consisted of 25 g of EGDMA (density of 1.05 g/cc) and 125 mg of TPO and the same volume of porogen to monomer. For toluene (density of 0.87 g/cc) that amount was 20.7 g; for n-heptane (density of 0.68 g/cc) that amount was 16.2 g; and for n-butanol (density of 0.81 g/cc) that amount was 19.3. The porogen to monomer ratio is critical especially when considering each porogen per trial has different densities, by fixing the volume ratio at 50/50 this ensure each droplet or particle that will be formed has the same potential to form porosity when the phase separation occurs.

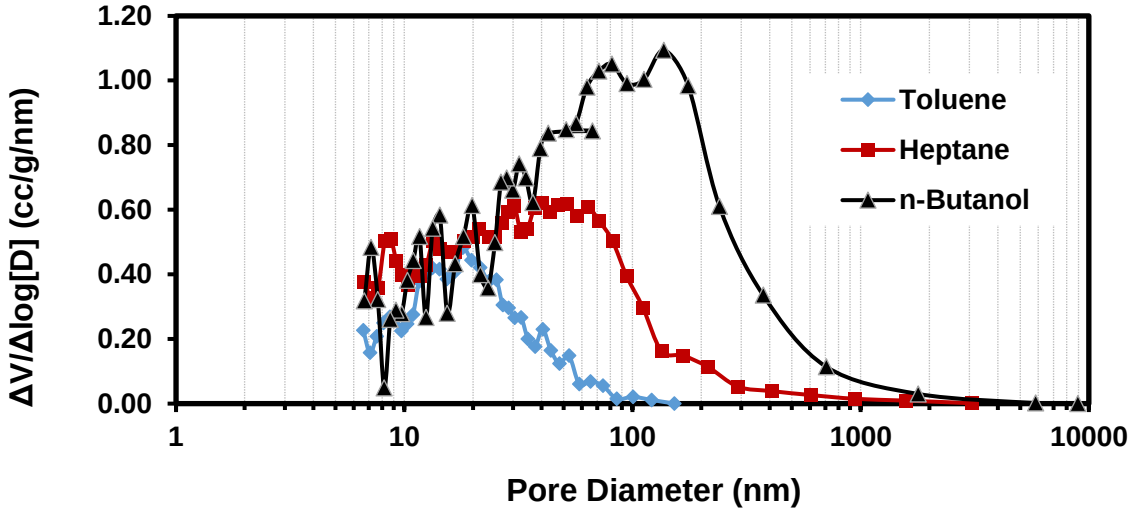

Figure 3.5. Pore size distribution by mercury intrusion porosimetry of polymer particles formed with different porogens.

The organic phase was mixed for 5 minutes covered to prevent exposure to UVA. 200 g of the aqueous 0.5% polyvinyl alcohol solution was placed in a clear plastic container and a paddle agitator was used to impart shear. The organic phase was then poured into the aqueous with the agitator at 225 rpm and left to stir for a minimum of 15 minutes. This time was to narrow the particle size distribution of the oil droplets.

Afterwards the UV curing lamp was turned on and set for 30 minutes, though within 5 minutes the particles were formed.

After the reaction is complete, the particles were screened and washed with successive amounts of acetone, 100 mL. Initially some batches were steam stripped due to the azeotrope exhibited by all three of these solvents, but this was not realistic of what would be done for the particles with encapsulated enzyme. After the washes, they were soaked in 150 mL of acetone, and sonicated for 1 hour. Then the samples were placed on an orbital shaker table to be shaken for 1 day, after which the acetone was decanted and fresh acetone was replaced. This then was repeated for a total of three fresh acetone washes each day. Each trial batch was screened and washed in the same fashion. Then the samples were filtered of the acetone, air dried overnight, then dried in the vacuum oven at 35 °C at 30 inHg to remove any residual solvent.

Two common methods to examine the internal pore structure are porosimetry by mercury intrusion or nitrogen adsorption. Mercury is more suited for meso to macro porosity, where nitrogen is correspondingly micro to meso porosity. By mercury intrusion porosimetry, the pore size distribution of each particle (Figure 3.5) was performed to have a comparison of the porogen's effect on the porosity of each polymer bead. It is clearly seen that based on the distribution that n-butanol had some truly large pores, with toluene being the smallest. This in turn narrows down the next set of experiments to screen with n-butanol being chosen as the porogen. Tuning the amount of porogen to monomer, a 70% v/v of n-butanol porogen under the same conditions above yielded too friable a polymer. Four trials are studied with the encapsulation of WMSP in mind—1) 60% v/v n-BuOH/EGDMA, 2) 56.5% v/v n-BuOH/EGDMA, 3) 56.5%

v/v n-BuOH/EGDMA with 5% (w/w of polymer) Hydrophobic Fumed Silica, 4) 56.5% v/v n-BuOH/EGDMA with 7% (w/w of solids) Hydrophobic Fumed Silica and internal water phase for water in oil in water emulsion. The hydrophobic fumed silica, Aerosil® R 972 (SA: 90-130 m^2/g), will be used to suspend the WMSP in later formulations, and thus was in this comparative study to see its effect on the particles' morphologies.

Table 2. Formulations of photopolymerization of porous macroparticles for use in encapsulation of WMSP.

Formulation						**Nitrogen Adsorption**	
Trial	n-BuOH (g)	EGDMA (g)	Internal H2O (g)	Aerosil (g)	TPO (g)	SA (m^2/g)	PV (cc/g)
1	27	23	0	0	0.125	155 ± 10	0.61 ± 0.03
2	25	25	0	0	0.125	188 ± 9	0.62 ± 0.03
3	25	25	0	1.5	0.125	264 ± 13	0.64 ± 0.04
4	25	25	25	2.1	0.125	293 ± 14	0.35 ± 0.02

The formulations are listed in Table 2, with the nitrogen physisorption analytical results for their corresponding trials. The surface area measurements followed the BET[96] method, and the pore volume measurements used the BJH[81] method, both of which were performed under nitrogen adsorption.

The process to form the particles in formulation 4 was slightly different due to the internal water phase to create a double emulsion (w/o/w). The motivation behind this was to artificially induce porosity within a particle by not only having a solvent porogen but also now water as a porogen. To the BuOH/EGDMA/TPO mixture, 25 g of deionized water with 2% sodium chloride was added and homogenized at 10000 rpm for 5

minutes. This emulsion was then added to the 0.5% PVOH aqueous phase as per the reactions of trials 1-3. The amount of R 972 silica added in 3 and 4 were not arbitrary as well, they were an optimized amount in later formulations to properly suspend 3.0 g of WMSP.

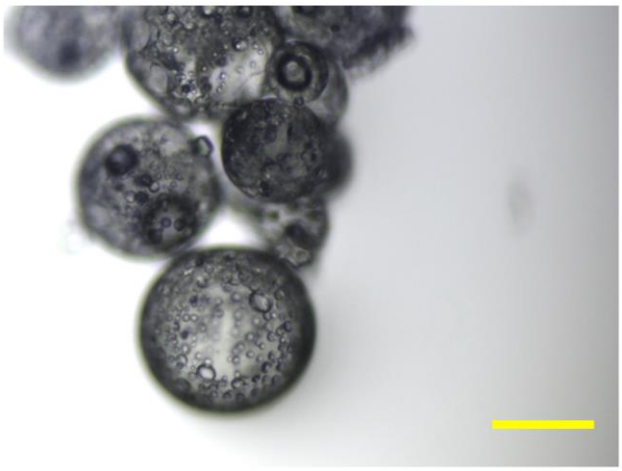

Figure 3.6. Light microscopy image of W/O/W particles showing internal water phase in an otherwise usually transparent particle, scale bar is 500 µm.

A visual confirmation of the internal aqueous phase can be seen by light microscopy (Figure 3.6). SEM images of the four trials can be seen in Figure 3.7. The higher magnification images show the surface and internal porous morphologies that confirm the surface area measurements. In trial 4 with the water-in-oil-in-water particles, the internal phase can be seen on a cross sectioned particle. The areas within the particle look like aggregates but are in fact voids created by the internal aqueous phase. Though there seems to be a loss of pore volume from the nitrogen adsorption measurements, but visually the spheres should have more PV. This is possibly due to the method being nitrogen adsorption instead of mercury intrusion, since nitrogen is better suited for micropores and mesopores.

Photopolymerization of the particles were also tested in a semi-batch process which uses a flow of the suspension through a curing zone.

Figure 3.7. Semi-continuous reaction zone by which the suspension fluid is pumped with a peristaltic pump to the top of the coil, then the oil in water mixture is polymerized along the revolutions of the coil, and final cured material is attained from the outflow.

This semi-continuous method allows for scalability of the polymerization process, as penetration of the UV light can be quite diffused as the phase separation occurs in each droplet. Also, the scale of the reactor and strength of the lamps can be a factor when in commercial applications. The pump flow rate and the length of the tubing in the polymerization zone then determines the residence time each droplet gets with exposure to UV.

With these porous substrates polymerized, trials can now include WMSP in the matrix. The polymer formulations chosen to incorporate the WMSP were the 50/50 (wt/wt) of n-BuOH to EGDMA and the same with W/O/W formulation.

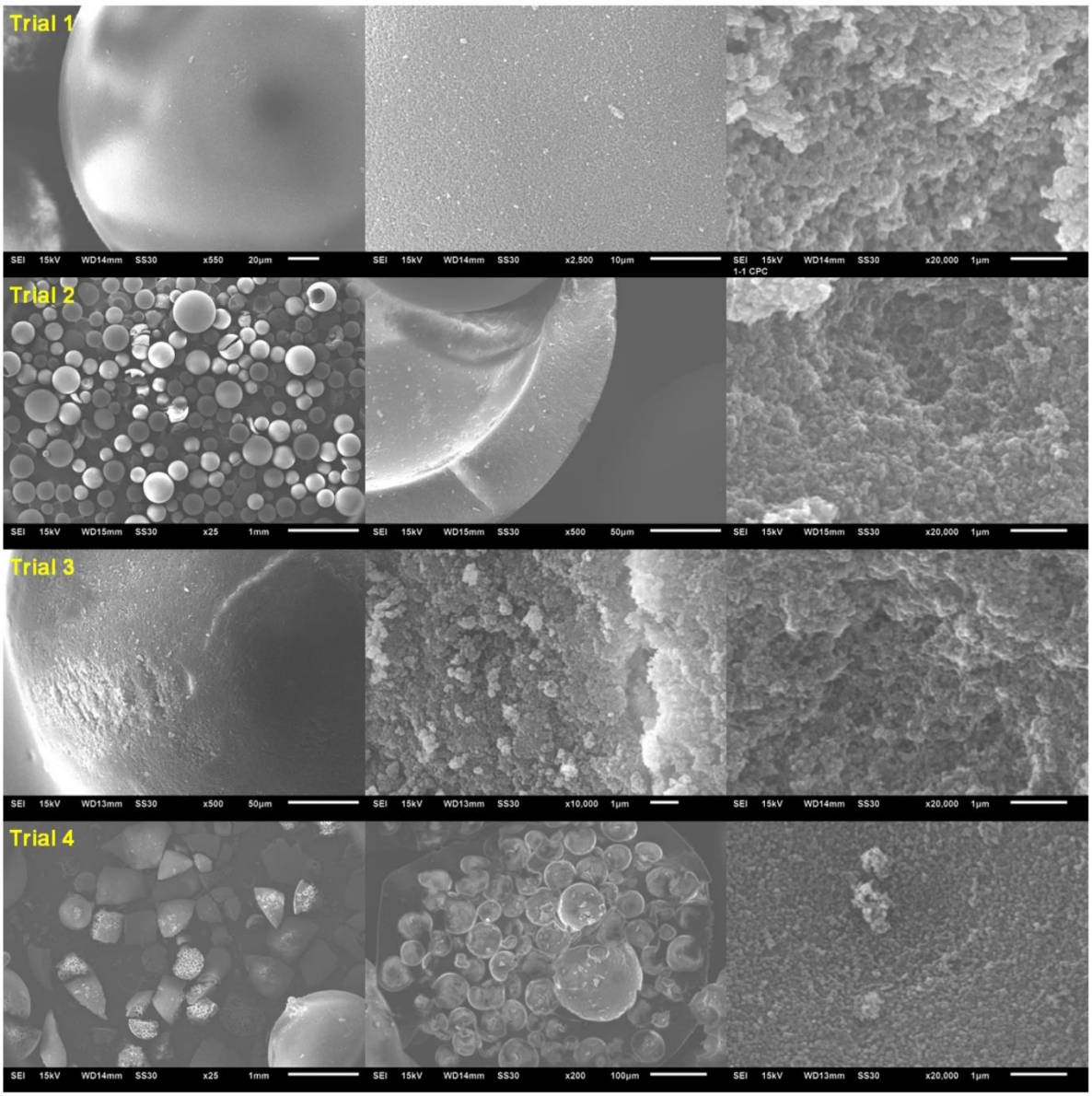

Figure 3.8. SEM microscopy of porous particles from EGDMA and n-BuOH, each row corresponds to the trial in the first image.

Three batches were polymerized to study the possible effect of the filler modification: 1) 100% hydrophobic fumed silica, 2) 50% hydrophobic, 50% hydrophilic fumed silica 3) W/O/W with 100% hydrophobic fumed silica. The WMSP content was set at 10% by weight of the solids amount (EGDMA and fumed silica weight).

The polymerization steps for the WMSP encapsulated porous particles were similar to the non-enzyme batches. With the extra addition of WMSP, a shearing step of the organic phase was required to properly disperse the powder. 3 g of WMSP was added to the 25 g EGDMA, 25 g n-BuOH batches, 0.125 g TPO, and 1.5 g fumed silica (of whichever type was being tested). This organic phase was then homogenized at 10000 rpm for 2 minutes, then introduced into the outer aqueous phase for photopolymerization. In the case of the W/O/W particles, the organic phase was first homogenized with WMSP followed by the internal aqueous phase addition and homogenization.

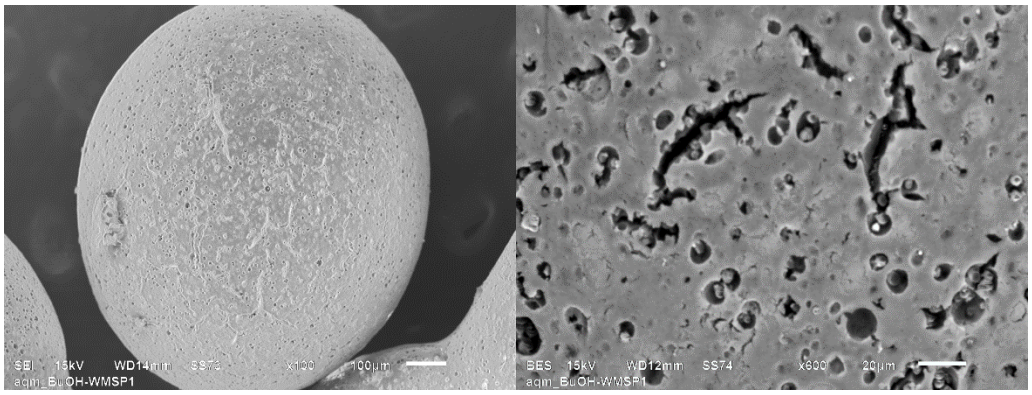

Figure 3.9. SEM imaging of WMSP in porous polymer particles, the left image is secondary imaging, while the right image is backscatter imaging of the particle surface showing pores with WMSP.

Once the particles have been properly sized and reacted under the UV light, they were decanted and washed with acetone accordingly. The same washing sonication and shaker table washings were performed, with the final air dry and vacuum oven dry conditions as the non-WMSP particles. In Figure 3.8, it is seen that the polymer particles with WMSP have dimples where the WMSP are on the surface. The WMSP encapsulated particles can either be stored dry or as an acetone wet-cake under ambient conditions.

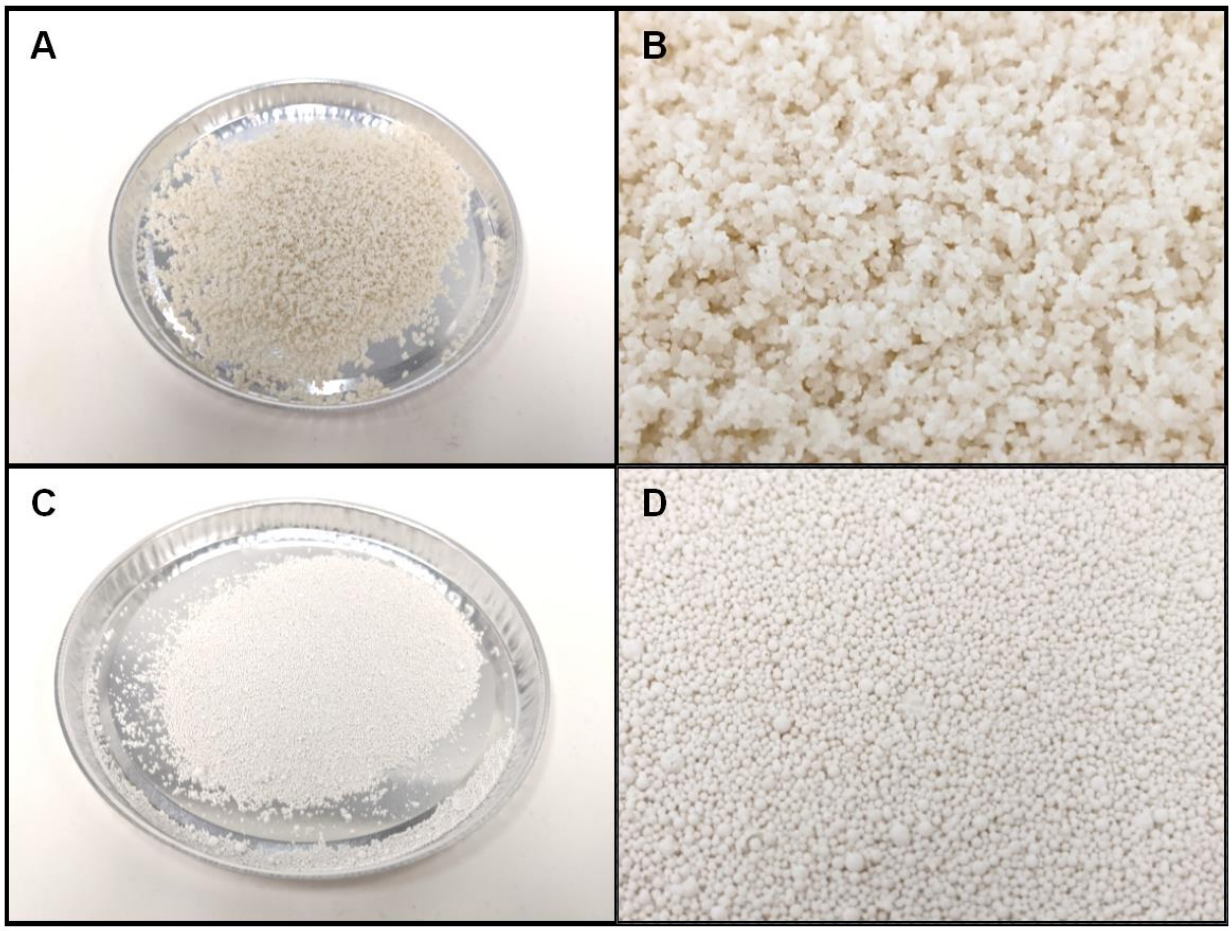

Figure 3.10. Porous polymer particles with 10% WMSP, A & B are acetone wetted samples in which the brown coloring from the WMSP is more easily observable, whereas C & D are the same batch but dried of the acetone.

3.3.3. Adsorption of WMSP on Polymer Particles

Many are endeavoring to create sustainable materials to supplement the large thermoset market. One example of a renewable material is from the epoxidation of common vegetable oils.[97] Most notably are the soybean oil and linseed oil variants.[98] They are currently in mass production and are primarily used as a biobased plasticizer for PVC. Many are studying the polymerization of these monomers with small molecules

or traditional amines.[99-107] Some use naturally occurring carboxylic acids to cure the epoxidized vegetable oils.[108-114] With the use of these water soluble acids, a dispersion is usually created of aqueous acid and epoxidized oil.[115] The curing then occurs at elevated temperature, which requires more energy and requires extra steps to attain usable polymer.

In keeping with the green chemistry trend, biobased polymer particles have been synthesized with epoxidized linseed oil (ELO) and aconitic acid (AA). One main source of aconitic acid is from sugarcane biomass. Every ton of sugarcane leaf matter yields an extracted 2-3 kilograms of aconitic acid.[116, 117] The reaction is a crosslinking of the epoxy functionalized triglyceride with the multifunctional carboxylic acid. These particles exhibit adhesion to many surfaces, due to possible hydrogen bonding from the ring opening of the epoxy groups.

3.3.4. Synthesis of ELO and AA Particles

The particles of this system will be utilized as a solid substrate to which WMSP can be bound. Suspension polymerization was the method to form the ELO and AA particles. The aqueous phase was made by adding 0.4 g of 30% sodium lauryl sulfate (SLS) in deionized water to a total water amount of 171 g, then slowly dissolving 0.9 g of polyvinyl alcohol (up to 2% of the phase). 5-7 drops of 10% antifoam AF in deionized water was metered in while agitating using an overhead stirrer with paddle impeller. The addition of the stabilizers should be performed with suitable shearing and timing to prevent agglomeration or skin from forming on the powder. After a clear solution is seen, 3.9 g aconitic acid was added (a minimum of 2% by weight of the total aqueous phase). The inner oil phase was made of 58.7 g of ELO. The formulation as mentioned

has been optimized to minimize surfactant amount while maximizing the yield of polymer. The oil-in-water suspension was then agitated for a minimum of 30 minutes to stabilize the oil droplet size distribution. Heat was then applied to polymerize the droplets, maintaining a minimum of 80 °C and overhead agitation for a minimum of 10 h.

Once the particles had cured, they can be filtered and washed with deionized water until no more foaming or bubbles can be seen, thus ensuring no residual surfactants on the particles. The particles were then air dried or oven dried to remove any surface moisture. For the application of watermelon seed powder substrate, the desired particle size is 500+ µm, which was achieved at 300 rpm agitation with a paddle impeller. These epoxy particles then were surface coated with WMSP dispersed in an acetone solution with cellulose acetate as a binder. The cellulose acetate used is 50000 MW.

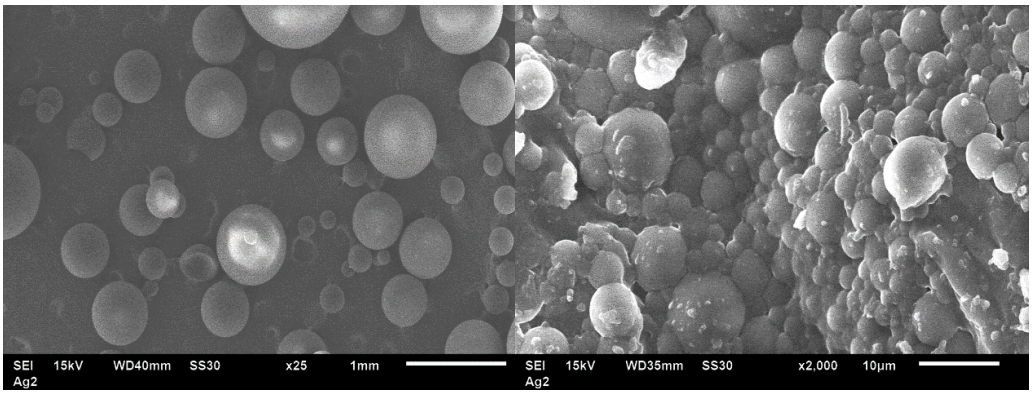

Figure 3.11. SEM imaging of ELO and AA particles created via suspension polymerization, left image are larger particles from impeller blade agitation and right image are a latex from homogenization of the batch.

To 20 g of acetone, 1 g of cellulose acetate was added and mixed until the solution was clear without any undissolved polymer. Vortex mixing initially was performed followed by shearing with a dispersion blade. Then 1.5 g of WMSP was added to this mixture and is homogenized at 10000 rpm for 30 seconds.

Figure 3.12. Epoxidized linseed oil (ELO) particles crosslinked with aconitic acid (AA) on left, WMSP with cellulose acetate coated ELO/AA particles on right.

The coating of the ELO/AA particles were carried out under ambient conditions with simple spray tumbling with air or nitrogen current drying. With the acetone, cellulose acetate, and WMSP solution in a spray bottle, the rotating beads were then spray coated and dried in between sprays. When the required thickness of coating was achieved, the particles were then air dried or vacuum oven dried to remove residual acetone. A qualitative test of the WMSP on ELO/AA beads was carried out in urea solution with universal indicator to determine if the WMSP had been fully occluded showing no reaction, or if there were any unbound WMSP which would result in a cloudy solution.

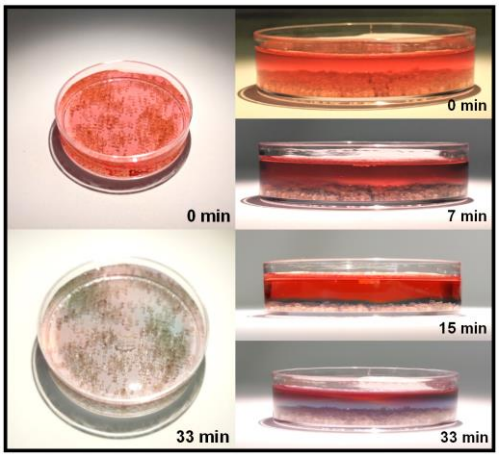

Figure 3.13. WMSP coated ELO/AA particles in solution with universal indicator, pHi = 3.0 and [urea] = 0.03 M.

Since the hydrolysis of urea occurred, with no clouding of solution, the WMSP coated particles were ready to be studied along the other two variants. These particles should have the most accessible WMSP since they were not constrained within a substrate.

3.4. Clock Reaction Kinetics with Immobilized WMSP

A study similar to section 2.4 was carried out to investigate the pH profiles of the various immobilized WMSP. The base conditions to be tested were 5.7 mM of urea, 3.54 units/mL, and a starting pH of 4.0. Three kinds of immobilized WMSP were tested—WMSP in agar hydrogels, WMSP in porous methacrylate particles, and WMSP on solid epoxidized linseed oil particles. The agar hydrogel should allow for faster diffusion due to the amount of water in each particle; the porous particles reaction with urea should be slower due to diffusion properties through the more rigid polymer pores; and lastly the solid particles should exhibit a high exposure of the WMSP enabling faster interaction with aqueous media.

For the trials with different WMSP-urease amounts (Figure 3.14), there was no clear distinction between immobilizations. At the lowest concentration of WMSP, the

ELO particles seemed the faster of the three, being the first to clock. With regards to the free WMSP, there shows no significant difference. In Figure 3.15, the urea concentration was varied and shows almost completely identical behavior. Compared to the free WMSP, all three techniques were slightly slower. Lastly, the initial pH is varied from 3.0 to 4.2 pH (Figure 3.16). Here there are drastic differences, with all three profiles being able to clock at lower pH faster than the free WMSP. The porous particle seems to be the most reactive, possibly due to the particle's production of ammonia not being able to be neutralized as fast by the surrounding solution.

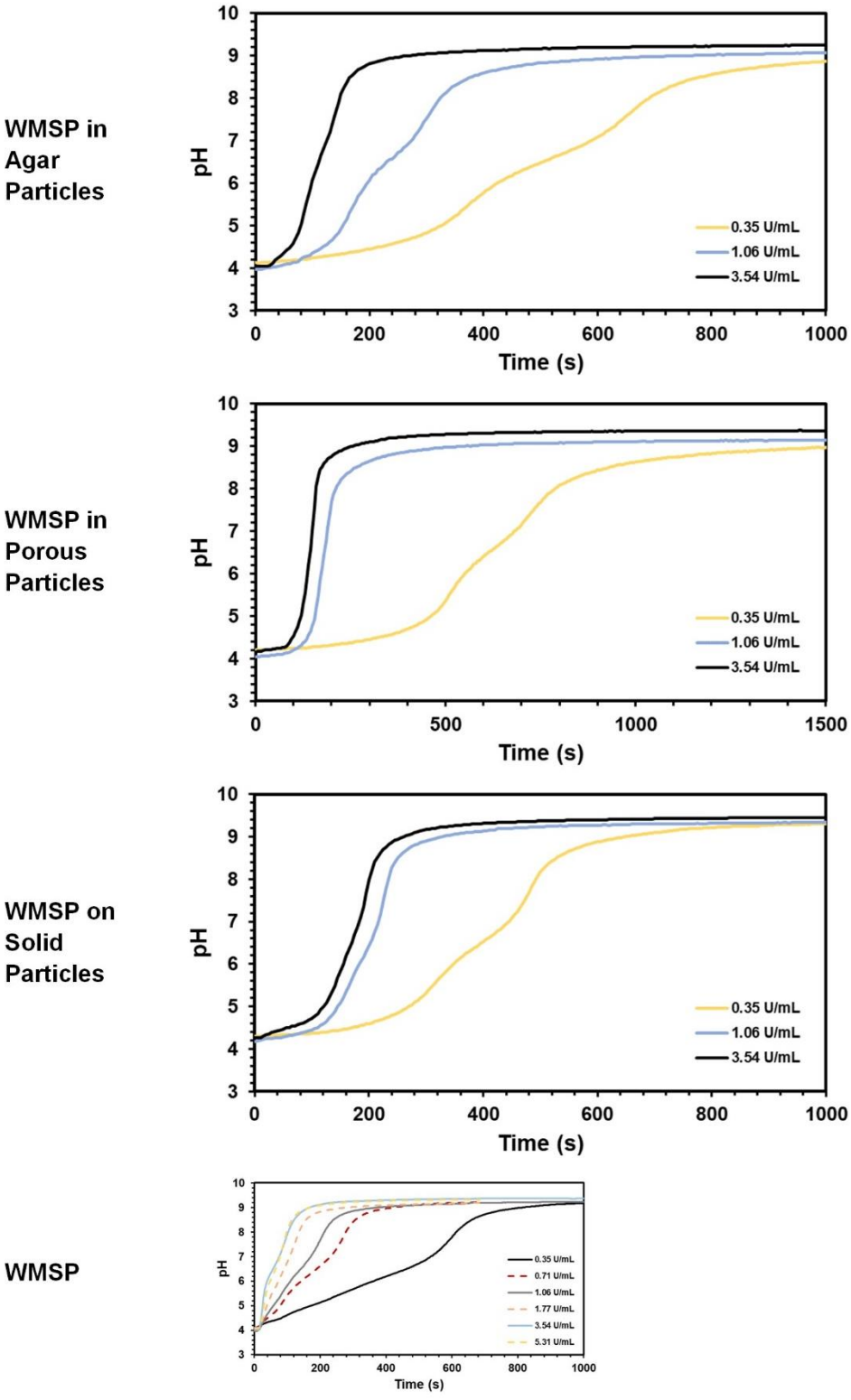

Figure 3.14. Variation of WMSP-urease concentration with different immobilization techniques, [urea] = 5.7 mM, pHi = 4.0.

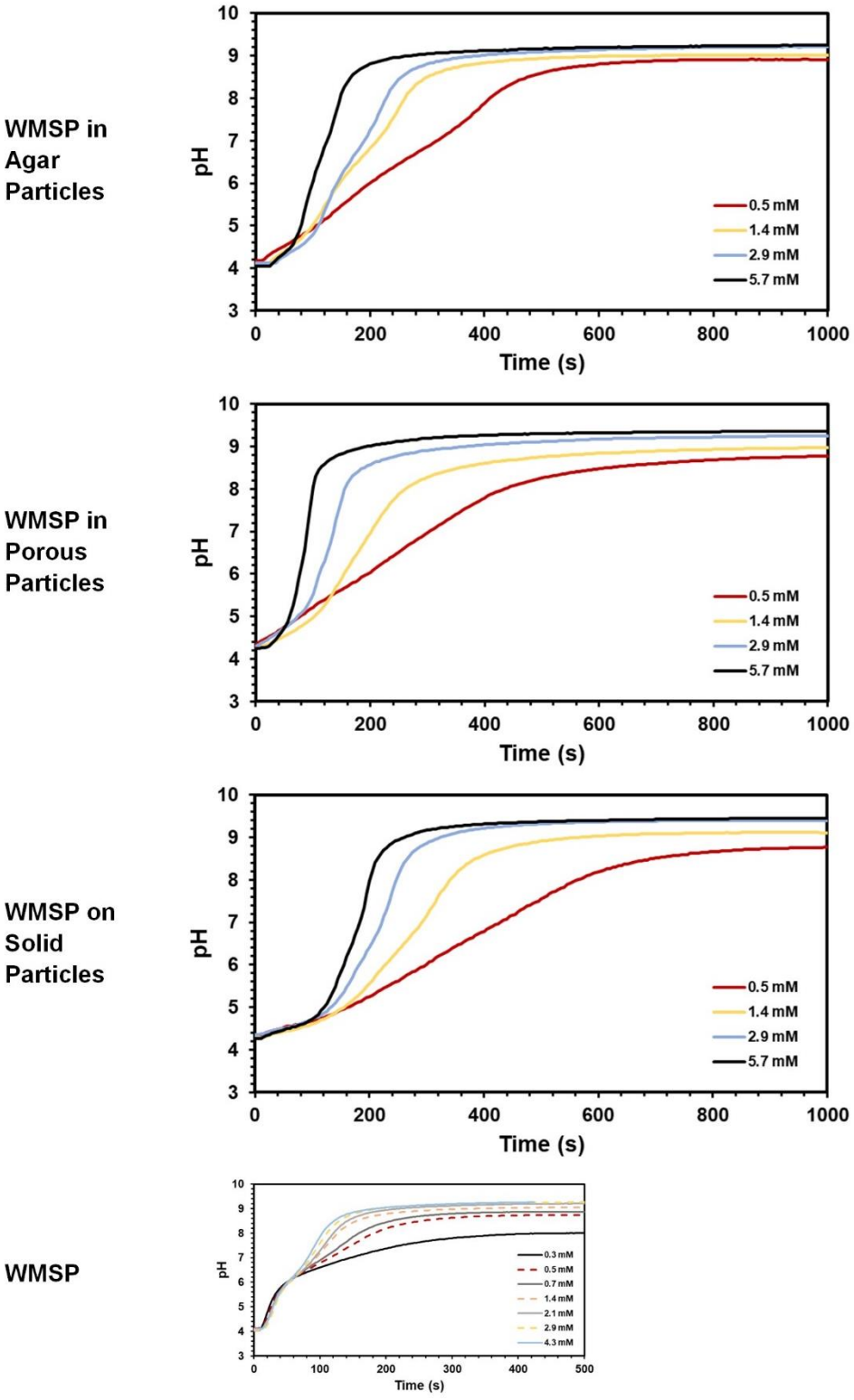

Figure 3.15. Variation of urea concentration with different immobilization techniques, [urease] = 3.54 U/mL, pHi = 4.0.

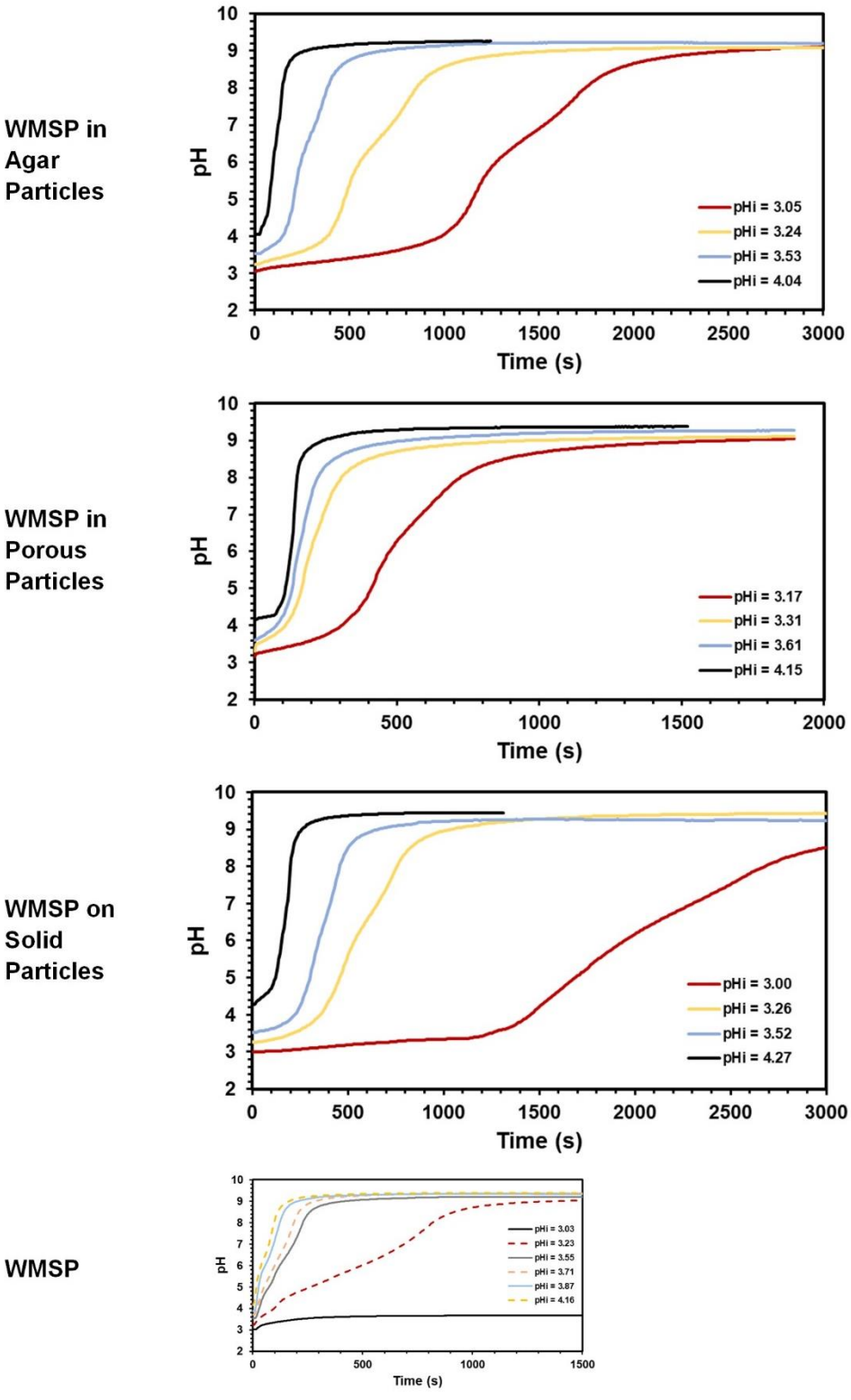

Figure 3.16. The effect of initial pH with different immobilization techniques, [urea] = 5.7 mM, [urease] = 3.54 U/mL.

Three batches of porous EGDMA-BuOH particles with 10% WMSP were made to test the effect of the type of fumed silica filler on the particles. It was predicted that the particle's internal hydrophobicity or hydrophilicity could be tuned. However, the difference in addition of hydrophilic fumed silica showed not difference in the clock behaviors of the urea-urease reaction.

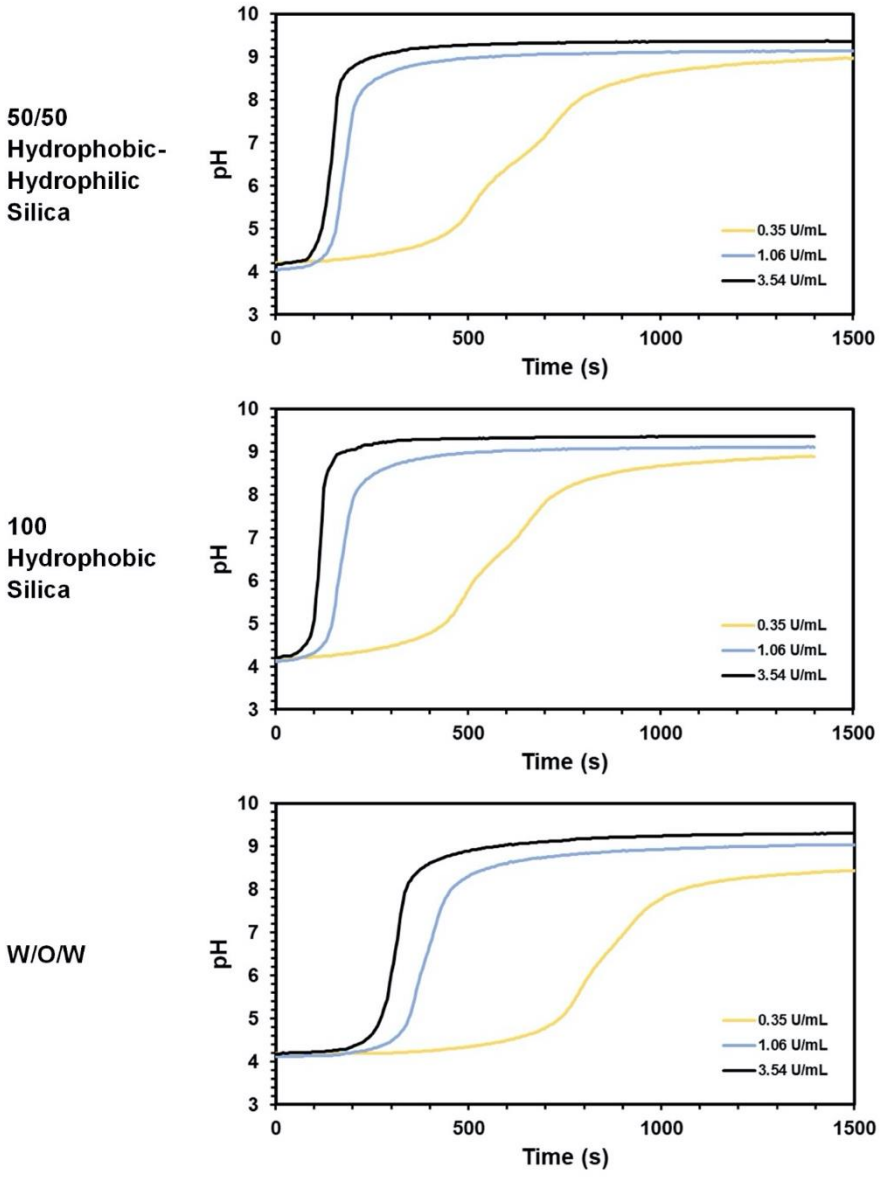

Figure 3.17. Urea-urease pH clock profiles for three types of porous particles with WMSP, [urea] = 5.7 mM and pHi = 4.0.

One possible explanation for the lack of effect of the filler type could be the filler concentration (6% by weight) is too low to show any true variance. Another rationalization could be that the filler had no interaction with the internal or external surfaces of the particle and was simply embedded within the matrix. The third plot in Figure 3.17 details the clock behavior for the W/O/W particle, which surprisingly was the slowest. Even though there were large voids inside the particle, the wettability and density of the particles changed.

3.5. Recyclability of Immobilized WMSP

One of the main motivations for enzyme immobilization besides improving stability is the recyclability of the enzyme and substrate. Not only does entrapping the WMSP allow for the enzyme to be recycled in subsequent reactions, but also it allows for easier manipulation of the enzyme or in this case the WMSP. As the powder's particles are around 5 microns, filtering the WMSP between usage would be intensive with a significant loss of material. By having them in agar or particles that are in the mm or 500+ µm range, it becomes much easier to simply wash and filter with a 200 mesh screen. Agar particles and porous particles were used in 10 successive urea-urease clock reactions, with acid washes in between to ensure that any internal ammonia would be neutralized.

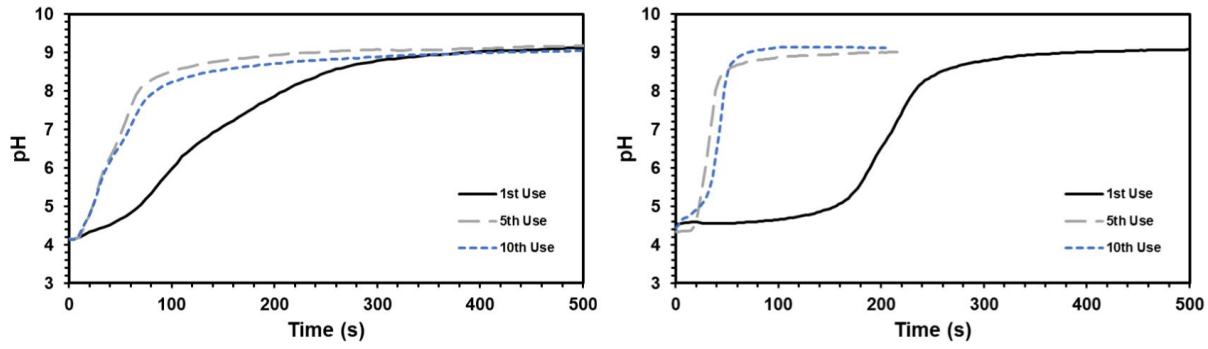

Figure 3.18. Recycling clock urea-urease reactions with agar particles (left) and porous particles (right), [urea] = 5.7 mM and [urease] 3.54 U/mL.

After 10 reaction cycles, both substrates showed no retardation of the clock reaction. Though in the agar particles, since they are slightly friable continued use was imparting some damage to some. Both showed an acceleration of the clock at after subsequent reactions. Unlike the hydrogel, the porous particles were much stiffer and resitant to breaking. They also can be subsequently dried and stored for later use.

3.6. Conclusions

Immobilization can improve the stability, reusability, and activity of enzymes in certain conditions. In the case of WMSP, the enzyme is already well protected and was shown to be highly stable. Three different approaches were then studied to immobilize the powder—agar hydrogel encapsulation, porous particle entrapment, and surface coated on a polymer particle. The hydrogel provides a particle already with an aqueous environment ready for urea. The porous particle is a durable and tunable matrix. And the surface modified particle is a simple yet green approach.

By encapsulating the WMSP with these methodologies, they became more user friendly when performing reactions. The particles increased the activity at lower pH and performed even faster with consecutive use. Notably, by having them in the porous particles, the material is now essentially an ion exchange resin—specifically a WMSP ion exchange resin catalyzing the decomposition urea to ammonia and carbon dioxide.

CHAPTER 4. APPLICATIONS OF WATERMELON SEED POWDER

4.1. Quorum Sensing and Reaction Diffusion Gel Growth

4.1.1. Introduction

Quorum sensing (QS) is a biological phenomenon that can induce biofilm formation and bacterial colony growth.[118, 119] This is generally a function of population density i.e. when bacteria are in a favorable colony size, a certain gene expression is triggered spending resources to propagate for example. These factors can then affect the virulence of bacterial growth.[119] The formation of biofilms is a means to aid in communication of the bacterial colony, which is further enhanced by their proximal intimacy. In bacteria specifically, quorum sensing can regulate motility, symbiosis, even antibiotic production.[120]

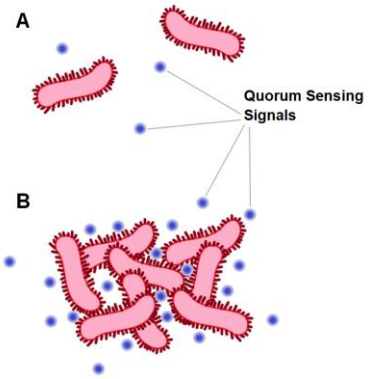

Figure 4.1. Quorum sensing example, with low density of cells (A) and high density of cells (B). Once the quorum is reached, gene expression is prompted.

There is current discussion on the behavior of quorum sensing with relation to diffusion sensing and even gradient sensing. Spatial density, diffusion limitations, and their combination are all properties that can be attributed to some form of "communication" between individuals.[121-123] Biofilm formation is quorum dependent, and additionally the dynamics of substrates and nutrients in the films are primarily through

diffusion. Reaction-diffusion systems[124-130] are used to model the exchange and flow of different compounds where convection is limited, e.g., a biofilm or gel.

4.1.2. Reaction-Diffusion Hydrogel Growth with WMSP in Agar Particles

The urea-urease system has been previously coupled with the thiol-acrylate system to create a temporal controlled gelation of the monomers.[77] By using the tunable clock of the urea-urease reaction to produce base, a Michael-addition type polymerization occurs. The reaction was performed using a trifunctional thiol and difunctional acrylate--ethoxylated trimethylolpropane tri(3-mercaptopropionate) (THIOCURE® ETTMP 1300) and poly(ethylene glycol) diacrylate (PEGDA, average M_n = 700).

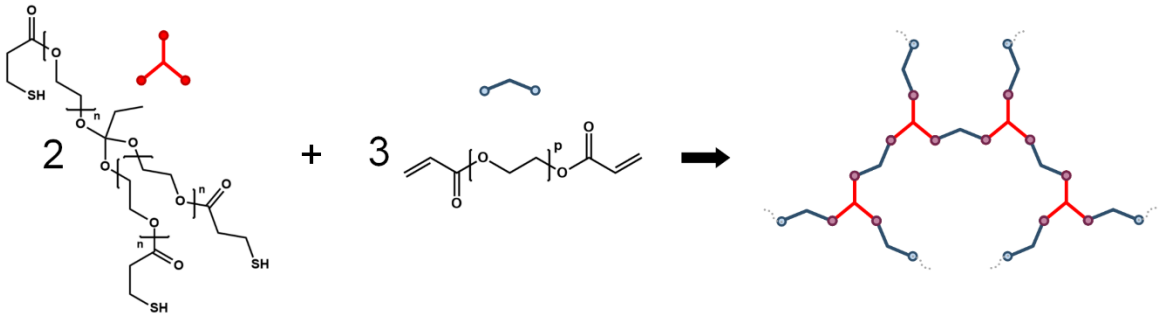

Figure 4.2. Base-catalyzed reaction of ETTMP 1300 and PEGDA 700 to form the hydrogel network.

This system can then be used in conjunction with the immobilized WMSP created to be a gelling agent or film forming agent for the particles. The solution prepared was 180 g of Nanopure™ water, with 1.8 g of urea (0.15 M), 13.12 g of ETTMP 1300 (0.05 M), 10.59 g of PEGDA 700 (0.075 M), 3 drops of 1% antifoam AF, 0.5 g xanthan gum, and 5 drops of 1% bromocresol purple in ethanol. Bromocresol purple has a pK_a of 6.3 and is yellow below 5.2 pH and purple above 6.8 pH. This means that when urea was hydrolyzed by the WMSP to form ammonia, a blue-purple color should be seen.

Because the thiol in the formulation is acidic, the solution color should remain yellow until ammonia was produced. Production of the above mixture required homogenization at 10000 rpm for 1 minute, as the xanthan gum needed to be properly dispersed. A degassing step was performed to remove any access bubbles. To accomplish this since the mixture is highly viscous, it was poured into a larger container to increase surface area contact with the negative pressure. Then that container was placed in a chamber and treated with successive vacuum and release iterations with mixing in between to collapse the bubbles or foam.

Once the translucent yellow solution was made, it was poured into petri dishes, and WMSP immobilized in agar particles was introduced. The urea hydrolysis from the urease contained within the WMSP then generated ammonia that would gel the mixture turning it blue. To confirm that the indicator color change was showing the front of the gel formation, a side-by-side test of solution with WMSP was done with indicator and without indicator.

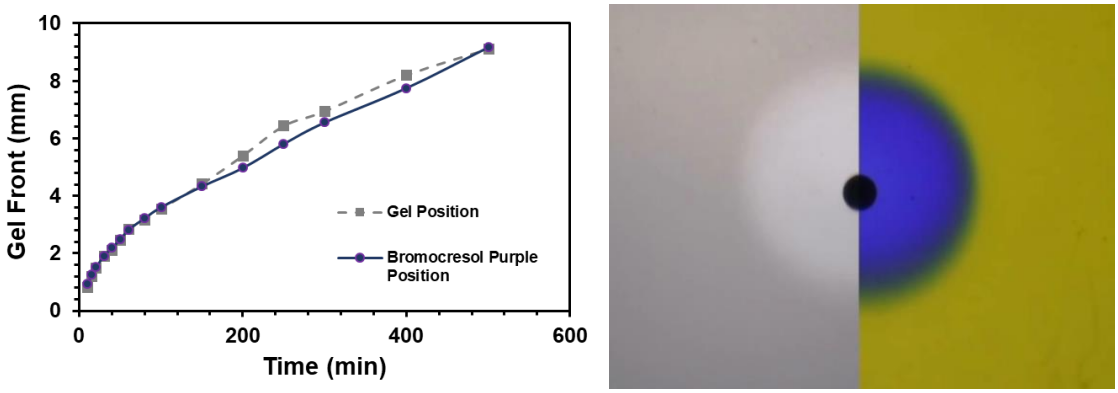

Figure 4.3. Plot detailing the position of the hydrogel formation compared to the pH indicator, bromocresol purple, propagation in solution.

A time lapse recording was done on both trials to compare the two. From Figure 4.3, the position versus time plot shows that there is negligible difference between the hydrogel and blue indicated areas.

A flow cell was setup with camera attached to investigate multiple layered hydrogel formation around the WMSP in agar particles. Since the particles had iron oxide in them, they can be positioned in the cell prior to adhesion. Once they were appropriately placed, three differently colored PEGDA/ETTMP solutions were flowed through the cell: 1) with bromocresol purple indicator to form a blue layer, 2) with no indicator to form a colorless layer, and 3) with a water dispersible red oil color to form a red layer. The first layer adhered the WMSP particles to the glass surface, and removal of the magnets can be done after just a few seconds.

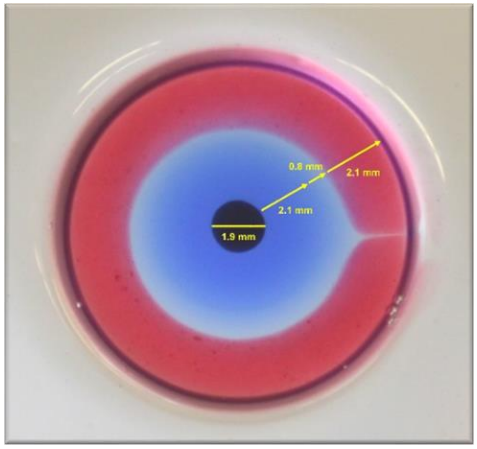

Figure 4.4. WMSP in agar particle with three ETTMP-PEGDA hydrogel layers made with bromocresol purple indicator, no indicator, and red oil colorant.

After the three layers were visualized, a solution of 10 pH NaOH in deionized water was continuously recycled through the cell. This then hydrolyzed the ester bonds in the hydrogel which in turn degraded the gel. After 450 minutes, the three layers had degraded and the WMSP particle detaches from the surface (Figure 4.5). Since the

WMSP in agar particles adhered to a surface, it was feasible to determine the strength of the ETTMP-PEGDA hydrogel. Initially it was thought that using the same flow cell, adhesion strength could be gauged by changing the flow rate and seeing detachment.

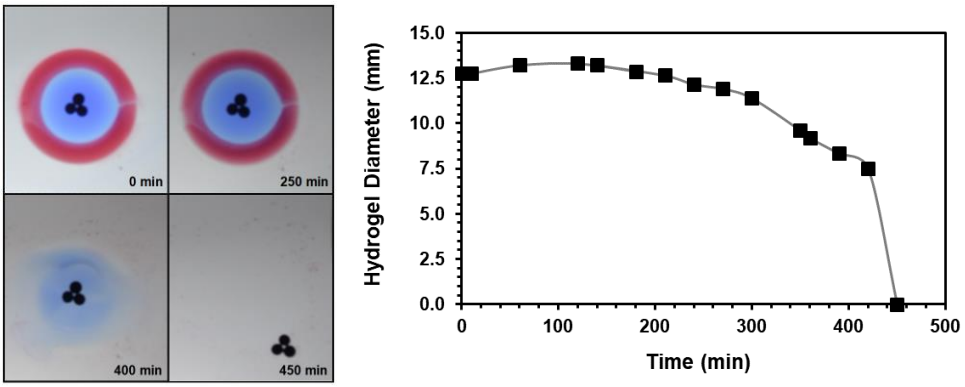

Figure 4.5. Degradation of the hydrogel layered WMSP in agar with recycled 10 pH aqueous NaOH, right plot is the hydrogel diameter versus time plot.

This proved not to be the case, as flow rates of above 2 L/min resulted in no detachment of any sized particle. Geometry was thought to be a factor, and WMSP agar particles were adhered inside the tubing in which fluid would flow; this also had no detachment. Scale up of the hydrogel was then done for mechanical testing.

Two types of test were carried out on the ETTMP-PEGDA hydrogel formulation: a lap shear test (based on ASTM F2255-03) and a peel test (based on ASTM D2861-87). The lap shear test pulls on a thin sheet of polyethylene that was adhered to various size discs of hydrogel. The peel test is a perpendicular pull of the adhered polyethylene, here the polyethylene sheet width was varied. The hydrogel was made by spiking the monomer solution with 10% (wt) ammonium hydroxide in deionized water with a ratio of 4 g of ETTMP-PEGDA solution to 40 µL of spike solution. The reasoning behind this is that the testing is already sensitive for a hydrogel, and the addition of a WMSP agar particle imparts heterogeneity into the material. However, several tests of hydrogels

formed by the WMSP particle were done and plotted on the same graph to show that there was no strength difference between the ammonium hydroxide polymerized gel versus WMSP particle polymerized gel.

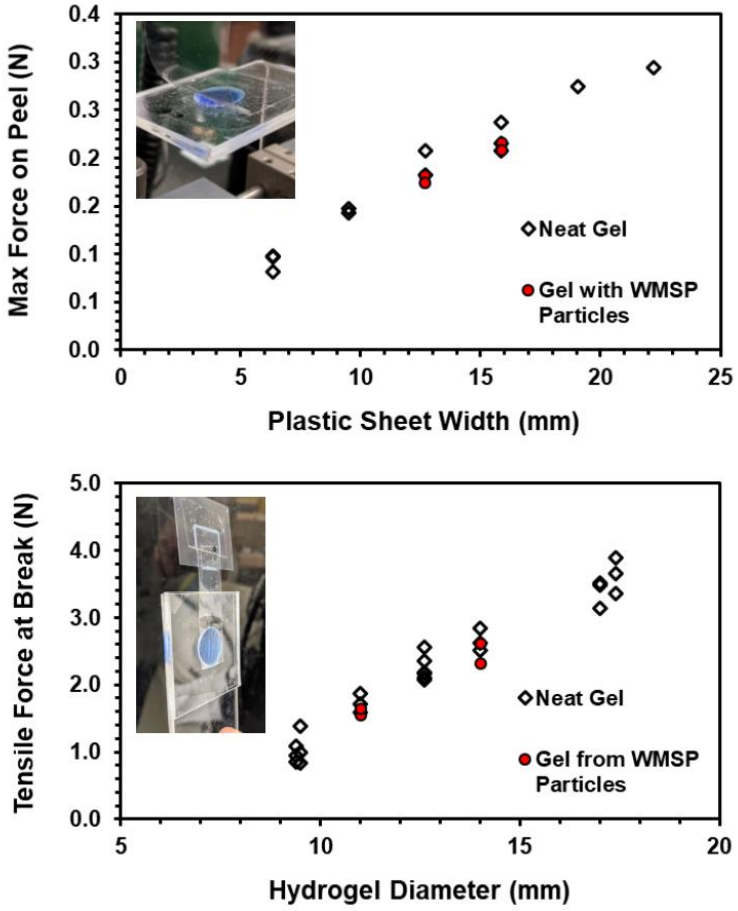

Figure 4.6. Mechanical testing of ETTMP-PEGDA hydrogel; peel test (top) and lap shear test (bottom).

The testing was performed on an Instron 5582 Universal Tester equipped with a 2 kN load cell at a constant crosshead rate of 2 mm/min.

4.1.3. Quorum Behavior with WMSP in Agar Particles

Synthetic quorum sensing is an important study as analogues to the biological phenomena[131-133]. By modeling the biological communication with synthetic materials, perhaps some dynamics can be seen to mitigate biofilm formation or to utilize it in a beneficial way. Previously,[134] agarose beads with watermelon seeds showed quorum behavior with reaction-induced convection. This has also been observed with the WMSP in agar particles with the ETTMP-PEGDA solution.

A quorum with the WMSP particles occurs due to an acidic environment neutralizing the produced ammonia from the urea hydrolysis. Though with a “quorum” number of particles, the ammonia produced was enough to locally raise the pH, which in turn accelerates the urea-urease reaction. Coupling this behavior with the hydrogel solution, a biofilm analogue can be visually seen.

Figure 4.7. Quorum behavior of WMSP agar particles in a solution of aqueous ETTMP-PEGDA with bromocresol purple indicator, clusters of particles react faster (left) and larger particles and clusters react faster (right).

Several parameters could influence the quorum sensing of these particles: number of particles, size of the particles, and all the solution concentrations (acidity, urea amount, WMSP concentration of particles). Investigating 0.05 M, 0.075 M, and 0.100 M

concentrations of urea in the ETTMP-PEGDA solution, particles were purposefully placed in group configurations and discretely by size.

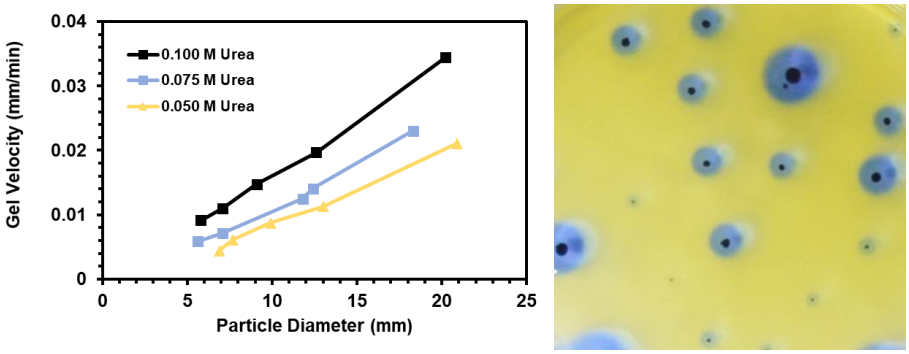

Figure 4.8. Plot of three different urea concentrations of ETTMP-PEGDA solution with different sized particles versus the gel growth velocity.

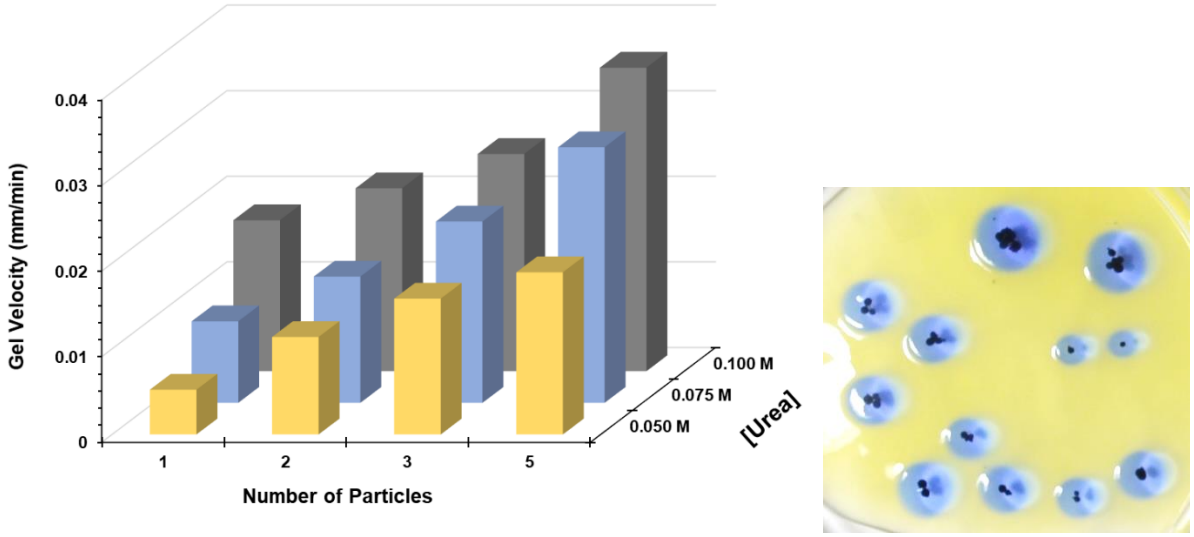

Figure 4.9. Hydrogel growth velocity versus the number of particles and with their corresponding urea concentrations.

In both plots of Figure 4.8 and Figure 4.9, larger particles or more particles do indeed stimulate hydrogel growth. One of the theories for quorum is a gradient or diffusion sensing, in this system the smaller particles when in proximity of the larger ones could be starved of urea, or there is a urea gradient.

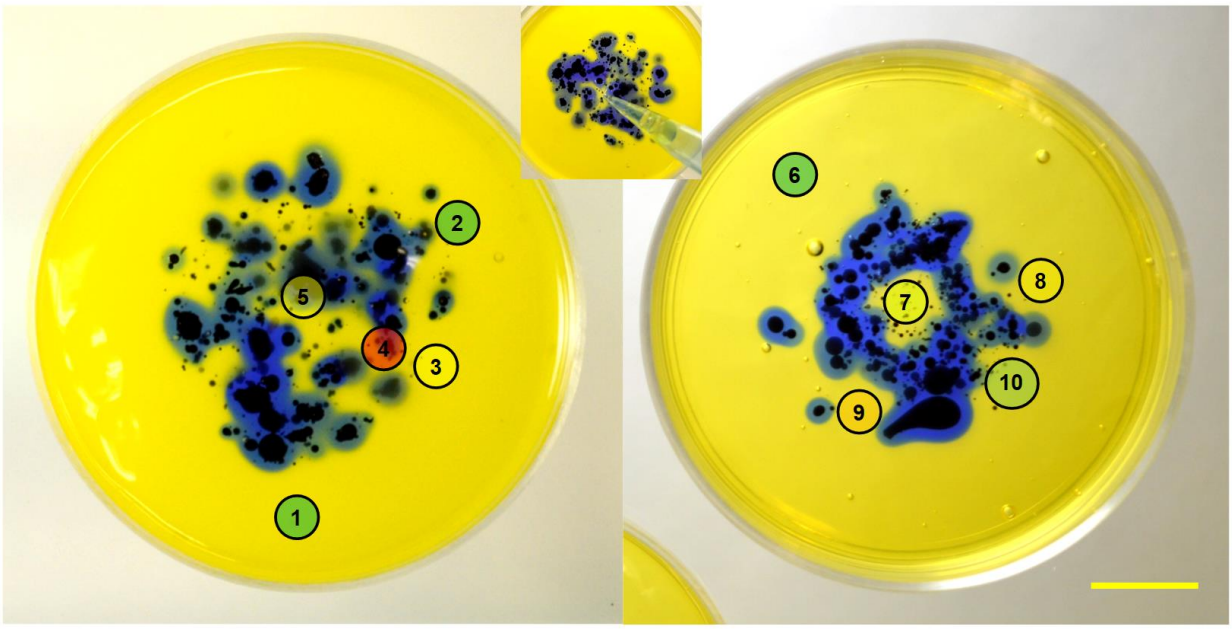

Figure 4.10. Urea gradient testing of ETTMP-PEGDA solution reacted with WMSP in agar particles.

Table 3. Spot analysis results of urea concentration losses from Figure 4.10.

Spot	**1**	**2**	**3**	**4**	**5**
Urea Loss	0.0%	2.4%	20.6%	42.4%	24.7%
Spot	**6**	**7**	**8**	**9**	**10**
Urea Loss	0.0%	13.5%	20.9%	23.7%	4.7%

To visualize the urea concentrations of certain areas, spot testing was performed of various locations in the WMSP reacted ETTMP-PEGDA system. To analyze the urea content, the Nessler's assay was utilized—instead of analyzing an unknown enzyme sample, the same known activity sample was used in each trial. The unknown now comes in the form of 200 µL of urea consumed ETTMP-PEGDA solution, as 200 µL of a 3% urea solution was the original assay amount. The assays did show that there was loss of urea in the solution of confined areas between particles.

Since all the pH profiles from the previous sections used constant stirring, it is likely that a similar density dependent behavior could be seen. The uniform squares (Figure 3.3) made from the casting the WMSP in agar would be the ideal case to test for this dynamic density dependent phenomena.

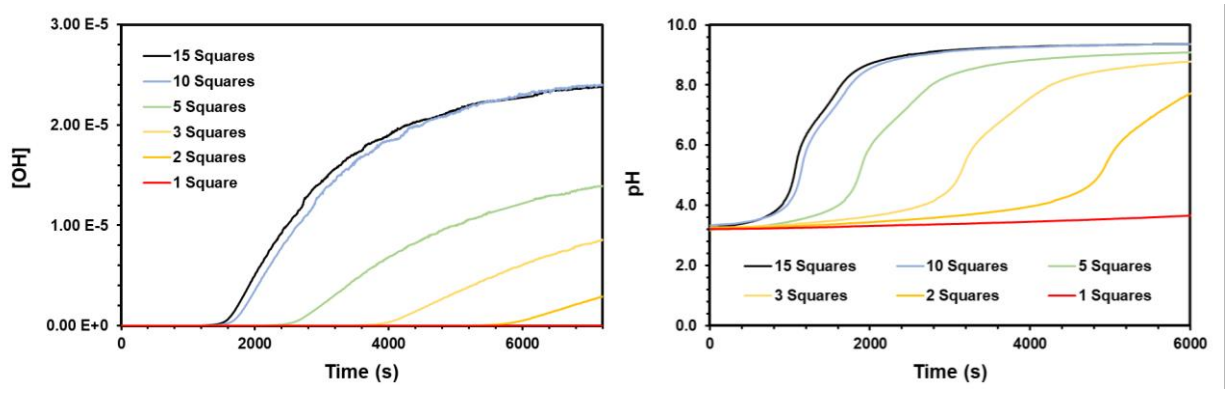

Figure 4.11. pH and [OH] profiles for various counts of square agar individuals with WMSP [urea] = 13.9 mM with initial pH at 3.0.

The testing conditions are 3.0 pH and a 500 µL spike of 10% (wt/wt) of aqueous urea. The solution volume was kept constant at 60 mL. Weighing at least 10 squares, an average weight per square is 72 mg, 5% of which is WMSP (14.4 mg/square). It is clear in this time frame, 2 squares in this solution is the minimum number needed to clock.

4.2. Conclusions

Quorum sensing and biofilm formation are important biological concepts that can be studied in various ways. Using WMSP encapsulated in agar particles and uniform squares is a synthetic approach to study a quorum-type behavior. Coupling this communicative property with thiol-acrylate monomers leads to a system that not only clocks when they are suitable in size or count, but also self-adheres and forms a gel biofilm analog. The reaction-diffusion growth of this gel can be layered to study different

diffusion or encapsulating technologies. Moreover, the gel when formed is quite resilient to fluid shearing motion on surfaces from glass to plastics.

4.3. Future Work

4.3.1. Temporal Controlled Adhesive with WMSP

Preliminary work has been done to create an adhesive using WMSPs. Since the thiol-acrylate system has been done in a hydrogel, concentrating the monomer content should make for a stronger adhesive. An unfortunate property of a one-pot thiol-acrylate glue is a short shelf-life due to free radical reactions of the monomers even with the inhibitors present. There are two ways to mitigate this: 1) use an alternative system or 2) separate the two monomers for a two-pot system. To use the WMSP as a form of delayed base release, the adhesive would already have to be two parts—urea in one portion and the WMSP in the other.

The thiol-acrylate system is very difficult to use in concentrated solutions for base catalyzed reactions: 1) low shelf life due to free-radical reactions and 2) addition of base causes heterogeneous phase separation. This means that the WMSP urea-urease reaction can be applied, as the clock can be tuned to release base after a user-defined induction period—e.g. lowering the initial pH, lowering the [urea], or WMSP amounts all can slow the clock reaction, and vice versa.

Initial trials were studied with ETTMP 1300-PEGDA 700 with high monomer ratios +30% (wt/wt) formulated with anhydrous ethanol, WMSP, urea, and bromocresol purple indicator. Fumed silica was added to viscosify the mixture into a paste. Urea has slight solubility in ethanol, but the alcohol allows for use of less ethoxylation and even water insoluble monomers. By removing water from the formulation, the urea-urease

reaction cannot take place. This means to activate the curing, the addition of water to the total formulation would drive the urea hydrolysis.

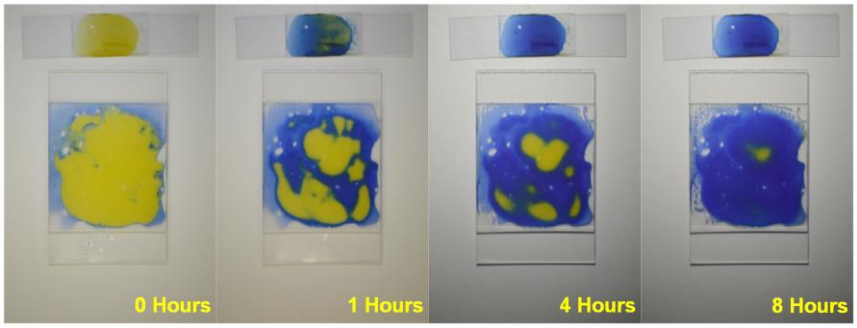

Figure 4.12. Water activated, ethanolic formulation of ETTMP-PEGDA adhesive with WMSP and urea.

This formulation was strong but only had a pot life of 1-2 months. It was then proposed to study the thiol-epoxy reactions. Not only do you gain pot life, but the –OH groups on the ring opening of the glycidyl groups should provide adhesion. Formulations were tried with three kinds of activation: water activation, where urea and WMSP are in formulation; WMSP activation, where urea-water is in the mixture; and lastly 2-part where part-a had WMSP and part-b had urea-water. The four of the most promising formulations are detailed in Table 4. Other monomers were added to the list of potential thiol-acrylate and thiol-epoxy formulations: 2,2′-(ethylenedioxy)diethanethiol (EDDT), trimethylolpropane triacrylate (TMPTA), trimethylolpropane triglycidyl ether (TMPTGE), trimethylolpropane tris(3-mercaptopropionate) (TMPTMP), and poly(ethylene glycol) diglycidyl ether (PEDGE M_n = 500).

Table 4. Adhesive formulations with WMSP and corresponding bond strength testing.

	Part A	Mass (g)	Part B	Mass (g)	Lap Shear Test (psi)
#7	TMPTGE	3.78	WMSP	1.3	88.0 ± 8.4
	ETTMP 1300	16.22			
	20% Urea in 3 pH H2O	4			
	Fumed Silica	2			

	Part A	Mass (g)	Part B	Mass (g)	Lap Shear Test (psi)
#8	TMPTGE	11.24	WMSP	1.3	49.7 ± 1.0
	EDDT	9.48			
	20% Urea in 3 pH H2O	4			
	Fumed Silica	1.36			

	Part A	Mass (g)	Part B	Mass (g)	Lap Shear Test (psi)
#9	PEDGE 500	13.08	WMSP	1.26	53.4 ± 15.1
	TMPTMP	6.92			
	20% Urea in 3 pH H2O	4			
	Fumed Silica	1.19			

	Part A	Mass (g)	Part B	Mass (g)	Lap Shear Test (psi)
#10	TMPTMP	10	TMPTA	7.4	TBD - Exceeded Force Gauge
	WMSP	1	30% Urea in 3 pH H2O	2.6	
	Fumed Silica	0.23	Fumed Silica	0.5	

Testing for the formulations were assessed on a 100 kgf force gauge with a manual screw and clamps Figure 4.13. The samples to be glued were two vinyl microscope slides, with 1 inch or ½ inch overlap depending on the strength of the glue. Once the samples were cured, they were clamped and broken until a peak force at break is read. Formulation #10 showed excess of 260 psi but had yet to break. For the formulations, the usual cure time is 5 hours, whereas formulation #10 hardened in 1-2 hours. Full cure time for #10 is at least 4 hours; at 2 hours the sample had a strength of 150 psi.

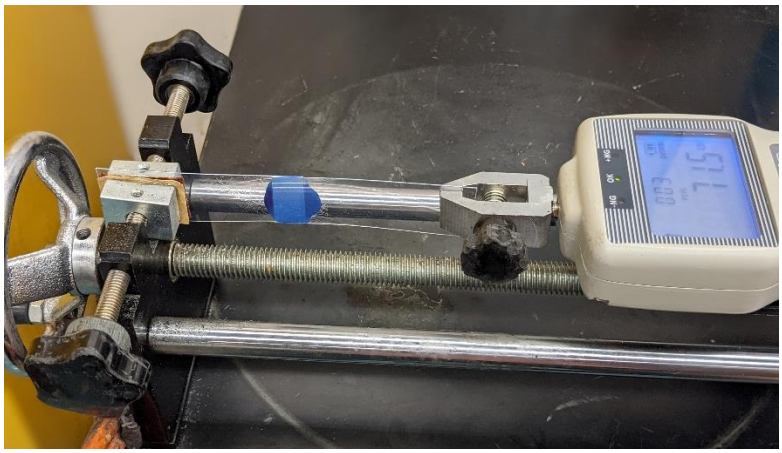

Figure 4.13. 100 kgf force gauge with aluminum clamps, mounted on a movable manual screw crank.

4.3.2. Other Potential Applications

With the layering trials of the WMSP, it is possible to have sensors or active pharmaceutical ingredients in each layer, that could peel or erode away with certain stimuli. Also the WMSP in agar particles reaction with ETTMP-PEGDA solution can take place in a 3D environment making spherical particles. Urease can also be used in bio-mineralization of cement,[135, 136] which would require an inexpensive and available enzyme source, namely WMSP. WMSP is a highly stable, active, and cost effective material. Industrial applications generally optimize time and raw material costs which usually eliminate costly enzymes from consideration, but with WMSPs it is very much a possibility.

APPENDIX. ADDITIONAL FIGURES

Table A.1. Dilutions of ammonium sulfate stock solution for calibration curve of Nessler's urease assay

Stock Concentration:
3.41 mg NH3 / mL

Spikes of Stock (uL)	NH3 (mg)	ABS
0	0.00	0.051
150	0.51	0.709
200	0.68	0.898
300	1.02	1.307
450	1.53	1.582
250	0.85	1.091
350	1.19	1.347

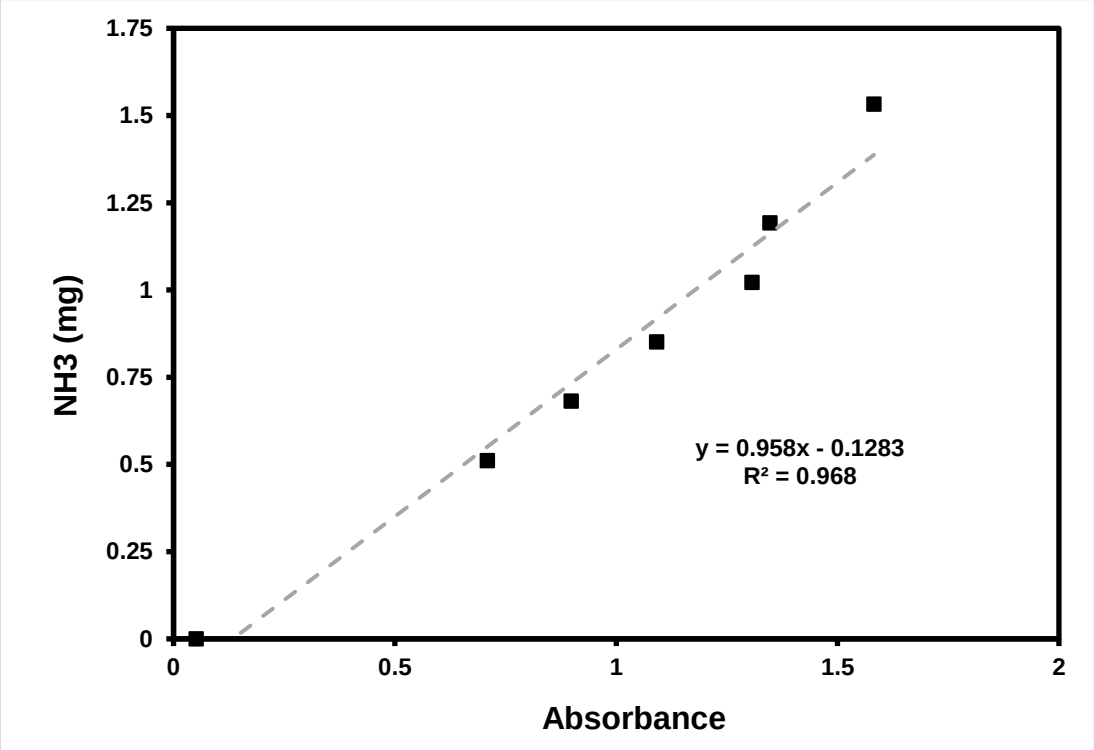

Figure 0.2. Calibration curve of absorbance measured ate 420 nm versus ammonia (mg) produced

REFERENCES

1. Sumner, J. B., The chemical nature of enzymes. 1946.

2. Mateer, J. G.; Marshall, E. K., The Urease Content of Certain Beans, with Special Reference to the Jack Bean. *J. Biol. Chem.* **1916,** *25*, 297-305.

3. Sumner, J. B.; Graham, V. A.; Noback, C. V., The purification of jack bean urease. *Experimental Biology and Medicine* **1924,** *21* (8), 551-552.

4. Karplus, P. A.; Pearson, M. A.; Hausinger, R. P., 70 Years of Crystalline Urease: What Have We Learned? *Accounts of Chemical Research* **1997,** *30* (8), 330-337.

5. Sirko, A.; Brodzik, R., Plant ureases: roles and regulation. *Acta Biochimica Polonica* **2000,** *47* (4), 1189-1195.

6. Venkatasubban, A.; Karnad, R., Urease activity of germinated seeds. *Proceedings of the Indian Academy of Sciences* **1936,** *4*, 370-375.

7. Webster, G. C.; Varner, J. E.; Gansa, A. N., Conversion of Carbon-14-Labeled Urea into Amino Acids in Leaves. *Plant Physiol* **1955,** *30* (4), 372-4.

8. Adams, C. A.; Rinne, R. W., The Occurrence and Significance of Dispensable Proteins in Plants. *New Phytologist* **1981,** *89* (1), 1-14.

9. Zonia, L. E.; Stebbins, N. E.; Polacco, J. C., Essential role of urease in germination of nitrogen-limited Arabidopsis thaliana seeds. *Plant Physiol* **1995,** *107* (4), 1097-103.

10. El-Hefnawy, M. E.; Sakran, M.; Ismail, A. I.; Aboelfetoh, E. F., Extraction, purification, kinetic and thermodynamic properties of urease from germinating Pisum Sativum L. seeds. *BMC Biochem* **2014,** *15*, 15.

11. Das, N.; Kayastha, A. M.; Srivastava, P. K., Purification and characterization of urease from dehusked pigeonpea (Cajanus cajan L.) seeds. *Phytochemistry* **2002,** *61* (5), 513-521.

12. Rechenmacher, C.; Wiebke-Strohm, B.; Oliveira-Busatto, L. A.; Polacco, J. C.; Carlini, C. R.; Bodanese-Zanettini, M. H., Effect of soybean ureases on seed germination and plant development. *Genet Mol Biol* **2017,** *40* (1 suppl 1), 209-216.

13. Ha, N. C.; Oh, S. T.; Sung, J. Y.; Cha, K. A.; Lee, M. H.; Oh, B. H., Supramolecular assembly and acid resistance of Helicobacter pylori urease. *Nat Struct Biol* **2001,** *8* (6), 505-9.

14. Debowski, A. W.; Walton, S. M.; Chua, E. G.; Tay, A. C.; Liao, T.; Lamichhane, B.; Himbeck, R.; Stubbs, K. A.; Marshall, B. J.; Fulurija, A.; Benghezal, M., Helicobacter pylori gene silencing in vivo demonstrates urease is essential for chronic infection. *PLoS Pathog* **2017,** *13* (6), e1006464.

15. Celli, J. P.; Turner, B. S.; Afdhal, N. H.; Keates, S.; Ghiran, I.; Kelly, C. P.; Ewoldt, R. H.; McKinley, G. H.; So, P.; Erramilli, S.; Bansil, R., Helicobacter pylori moves through mucus by reducing mucin viscoelasticity. *Proc Natl Acad Sci U S A* **2009,** *106* (34), 14321-6.

16. Malfertheiner, P.; Megraud, F.; O'Morain, C.; Bazzoli, F.; El-Omar, E.; Graham, D.; Hunt, R.; Rokkas, T.; Vakil, N.; Kuipers, E. J., Current concepts in the management of Helicobacter pylori infection: the Maastricht III Consensus Report. *Gut* **2007,** *56* (6), 772-81.

17. Keeken, N.; Hattum, E.; de Boer, W., Validation of a new, commercially available dry rapid urease test for the diagnosis of Helicobacter pylori infection in gastric biopsies. *Neth J Med.* **2006,** *64* (9), 329-333.

18. Graham, D. Y.; Miftahussurur, M., Helicobacter pylori urease for diagnosis of Helicobacter pylori infection: A mini review. *J Adv Res* **2018,** *13*, 51-57.

19. Chomicki, G.; Renner, S. S., Watermelon origin solved with molecular phylogenetics including Linnaean material: another example of museomics. *New Phytol* **2015,** *205* (2), 526-32.

20. Paris, H. S., Origin and emergence of the sweet dessert watermelon, Citrullus lanatus. *Ann Bot* **2015,** *116* (2), 133-48.

21. Strauss, M. The 5,000-Year Secret History of the Watermelon. https://www.nationalgeographic.com/news/2015/08/150821-watermelon-fruit-history-agriculture/.

22. Paris, H. S.; Daunay, M. C.; Janick, J., The Cucurbitaceae and Solanaceae illustrated in medieval manuscripts known as the Tacuinum Sanitatis. *Ann Bot* **2009,** *103* (8), 1187-205.

23. Dikhtyarev, S. I.; Yanina, M. M.; Kuznetsova, R. G.; Kurganov, B. I.; Chernobai, V. T., Isolation of a urease from watermelon seeds and the study of its properties. *Chemistry of Natural Compounds* **1983,** *19* (5), 587-591.

24. Prakash, O.; Bhushan, G., Isolation, Purification and Partial Characterisation of Urease from Seeds of Water Melon (*Citrullus vulgaris*). *J. Plant Biochemistry & Biotechnology* **1997,** *6*, 45-47.

25. Prakash, O.; Bhushan, G., A study of inhibition of urease from seeds of the water melon (Citrullus vulgaris). *J Enzyme Inhib* **1998,** *13* (1), 69-77.

26. Mohamed, T., Purification of urease from water melon seeds for clinical diagnostic kits. *Bioresource Technology* **1999,** *68* (3), 215-223.

27. Behere, M.; Patil, S. S.; Rathod, V. K., Rapid extraction of watermelon seed proteins using microwave and its functional properties. *Prep Biochem Biotechnol* **2020**, 1-8.

28. Khaleque, K. A.; Muazzam, M. G.; Ispahani, P., A Simple Method for the Use of Water Melon Seed Preparations in the Estimation of Blood Urea. *J Clin Pathol* **1964,** *17*, 97-8.

29. Liu, S.; Jiang, L.; Li, Y., Research of aqueous enzymatic extraction of watermelon seed Oil of ultrasonic pretreatment assisted. *Procedia Engineering* **2011,** *15*, 4949-4955.

30. Wani, A. A.; Sogi, D. S.; Singh, P.; Shivhare, U. S., Characterization and functional properties of watermelon (Citrullus lanatus) seed protein isolates and salt assisted protein concentrates. *Food Science and Biotechnology* **2011,** *20* (4), 877-887.

31. Javadi, N.; Khodadadi, H.; Hamdan, N.; Kavazanjian, E., EICP Treatment of Soil by Using Urease Enzyme Extracted from Watermelon Seeds. In *IFCEE 2018*, American Society of Civil Engineers: Orlando, Florida, 2018; pp 115-124.

32. Williams, W. T., Function of Urease in Citrullus Seeds. *Nature* **1950,** *165* (4185), 79-79.

33. Williams, W. T.; Sharma, P. C., The Function of Urease inCitrullusSeeds. *Journal of Experimental Botany* **1954,** *5* (1), 136-157.

34. Kagawa, T.; McGregor, D. I.; Beevers, H., Development of Enzymes in the Cotyledons of Watermelon Seedlings. *Plant Physiol.* **1973,** *51*, 66-71.

35. Sautter, C.; Hock, B., Fluorescence Immunohistochemical Localization of Malate Dehydrogenase Isoenzymes in Watermelon Cotyledons. *Plant Physiol.* **1982,** *70*, 1162-1168.

36. (AIST), N. I. o. A. I. S. a. T., SDBS-1936 Castor Oil 1999.

37. Thomas, A., *Ullmann's Encyclopedia of Industrial Chemistry*. 2000.

38. Weber, E.; Neumann, D., Protein bodies, storage organelles in plant seeds. *Biochemie und Physiologie der Pflanzen* **1980,** *175* (4), 279-306.

39. Wang, T.; Cobb, B. G.; Sittertz-Bhatkar, H.; Leskovar, D. I., An Ultrastructural Study of Seed Reserves in Triploid Watermelons. *Acta Horticulturae* **2004,** (631), 71-77.

40. Tanaka, K.; Sugimoto, T.; Ogawa, M.; Kasai, Z., Isolation and Characterization of Two Types of Protein Bodies in the Rice Endosperm. *Agricultural and Biological Chemistry* **2014,** *44* (7), 1633-1639.

41. Giuliani, C.; Tani, C.; Maleci Bini, L., Micromorphology and anatomy of fruits and seeds of bitter melon (Momordica charantia L., Cucurbitaceae). *Acta Societatis Botanicorum Poloniae* **2016,** *85* (1).

42. Eden Brothers(R) The Seediest Place on Earth. https://www.edenbrothers.com/.

43. Vogel, A., *Vogel's Textbook of Macro and Semimicro Qualitative Inorganic Analysis*. Longman Group: London and New York, 1979.

44. Leonard, R. H., Quantitative Range of Nessler's Reaction with Ammonia. *Clinical Chemistry* **1963,** *9* (4), 417-422.

45. Phosphate Buffer (pH 5.8 to 7.4) Preparation. https://www.aatbio.com/resources/buffer-preparations-and-recipes/phosphate-buffer-ph-5-8-to-7-4.

46. Bubanja, I. N.; Bánsági, T.; Taylor, A. F., Kinetics of the urea–urease clock reaction with urease immobilized in hydrogel beads. *Reaction Kinetics, Mechanisms and Catalysis* **2017,** *123* (1), 177-185.

47. Wrobel, M. pH-driven instabilities in chemical systems. University of Leeds, 2012.

48. Hu, G.; Pojman, J. A.; Scott, S. K.; Wrobel, M. M.; Taylor, A. F., Base-catalyzed feedback in the urea-urease reaction. *J Phys Chem B* **2010,** *114* (44), 14059-63.

49. Krajewska, B.; Ciurli, S., Jack bean (Canavalia ensiformis) urease. Probing acid-base groups of the active site by pH variation. *Plant Physiol Biochem* **2005,** *43* (7), 651-8.

50. Lim, K.; Leverenz, H., Characterization of urease derived from Citrullus lanatus (watermelon) seeds to estimate total Kjeldahl nitrogen in human urine. *International Journal of Environmental Analytical Chemistry* **2019,** *99* (5), 486-499.

51. Tetiker, A.; Ertan, F., Investigation of some properties of immobilized urease from Cicer arietinum and its using in determination of urea level in some animal feed. *Journal of Innovations in Pharmaceutical and Biological Sciences* **2017,** *4* (2), 01-06.

52. Yang, D.; Fan, J.; Cao, F.; Deng, Z.; Pojman, J. A.; Ji, L., Immobilization adjusted clock reaction in the urea–urease–H+ reaction system. *RSC Advances* **2019,** *9* (7), 3514-3519.

53. Colon, H. D.; Walt, D. R., Immobilization of enzymes in polymer supports. *Journal of Chemical Education* **1986,** *63* (4).

54. Matsuno, H.; Nagasaka, Y.; Kurita, K.; Serizawa, T., Superior Activities of Enzymes Physically Immobilized on Structurally Regular Poly(methyl methacrylate) Surfaces. *Chemistry of Materials* **2007,** *19* (9), 2174-2179.

55. Chen, B.; Hu, J.; Miller, E. M.; Xie, W.; Cai, M.; Gross, R. A., Candida antarctica lipase B chemically immobilized on epoxy-activated micro- and nanobeads: catalysts for polyester synthesis. *Biomacromolecules* **2008,** *9* (2), 463-71.

56. Suraniti, E.; Studer, V.; Sojic, N.; Mano, N., Fast and easy enzyme immobilization by photoinitiated polymerization for efficient bioelectrochemical devices. *Anal Chem* **2011,** *83* (7), 2824-8.

57. Tran, D. N.; Balkus, K. J., Perspective of Recent Progress in Immobilization of Enzymes. *ACS Catalysis* **2011,** *1* (8), 956-968.

58. Ai, Q.; Yang, D.; Zhu, Y.; Jiang, Z., Fabrication of Boehmite/Alginate Hybrid Beads for Efficient Enzyme Immobilization. *Industrial & Engineering Chemistry Research* **2013,** *52* (42), 14898-14905.

59. Tang, C.; Saquing, C. D.; Morton, S. W.; Glatz, B. N.; Kelly, R. M.; Khan, S. A., Cross-linked polymer nanofibers for hyperthermophilic enzyme immobilization: approaches to improve enzyme performance. *ACS Appl Mater Interfaces* **2014,** *6* (15), 11899-906.

60. Zhu, X.; Ma, Y.; Zhao, C.; Lin, Z.; Zhang, L.; Chen, R.; Yang, W., A mild strategy to encapsulate enzyme into hydrogel layer grafted on polymeric substrate. *Langmuir* **2014,** *30* (50), 15229-37.

61. Che, H.; Buddingh, B. C.; van Hest, J. C. M., Self-Regulated and Temporal Control of a "Breathing" Microgel Mediated by Enzymatic Reaction. *Angew Chem Int Ed Engl* **2017,** *56* (41), 12581-12585.

62. Mondal, S.; Malik, S.; Sarkar, R.; Roy, D.; Saha, S.; Mishra, S.; Sarkar, A.; Chatterjee, M.; Mandal, B., Exuberant Immobilization of Urease on an Inorganic SiO2 Support Enhances the Enzymatic Activities by 3-fold for Perennial Utilization. *Bioconjug Chem* **2019,** *30* (1), 134-147.

63. Yushkova, E. D.; Nazarova, E. A.; Matyuhina, A. V.; Noskova, A. O.; Shavronskaya, D. O.; Vinogradov, V. V.; Skvortsova, N. N.; Krivoshapkina, E. F., Application of Immobilized Enzymes in Food Industry. *J Agric Food Chem* **2019,** *67* (42), 11553-11567.

64. Zezzi do Valle Gomes, M.; Nabavi Zadeh, P. S.; Palmqvist, A. E. C.; Åkerman, B., Spatial Distribution of Enzymes Immobilized in Mesoporous Silicas for Biocatalysis. *ACS Applied Nano Materials* **2019,** *2* (11), 7245-7254.

65. Kim, H.; Hassouna, F.; Muzika, F.; Arabacı, M.; Kopecký, D.; Sedlářová, I.; Šoóš, M., Urease adsorption immobilization on ionic liquid-like macroporous polymeric support. *Journal of Materials Science* **2019,** *54* (24), 14884-14896.

66. Burns, T.; Breathnach, S.; Cox, N.; Griffiths, C., Rook's Textbook of Dermatology. Wiley-Blackwell: 2010.

67. Wrobel, M. M.; Bansagi, T., Jr.; Scott, S. K.; Taylor, A. F.; Bounds, C. O.; Carranza, A.; Pojman, J. A., pH wave-front propagation in the urea-urease reaction. *Biophys J* **2012,** *103* (3), 610-615.

68. Bansagi, T., Jr.; Taylor, A. F., Role of differential transport in an oscillatory enzyme reaction. *J Phys Chem B* **2014,** *118* (23), 6092-7.

69. Jee, E. Time-Lapse Polymerizations Triggered by pH clock Reactions. Louisiana State University and Agricultural and Mechanical College, Baton Rouge, Louisiana, 2016.

70. Herman, E. M.; Larkins, B. A., Protein storage bodies and vacuoles. *Plant Cell* **1999,** *11* (4), 601-14.

71. Aguilera, J. M., Protein extraction from lupin seeds: microstructural aspects and hypothesis of mechanism. *International Journal of Food Science & Technology* **2007,** *24* (1), 29-37.

72. Li, D.; Xia, Y., Electrospinning of Nanofibers: Reinventing the Wheel? *Advanced Materials* **2004,** *16* (14), 1151-1170.

73. Reneker, D. H.; Yarin, A. L., Electrospinning jets and polymer nanofibers. *Polymer* **2008,** *49* (10), 2387-2425.

74. Wang, Z.-G.; Wang, J.-Q.; Xu, Z.-K., Immobilization of lipase from Candida rugosa on electrospun polysulfone nanofibrous membranes by adsorption. *Journal of Molecular Catalysis B: Enzymatic* **2006,** *42* (1-2), 45-51.

75. Yujun, W.; Jian, X.; Guangsheng, L.; Youyuan, D., Immobilization of lipase by ultrafiltration and cross-linking onto the polysulfone membrane surface. *Bioresour Technol* **2008,** *99* (7), 2299-303.

76. Pritchard, C. D.; O'Shea, T. M.; Siegwart, D. J.; Calo, E.; Anderson, D. G.; Reynolds, F. M.; Thomas, J. A.; Slotkin, J. R.; Woodard, E. J.; Langer, R., An injectable thiol-acrylate poly(ethylene glycol) hydrogel for sustained release of methylprednisolone sodium succinate. *Biomaterials* **2011,** *32* (2), 587-97.

77. Jee, E.; Bansagi, T., Jr.; Taylor, A. F.; Pojman, J. A., Temporal Control of Gelation and Polymerization Fronts Driven by an Autocatalytic Enzyme Reaction. *Angew Chem Int Ed Engl* **2016,** *55* (6), 2127-31.

78. Fatin-Rouge, N.; Starchev, K.; Buffle, J., Size Effects on Diffusion Processes within Agarose Gels. *Biophysical Journal* **2004,** *86* (5), 2710-2719.

79. Williams, P.; Phillips, G., *Handbook of Hydrocolloids*. 2000.

80. Griffin, W., Classification of Surface-Active Agents by HLB. *Journal of the Society of Cosmetic Chemists* **1949,** *1* (5), 311-326.

81. Barrett, E. P.; Joyner, L. G.; Halenda, P. P., The Determination of Pore Volume and Area Distributions in Porous Substances. I. Computations from Nitrogen Isotherms. *Journal of the American Chemical Society* **1951,** *73* (1), 373-380.

82. Xie, S.; Svec, F.; Fréchet, J. M. J., Porous Polymer Monoliths: Preparation of Sorbent Materials with High-Surface Areas and Controlled Surface Chemistry for High-Throughput, Online, Solid-Phase Extraction of Polar Organic Compounds. *Chemistry of Materials* **1998,** *10* (12), 4072-4078.

83. Erbay, E.; Okay, O., Pore memory of macroporous styrene–divinylbenzene copolymers. *Journal of Applied Polymer Science* **1999,** *71* (7).

84. Okay, O., Macroporous Copolymer Networks. *Progress in Polymer Science* **2000,** *25*, 711-779.

85. Li, L.; Cheng, J.; Wen, X.; Pi, P.; Yang, Z., Synthesis and Characterization of Suspension Polymerized Styrene-Divinylbenzene Porous Microsphere Using as Slow-Release-Active Carrier. *Chinese Journal of Chemical Engineering* **2006,** *14* (4), 471-477.

86. Fang, D. Synthesis, Characterization and Modeling of Porous Copolymer Particles. Ontario, Canada, 2007.

87. Al-Sabti, M.; Jawad, J.; Jacob, W., Preparation of Macroporous Styrene-Divinyl Benzene Copolymers. *Eng. & Technology* **2007,** *25* (9), 1041-1048.

88. Abdel-Azim, A.-A. A.; Abdul-Raheim, A. M.; Atta, A. M.; Brostow, W.; El-Kafrawy, A. F., Synthesis and Characterization of Porous Crosslinked Copolymers for Oil Spill Sorption. *e-Polymers* **2007,** *7* (1).

89. Mohamed, M. H.; Wilson, L. D., Porous Copolymer Resins: Tuning Pore Structure and Surface Area with Non Reactive Porogens. *Nanomaterials (Basel)* **2012,** *2* (2), 163-186.

90. Alvim, I. D.; Grosso, C. R. F., Microparticles obtained by complex coacervation: influence of the type of reticulation and the drying process on the release of the core material. *Ciência e Tecnologia de Alimentos* **2010,** *30* (4), 1069-1076.

91. Zhao, T.; Qiu, D., One-pot synthesis of highly folded microparticles by suspension polymerization. *Langmuir* **2011,** *27* (21), 12771-4.

92. Gokmen, M. T.; Du Prez, F. E., Porous polymer particles—A comprehensive guide to synthesis, characterization, functionalization and applications. *Progress in Polymer Science* **2012,** *37* (3), 365-405.

93. Zhan, S.; Chen, C.; Zhao, Q.; Wang, W.; Liu, Z., Preparation of 5-Fu-Loaded PLLA Microparticles by Supercritical Fluid Technology. *Industrial & Engineering Chemistry Research* **2013,** *52* (8), 2852-2857.

94. Yang, S.; Wang, Y.; Jiang, Y.; Li, S.; Liu, W., Molecularly Imprinted Polymers for the Identification and Separation of Chiral Drugs and Biomolecules. *Polymers (Basel)* **2016,** *8* (6).

95. Yan, H.; Row, K., Characteristic and Synthetic Approach of Molecularly Imprinted Polymer. *International Journal of Molecular Sciences* **2006,** *7* (5), 155-178.

96. Brunauer, S.; Emmett, P. H.; Teller, E., Adsorption of Gases in Multimolecular Layers. *Journal of the American Chemical Society* **1938,** *60* (2), 309-319.

97. Pan, X.; Sengupta, P.; Webster, D. C., Novel biobased epoxy compounds: epoxidized sucrose esters of fatty acids. *Green Chemistry* **2011,** *13* (4).

98. Sitz, E. D.; Bajwa, D. S.; Webster, D. C.; Monono, E. M.; Wiesenborn, D. P.; Bajwa, S. G., Epoxidized sucrose soyate—A novel green resin for crop straw based low density fiberboards. *Industrial Crops and Products* **2017,** *107*, 400-408.

99. Rosch, J.; Mulhaupt, R., Polymers from renewable resoureces: polyester resins and blends based upon anhydride-cured epoxidized soybean oil. *Polymer Bulletin* **1993,** *31*, 679-685.

100. Hernandez, S.; Vigueras, E., Acrylated-Epoxidized Soybean Oil-Based Polymers and Their Use in the Generation of Electrically Conductive Polymer Composites. In *Soybean - Bio-Active Compounds*, 2013.

101. Liu, K. Novel plant oil-based thermosets and polymer composites. Iowa State University, 2014.

102. Gogoi, P.; Boruah, M.; Sharma, S.; Dolui, S. K., Blends of Epoxidized Alkyd Resins Based on Jatropha Oil and the Epoxidized Oil Cured with Aqueous Citric Acid Solution: A Green Technology Approach. *ACS Sustainable Chemistry & Engineering* **2015,** *3* (2), 261-268.

103. Wang, R. Manufacturing of vegetable oils-based epoxy and composites for structural applications. Missouri University of Science and Technology, 2014.

104. Jian, X.-Y.; An, X.-P.; Li, Y.-D.; Chen, J.-H.; Wang, M.; Zeng, J.-B., All Plant Oil Derived Epoxy Thermosets with Excellent Comprehensive Properties. *Macromolecules* **2017,** *50* (15), 5729-5738.

105. Jian, X.-Y.; He, Y.; Li, Y.-D.; Wang, M.; Zeng, J.-B., Curing of epoxidized soybean oil with crystalline oligomeric poly(butylene succinate) towards high performance and sustainable epoxy resins. *Chemical Engineering Journal* **2017,** *326*, 875-885.

106. Frias, C. F.; Serra, A. C.; Ramalho, A.; Coelho, J. F. J.; Fonseca, A. C., Preparation of fully biobased epoxy resins from soybean oil based amine hardeners. *Industrial Crops and Products* **2017,** *109*, 434-444.

107. Aouf, C.; Nouailhas, H.; Fache, M.; Caillol, S.; Boutevin, B.; Fulcrand, H., Multi-functionalization of gallic acid. Synthesis of a novel bio-based epoxy resin. *European Polymer Journal* **2013,** *49* (6), 1185-1195.

108. Ma, S.; Kovash, C. S.; Webster, D. C., Effect of solvents on the curing and properties of fully bio-based thermosets for coatings. *Journal of Coatings Technology and Research* **2016,** *14* (2), 367-375.

109. Ma, S.; Webster, D. C., Naturally Occurring Acids as Cross-Linkers To Yield VOC-Free, High-Performance, Fully Bio-Based, Degradable Thermosets. *Macromolecules* **2015,** *48* (19), 7127-7137.

110. Ma, S.; Webster, D. C.; Jabeen, F., Hard and Flexible, Degradable Thermosets from Renewable Bioresources with the Assistance of Water and Ethanol. *Macromolecules* **2016,** *49* (10), 3780-3788.

111. Chen, Y.; Xi, Z.; Zhao, L., New bio-based polymeric thermosets synthesized by ring-opening polymerization of epoxidized soybean oil with a green curing agent. *European Polymer Journal* **2016,** *84*, 435-447.

112. Chen, Y.; Xi, Z.; Zhao, L., Curing kinetics of bio-based epoxy resin based on epoxidized soybean oil and green curing agent. *AIChE Journal* **2017,** *63* (1), 147-153.

113. Pradhan, S.; Pandey, P.; Mohanty, S.; Nayak, S. K., Synthesis and characterization of waterborne epoxy derived from epoxidized soybean oil and bioderived C-36 dicarboxylic acid. *Journal of Coatings Technology and Research* **2017,** *14* (4), 915-926.

114. Zeng, R.-T.; Wu, Y.; Li, Y.-D.; Wang, M.; Zeng, J.-B., Curing behavior of epoxidized soybean oil with biobased dicarboxylic acids. *Polymer Testing* **2017,** *57*, 281-287.

115. Zhang, C.; Garrison, T. F.; Madbouly, S. A.; Kessler, M. R., Recent advances in vegetable oil-based polymers and their composites. *Progress in Polymer Science* **2017,** *71*, 91-143.

116. Naniwadekar, M. Y.; Jadhav, A. S.; Ghosh, A.; Sahu, A., Cost Estimation & Optimum Route Selection for the Production of Aconitic Acid. *Journal of Basic and Applied Chemical Sciences* **2013,** *3* (4), 79-87.

117. Zapata, N. J. G. Aconitic Acid from Sugarcane: Production and Industrial Application. Louisiana State University and Agricultural and Mechanical College, Baton Rouge, 2007.

118. Bassler, B. L., How bacteria talk to each other: regulation of gene expression by quorum sensing. *Current Opinion in Microbiology* **1999,** *2* (6), 582-587.

119. Rutherford, S. T.; Bassler, B. L., Bacterial quorum sensing: its role in virulence and possibilities for its control. *Cold Spring Harb Perspect Med* **2012,** *2* (11).

120. Miller, M. B.; Bassler, B. L., Quorum sensing in bacteria. *Annu Rev Microbiol* **2001,** *55*, 165-99.

121. Redfield, R., Is quorum sensing a side effect of diffusion sensing? *Trends in Microbiology* **2002,** *10* (8), 365-370.

122. Platt, T. G.; Fuqua, C., What's in a name? The semantics of quorum sensing. *Trends Microbiol* **2010,** *18* (9), 383-7.

123. West, S. A.; Winzer, K.; Gardner, A.; Diggle, S. P., Quorum sensing and the confusion about diffusion. *Trends Microbiol* **2012,** *20* (12), 586-94.

124. Lee, K.-J.; McCormick, W. D.; Pearson, J. E.; Swinney, H. L., Experimental observation of self-replicating spots in a reaction–diffusion system. *Nature* **1994,** *369* (6477), 215-218.

125. Lefebvre, J.; Vincent, J.-C., Diffusion-reaction-growth coupling in gel-immobilized cell systems: Model and experiment. *Enzyme and Microbial Technology* **1995,** *17* (3), 276-284.

126. Petroff, A. P.; Wu, T. D.; Liang, B.; Mui, J.; Guerquin-Kern, J. L.; Vali, H.; Rothman, D. H.; Bosak, T., Reaction-diffusion model of nutrient uptake in a biofilm: theory and experiment. *J Theor Biol* **2011,** *289*, 90-5.

127. Stewart, P. S.; Zhang, T.; Xu, R.; Pitts, B.; Walters, M. C.; Roe, F.; Kikhney, J.; Moter, A., Reaction-diffusion theory explains hypoxia and heterogeneous growth within microbial biofilms associated with chronic infections. *NPJ Biofilms Microbiomes* **2016,** *2*, 16012.

128. Yang, T.; Han, Y., Quantitatively Relating Diffusion and Reaction for Shaping Particles. *Crystal Growth & Design* **2016,** *16* (5), 2850-2859.

129. Lamotta, E. J., Internal diffusion and reaction in biological films. *Environ Sci Technol* **1976,** *10* (8), 765-9.

130. Stewart, P. S., Diffusion in biofilms. *J Bacteriol* **2003,** *185* (5), 1485-91.

131. Hong, S. H.; Hegde, M.; Kim, J.; Wang, X.; Jayaraman, A.; Wood, T. K., Synthetic quorum-sensing circuit to control consortial biofilm formation and dispersal in a microfluidic device. *Nat Commun* **2012,** *3*, 613.

132. Zhang, F.; Kwan, A.; Xu, A.; Suel, G. M., A Synthetic Quorum Sensing System Reveals a Potential Private Benefit for Public Good Production in a Biofilm. *PLoS One* **2015,** *10* (7), e0132948.

133. Shum, H.; Balazs, A. C., Synthetic quorum sensing in model microcapsule colonies. *Proc Natl Acad Sci U S A* **2017,** *114* (32), 8475-8480.

134. Markovic, V. M.; Bansagi, T., Jr.; McKenzie, D.; Mai, A.; Pojman, J. A.; Taylor, A. F., Influence of reaction-induced convection on quorum sensing in enzyme-loaded agarose beads. *Chaos* **2019,** *29* (3), 033130.

135. Dilrukshi, R. A. N.; Watanabe, J.; Kawasaki, S., Sand Cementation Test using Plant-Derived Urease and Calcium Phosphate Compound. *Materials Transactions* **2015,** *56* (9), 1565-1572.

136. Dilrukshi, R. A. N., Strengthening of Sand Cemented with Calcium Phosphate Compounds Using Plant-Derived Urease. *International Journal of Geomate* **2016**.

VITA

Anthony Mai was born and raised in Lafayette, Louisiana and received his B.S.'s in Chemistry and Mathematics from the University of Louisiana at Lafayette in December 2007. He then went to work in research and development at AMCOL in Lafayette and Sasol in Lake Charles. After 6 years working, he joined Dr. John Pojman's research team at Louisiana State University in August 2016. He has mentored many undergrads with individual projects in the lab, getting them ready for high level research. He's worked on several IP projects at his tenure in graduate school, including collaborations with the AgCenter's research on sweet potatoes, grass seeds, sugarcane biomass, and hog baits. He aims to return to industry and continue applied materials polymer research.